IMMOBILIZATION OF TETRABROMOBISPHENOL A ON PINECONE-DERIVED BIOCHAR

A Thesis

Submitted to the Faculty of Graduate Studies and Research

in Partial Fulfillment of the Requirements

for the Degree of

Master of Applied Science

in Environmental Systems Engineering

University of Regina

By

Jian Shen

Regina, Saskatchewan

August 2017

UNIVERSITY OF REGINA

FACULTY OF GRADUATE STUDIES AND RESEARCH

SUPERVISORY AND EXAMINING COMMITTEE

Jian Shen, candidate for the degree of Master of Applied Science in Environmental Systems Engineering**,** has presented a thesis titled, ***Immobilization of Tetrabromobisphenol A On Pinecone-Derived Biochar,*** in an oral examination held on August 19, 2017. The following committee members have found the thesis acceptable in form and content, and that the candidate demonstrated satisfactory knowledge of the subject material.

External Examiner:	Dr. Wei Peng, Industrial Systems Engineering
Supervisor:	Dr. Gordon Huang , Environmental Systems Engineering
Committee Member:	Dr. Chunjiang An, Adjunct
Committee Member:	Dr. Kelvin Ng, Environmental Systems Engineering
Chair of Defense:	Dr. Dianliang Deng, Department of Mathematics & Statistics

ABSTRACT

In the past decades, Tetrabromobisphenol A (TBBPA), one of brominated flame retardants (BFR), has been widely used in a variety of commercial and industry applications to improve fire resistance, and it is also commonly used in fire safety of laminates in printed circuit boards, plastics in electrical and electronic equipment. Due to its large part of world production of BFRs for covering around 60% of the total BFR market and the use of TBBPA is currently not restricted in many countries including America and China, TBBPA is of great concern as a relatively persistent organic pollutant released through manufacturing, recycling, and disposal of various fabrics and materials. Moreover, many studies suggest that TBBPA at environmentally relevant concentrations can induce a variety of adverse health effects including cytotoxicity, immunotoxicity, hepato-toxicity, disruption of thyroid homeostasis, and has potential to disrupt estrogen signaling. The aqueous toxicity of TBBPA has been demonstrated that the acute 48-h LC50 (lethal concentration of 50%) for Daphnia magna was reported to be 0.96 mg/L, and 96-h LC50 for fish ranged from 0.40 to 0.54mg/L. The acute oral toxicity of TBBPA for mammals is low. However, the International Agency for Research on Cancer has recently upgraded this flame retardant to group 2A (probably carcinogenic to humans) which was based on sufficient evidence of carcinogenicity in experimental animals and strong mechanistic evidence in humans. The immobilization of TBBPA from aqueous solution by pinecone-derived biochars was investigated. The surface structures and functional groups of biochars produced at different temperatures were characterized through synchrotron-assisted FTIR analysis. The adsorption isotherms were well described by the Langmuir model. The adsorption capacity of TBBPA varied as pH and TBBPA initial concentration

changed. The influences of inorganic fertilizer ions (NH_4^+, PO_4^{3-} and NO_3^-) on the immobilization of TBBPA by pinecone biochars were revealed through fractional-factorial assisted analysis. The results indicated the main effects include negative effects of PO_4^{3-}, positive effects of NH_4^+ and insignificant effects of NO_3^- ions in immobilization and there are interactions among these ions, pH and biochar properties.

Functionality and surface interaction between biochar and TBBPA were investigated under analysis of kinetic models, contact times, surface composition and synchrotron-based FTIR analysis. The results indicated that the interaction between TBBPA on biochar was mainly caused by hydroxyls. Their interactive effects of acid functional groups could be an important role in the adsorption of TBBPA. Moreover, under the high initial concentration, the adsorption process can be stabilized by other oxygen-containing groups. In addition, this study also revealed that π-π interactions could have insignificant impacts on TBBPA adsorption. The results can help understand migration patterns of TBBPA and analyze the immobilization on biochars in the presence of inorganic fertilizer ions. It will have important implications for environmental risk assessment and wastewater treatment.

ACKNOWLEDGEMENT

Firstly, I would like to address my utmost gratitude to my supervisor, Dr. Gordon Huang for his precious guidance and patent remarks. He constantly encourages me through my practical and theoretical studies in environmental engineering with extraordinary support on my thesis. It should acknowledge that, without his constant support, this study would not have been completed. I would also give my appreciation to thank my co-supervisor Dr. Chunjiang An for his kindly guiding and valuable comments.

I sincerely appreciate the help from Drs. Shan Zhao, Peng Zhang, and Shuo Wang. I would also like to thank Yao Yao, Xiaying Xin, Xiujuan Chen and other members in the Institute for Energy, Environment and Sustainable Communities at the University of Regina for their considerate help.

I gratefully acknowledge the Faculty of Graduate Studies and Research, the Faculty of Engineering, for their financial support during my study at the University of Regina.

Finally, I would like to give extend gratitude to my family for their continuous supporting me financially and mentally.

TABLE OF CONTENTS

ABSTRACT ..... **i**

ACKNOWLEDGEMENT ..... **iii**

LIST OF TABLES ..... **vii**

LIST OF FIGURES ..... **viii**

LIST OF ABBREVIATIONS ..... **x**

CHAPTER 1 INTRODUCTION **1**

1.1 Background **1**

1.2 Implications of Immobilizing TBBPA in the Environment **2**

1.3 Roles of Environmental Factors **2**

1.4 Objectives **3**

CHAPTER 2 LITERATURE REVIEW **5**

2.1 Environmental Applications of Biochars **5**

2.2 Fate and Transport of TBBPA in the Environment **8**

2.3 Immobilization of Environmental Pollutants on Adsorbents **11**

2.4. Literature Review Summary **14**

CHAPTER 3 ROLE OF INORGANIC FERTILIZER IONS IN THE IMMOBILIZATION OF TETRABROMOBISPHENOL A BY PINECONE-DERIVED BIOCHARS **16**

3.1 Background **16**

3.2 Materials and methods **19**

3.2.1 Chemicals 19

3.2.2 Biochar Preparation 21

3.2.3 Adsorption Studies.....21

3.2.4 Analytical Methods.....23

3.2.5 Data Analysis and Quality Assurance 25

3.3 Results and Discussion 26

3.3.1 Elemental Analysis and SEM Characterization of Pinecone-Derived Biochars 26

3.3.2 Synchrotron-Based FTIR Analysis of Pinecone Biochars.....30

3.3.3 Adsorption of TBBPA at Biochar-Water Interface 33

3.3.4 pH-Dependent Adsorption of TBBPA on Biochars 38

3.3.5 Factorial Analysis of Inorganic Fertilizer Ions Influencing the Adsorption Process 44

3.4 Conclusions 62

CHAPTER 4 KINETICS AND SURFACE FUNCTIONALITY IN THE REMOVAL OF TETRABROMOBISPHENOL A BY PINECONE-DERIVED BIOCHARS 63

4.1. Background.....63

4.2. Materials and Methods 65

4.2.1 Chemicals 66

4.2.2 Preparation of Acid Biochars.....66

4.2.3 Characterization of Charcoal Adsorbents.....67

4.2.4 Adsorption Experiments 68

4.2.5 Quality Assurance and Quality Control 69

4.3. Results and Discussion 70

4.3.1 Surface Characterization of Pinecone-Derived Biochars 70

4.3.2 Insight from Synchrotron FTIR Analysis 74

4.3.3. Effect of Contact time on the Adsorption of TBBPA by Biochars 82

4.3.4. Adsorption Kinetics 84

4.3.5. Effect of Biochar Dosage 90

4.3.6. Role of Charcoal Surface Functionality in the Adsorption of TBBPA 94

4.4. Conclusions 99

CHAPTER 5 CONCLUSIONS 102

5.1 Summary 102

5.2 Research Achievements 102

5.3 Recommendations for the Future Study 104

REFERENCES 105

LIST OF TABLES

Table 3.1 Characteristics of BCYP and BCBP biochars 29

Table 3.2: Calculated Langmuir and Freundlich coefficient of TBBPA adsorption. ..36

Table 3.3 Independent factors and their levels in 2^{5-1} fractional factorial design. 48

Table 3.4 Results of fractional factorial analysis for BCBP 49

Table 3.5 Results of fractional factorial analysis for BCYP 50

Table 3.6 Design matrix of 2^{5-1} fractional factorial design and corresponding responses for BCBP.....53

Table 3.7 Design matrix of 2^{5-1} fractional factorial design and corresponding responses for BCYP.....54

Table 4.1 Elemental composition of biochars 72

Table 4.2 Kinetic models and parameters of TBBPA adsorption on biochars 89

LIST OF FIGURES

Figure 3.1 Chemical structure of Tetrabromobisphenol A 20

Figure 3.2 FTIR end station at Canadian Light Source 24

Figure 3.3 The SEM images of (a) BCYP300 (b) BCYP600 (c) BCBP300 and (d) BCBP600 28

Figure 3.4: Second derivative FTIR spectra (3600–2600 cm^{-1}) and mid-infrared region (1800–800 cm^{-1}) of (A) BCYP and (B) BCBP biochars produced at various temperatures 31

Figure 3.5 Sorption isotherms of TBBPA on (A) BCBP and (B) BCYP biochars (biochar = 10 mg, pH=7; the solid line represents non-linear curve fitting by Langmiur model the dotted lines represents non-linear curve fitting by Freundlich model.) 35

Figure 3.6 Species distribution of TBBPA as a function of pH 39

Figure 3.7 Effect of pH on distribution coefficient of TBBPA on (A) BCYP and (B) BCBP 42

Figure 3.8 Influence of pH and concentration on distribution coefficient (K_d) 43

Figure 3.9 Half-Normal test for (a) BCYP and (b) BCBP 46

Figure 3.10 Interactive Effects of Inorganic Fertilizer Ions for adsorption of TBBPA on (A) BCYP and (B) BCBP biochars 47

Figure 3.11 Main factors for BCYP and BCBP 52

Figure 3.12 Effect of NaCl concentration for adsorption of TBBPA on (A) BCYP and (B) BCBP 56

Figure 4.1 SEM images of (a) BCSP400 (b) BCSP600 (c) BCYP400 (d) BCYP600 71

Figure 4.2 Synchrotron FTIR spectra of biochars BCSPs, BCYPs and TBBPA 76

Figure 4.3 Synchrotron FTIR spectra of (a) BCSP400 and adsorbed TBBPA, (b)

BCSP500 and adsorbed TBBPA, (c) BCSP600 and adsorbed TBBPA, (d) BCYP400 and adsorbed TBBPA, (e) BCYP500 and adsorbed TBBPA, (f) BCYP600 and adsorbed TBBPA 78

Figure 4.4 FT-IR spectrum of adsorbed TBBPA on BCYPs, BCBPs and TBBPA molecular in wavenumber 3600 to 2800 cm^{-1} 79

Figure 4.5 Possible mechanism in adsorption of TBBPA on biochar 81

Figure 4.6 Effect of contact time on the adsorption of TBBPA by BCYPs and BCSPs. 83

Figure 4.7 Kinetic analysis of pseudo-first model of (a) BCSP and (b) BCYP; pseudo-second model of (c) BCSP and (d) BCYP; intra-particle model of (e) BCSP and (f) BCYP 87

Figure 4.8 Effect of activated carbon dosage on the removal of TBBPA by BCSPs and (b) BCYPs. 91

Figure 4.9 Effect of initial TBBPA concentrations on the removal performance with (a) BCSPs and (b) BCYPs. 93

Figure 4.10 Interactions between TBBPA adsorption and (a) surface area of BCSPs; (b) surface area of BCYPs; (c) carbon content of BCSPs; (d) carbon content of BCYPs; (e) hydrogen-oxygen ratio of BCSPs; (f) hydrogen-oxygen ratio of BCYPs; (g) oxygen-carbon ratio of BCSPs, and (h) oxygen-carbon ratio of BCYPs. 95

LIST OF ABBREVIATIONS

BCBP	Biochar derived from Scot pinecones
BCSP	Black charcoal derived from Scot pinecones
BCYP	Biochar derived from Yellow pinecones
BFR	Brominated Flame retardant
BPA	Bisphenol A
DAD	Diode array detector
EDA	Electron donor-acceptor
LSD	Least significant difference
MCT	Mercury cadmium telluride
SR-FTIR	Synchrotron-based Fourier transform infrared spectroscopy
TBBPA	Tetrabromobisphenol A

CHAPTER 1

INTRODUCTION

1.1 Background

Brominated flame retardants (BFR) are present and can impact numerous aspects in our lives. They are used to merged with material to prevent fire spreading and slow down the combustion. The incorporated materials, such as plastics, textiles and electronic/electrical products are widely distributed around the world (Liu et al. 2016). TBBPA, the most extensively used BFRs uptakes around 60% of the total BFRs market (Law et al. 2006). Through the leaching from landfill site of electrical wastes, TBBPA can be easily transported into environment and contaminant ecosystems (Osako et al. 2004). Biochar, a carbon material produced by thermal heating under oxygen-limited condition, can be used as soil amendment to improve land fertility and help to enhance capture rate of carbon dioxide for plants (Joseph et al. 2015). As an adsorbent in the soil, biochar has the capability to immobilize pollutants from leachate and stormwater (Shimabuku et al. 2016). Such process can help to capture pollutants from their constant fate and transport in atmosphere and they can be finally mineralized through biodegradation effects of microorganisms. On the other hand, it can result in accumulation of pollutants on biochar material and instead of improving soil fertility as a soil amendment, may damage soil system, plants and microorganisms. Thus, the immobilization effect of biochar on the fate and transport of TBBPA in the environment need to be investigated to further understand biochar application and TBBPA transport between water and soil.

1.2 Implications of Immobilizing TBBPA in the Environment

As a widely used brominated flame retardant, TBBPA has multiple paths to enter the environment. By released from product, leached from TBBPA-containing wastes, and escaped during manufacture, TBBPA can access to atmosphere, soil and water (Liu et al. 2016). In addition, health problem can be a concern of TBBPA distributed in the ecosystem. As a disruptor for estrogen or thyroid hormonal system, an environmental relevant concentration of TBBPA can cause damage on aquatic organisms (Kuiper et al. 2007). Moreover, through the contamination of reservoir, river and lake, the threat of potential human exposure of TBBPA can be predictable. Furthermore, human can also contact to TBBPA in indoor environment via inhalation of contaminated air and duct and/or via intake of polluted food. Thus, the immobilization of TBBPA from environment is necessary.

1.3 Roles of Environmental Factors

As a complex and diverse system of biochar application field, the immobilization effect of TBBPA can be influenced by multiple factors including soil substances, biochar dosage and solution pH. The adsorption capacity of biochar was reported that related with ammonium, phosphors and nitrogen content in the soil (Gul and Whalen 2016). Large amount of ammonium, phosphors and nitrogen ions are present in agricultural field after the involvement of inorganic fertilizer or produced from natural nitro-cycle and phosphors-cycle. Besides, as an ionic compound, the form and relevant adsorption effects of TBBPA can be altered in pH levels and different adsorption mechanisms and

performances can be expected in acid, neutral and alkaline region. Moreover, considering varied distributed amount of TBBPA on biochar field, the effects of initial concentrations of TBBPA and biochar dosage can be implicated as environmental factors on immobilization of TBBPA. Such environmental factor can not only help to investigate the transport of TBBPA between soil and water conditions, but also help to outline the possible TBBPA adsorption mechanisms on biochar with solid-liquid interface.

1.4 Objectives

In this study, therefore, the immobilization of TBBPA by pinecone-derived biochars at solid-liquid interface was studied. In detail, (1) pinecone biochars produced from different species and temperatures were characterized through synchrotron-assisted FTIR analysis; (2) the sorption of TBBPA on pinecone biochars were elucidated through isotherm models and the sorption mechanisms were explicated; (3) the effects of aqueous chemistry characteristics (pH, ionic strength, etc.) on TBBPA adsorption were explored; (4) particularly, the influences of inorganic fertilizer ions (NH_4^+, PO_4^3-, and NO_3^-) on the immobilization of TBBPA by pinecone biochars were revealed through fractional-factorial assisted analysis. The results have important implications for risk assessment of brominated flame retardants in the environment.

This study also seeks to reveal the interactions between TBBPA and biochar surface, as well as the corresponding effects of functionality and adsorption capacities. The contact time, the removal efficiency, and the contribution of surface properties of

biochars on TBBPA adsorption will be investigated. In detail, (1) The change of surface functional groups and their interactions during TBBPA adsorption on biochars derived from different temperatures will be analyzed via Synchrotron-based FTIR (SR-FTIR) analysis. (2) The batch experiments including contact time analyses between TBBPA and biochars, calculations of removal percentages and corresponding kinetic models will be conducted to reveal the adsorption process and efficiency on the surface of biochar. (3) Surface behaviors and their interactions with TBBPA concentrations will be investigated by observing adsorption behaviors between TBBPA and compositions of surface on different biochar. The results could provide a feasible sorbent that can be utilized to remove TBBPA and BPA-derived compound in aqueous environment. The SR-FTIR analysis can help to reveal the interactions of TBBPA with certain functional groups on the biochar surface. By investigating of SR-FTIR results, kinetic models and surface compositions, the roles of function groups, carbon structures and porous sites will also be discovered to better understanding the process of TBBPA adsorption. Moreover, it is expected that the results of interactions and kinetic models of TBBPA on biochars can help to reveal the environmental factors of TBBPA transport, as the mobility and immobility of TBBPA on natural produced charcoals from wildfire or other natural factors, can be evaluated with the result of this study.

CHAPTER 2

LITERATURE REVIEW

Most of adsorption and immobilization studies could include the adsorbent, adsorption target and their interaction and effects. Thus, this chapter can be divided into three sections. Their universality of industrial utility and particularity of environmental activity can be demonstrated and illustrated based on related works. Section 2.1 is introduced the carbon-material biochar as the adsorbent in soil and water applications. Section 2.2 is reported the distribution of released TBBPA pollutant in ecology systems and their fate and transport. Section 2.3 is introduced the immobilization effects of TBBPA on other substances.

2.1 Environmental Applications of Biochars

Biochar, a solid material obtained from thermochemical conversion of biomass for a cost-efficient adsorbent, has been actively studied for removal of organic and inorganic contaminates and its biological interactions with microbes and plants (Jin et al. 2016, Taghizadeh-Toosi et al. 2012). Compared with the traditional adsorbents, like activated carbon, biochar has been applied as a novel and low-cost carbonaceous material for multiple use (Jin et al. 2016). Biochar can be produced from agricultural wastes and biomass by pyrolysis (Das et al. 2016, Fan et al. 2016). At a certain temperature and oxygen-limited conditions, biomass can be transformed into fine-grained, carbon-rich structure with porous and functional surface (Cao et al. 2016). Factors of biomass type, pyrolysis temperature and residence time, the activation post-treatment during the

biomass pyrolysis could affect the specific surface properties of biochar and its compositions (Jin et al. 2016). Substances, which include but not be limited in wheat straws (Bruun et al. 2012), pine needle (Chen et al. 2008), papermill waste (Van Zwieten et al. 2010), manures (Cao et al. 2009) and municipal sludges (Hossain et al. 2011), can be particularly used for its specified effects and/or efficient adsorption of certain organic or inorganic targets in the consider of green and cost-effective methods. Wheat straw-derived biochar was reported that the application of wheat straw-derived biochar could be a possible management strategy for long-term carbon sequestration in soils without the results of increased N_2O production rates as well as not effectively immobilize NO_3^- in the soil (Cheng et al. 2012). It was also reported that the biochar pyrolyzed from cereal straw, could significantly reduce CO_2 and N_2O emissions, with the changed enzyme activities, as the stale carbon form of biochar was increased the soil carbon pool (Wu et al. 2013). Such reports indicated that biochar derived from plant biomass via pyrolysis could show to be resistant to biodegradation in environment. Pine needle-derived biochar was reported efficient adsorption of nonpolar and polar aromatic contaminants (Chen et al. 2008) as well as lead and copper (Ahmad et al. 2016). The activities of soil microorganisms were reported that they could be affected by pine needle-derived or soybean stover-derived biochar through imparting positive and negative influences on cycling of nutrient, formation of structure and growth rate of plant in soil. As the agricultural crop residues-derived biochar showed effective in adsorption of organic compounds, manure-derived biochar exhibited high efficiency of adsorption to heavy metals and organic contaminants (Cao et al. 2009). Furthermore, high content of phosphorous in the manure-derived biochar was observed as the main factor for the retention of heavy metal by formation a stable compound. The adsorption of organic contaminants could be the result of partitioning

into the noncarbonized organic phase on the manure-derived biochar (Cao et al. 2009). Moreover, for its specified adsorption on Pb and atrazine, manure-derived biochar could be used for application in environmental remediation (Cao and Harris 2010).

The application of biochar was reported on agriculture land to help improve soil properties and enhance soil fertilities by improving the retention of nutrient and moisture (Buss et al. 2016, Cao et al. 2016). Biochar converted from wastewater sludge was recognized as an environmentally and economically method to address sludges via pyrolysis process (Cao and Harris 2010). Concentrations of nitrogen and trace metals were observed on the sludge-derived biochar as well as significantly increased soil electrical conductivity was found in the field under biochar application. Additionally, The yield of cherry tomato production was found increased at its maximum when sludge-derived biochar applied in the field with fertilizer (Hossain et al. 2010). Converting biomass into biochar as a soil remediator can also reduce the climate change by sequestering carbon form atmosphere (Ahmad et al. 2014). Such converting process into biochar on soil application can results in four co-products: a long term stable carbon in biochar, renewable energy generation, carbon soil amendment, and biomass waste management (Roberts et al. 2010). As the reported negative net greenhouse gas emissions from pyrolysis of agricultural wastes and estimated through life cycle assessment of climate change impacts, biochar may present mitigation benefits in climate change (Roberts et al. 2010). The water holding capacity and the enhancement of CH_4 uptake on biochar applied field were reported as an effect of mitigating climate change through the reduction of emission (Karhu et al. 2011).

2.2 Fate and Transport of TBBPA in the Environment

TBBPA is an intensively used brominated flame retardant (BFR) which is substances to prevent or slow down fire spreading or make materials self-extinguishing from flames (Liu et al. 2016). The application of TBBPA as BFR is involved primarily in materials including plastic, textiles, electrical products. Covering around 60% of total BFR market, TBBPA is recognized as the one of the most widely used BFRs (Birnbaum and Staskal 2004). The total global market of TBBPA was reported that over 120,000 tonnes of such compound in 2001 and over 170,000 tonnes in 2004 (Morose 2006). TBBPA, a white to off-white crystalline powder at room temperature, can be synthesized by bromination of bisphenol A (BPA) by using hydrobromic acid with the following properties: low vapor pressure at 20 ℃; moderately high octanol/water partitioning that can be dependent on the state of ionization and matrix pH levels. The solubility of TBBPA can be changed from low to moderate with the increased of pH levels (Liu et al. 2016, Meerts et al. 2001). In addition, epoxy, polycarbonate and phenolic resins are used to combined with TBBPA to form flame retardant material, and approximately 70% - 90% of TBBPA are estimated to be used as a reactive intermediate in the production of epoxy and polycarbonate (Alaee et al. 2003). As an additional material, TBBPA may leach out of the polymer matrix naturally as it does not react chemically with polymer compounds (Alaee et al. 2003). It was reported large amount of brominated flame retardants were observed with large amount of organics (Osako et al. 2004). The leaching characteristic of TBBPA and other brominated flame retardants was influenced by the co-interaction of dissolved humic matters (Osako et al. 2004). The TBBPA in leachate from waste circuit board in landfill site was reported that fast leaching process of TBBPA was found in landfill site and the leaching rate of

such compound could be strongly influenced by various factors including extracts, BFR congeners and specific surface areas of leaching materials (Zhou et al. 2013). Other e-waste, such as TV housing plastics as well as BFR-containing textiles and sludges can leach TBBPA. Its leachability was found intimately associated with landfill age, and characteristics of dumped waste (Choi et al. 2009). It indicated that the leaching problem of municipal solid landfills could be a great concern. The potential contamination of TBBPA from waste landfills and open dump site could be a considerable interest. Furthermore, with the involve of great amount of old organic wastes which imported via legal and illegal routes, the TBBPA contamination could be severe due to the enhancement of BFR leaching with the coefficient with high organic portion in soil.

The fate and transport of TBBPA was reported in soil, water and atmosphere. A serious environmental contamination was reported an accidentally TBBPA invasion to food supply at Michigan in USA in 1973, inducing a requiring of destruction of approximately 29,800 cattle, 5,920 hogs, 1,470 sheep, and 1.5 million chickens (Di Carlo et al. 1978). In 1983, TBBPA compound was reported exist in river sediments and mussels in Osaka (Watanabe et al. 1983). Since then, the existence of TBBPA in environment was continuously reported. In the Pearl River Delta, southern China, 0.06 to 304 ng/g dry weight of TBBPA from sediments and waterbody was found, and the concentration of TBBPA was reported that significantly correlate with local input sources (Feng et al. 2012). Enantiomeric fractions were reported different with rivers and estuary, indicating extent of enantioselective biotransformation in the sediments (Feng et al. 2012). In addition, sewage treatment works, landfill leachates, sediments, and food web organisms of the North Sea basin were investigated for TBBPA

contamination (Morris et al. 2004). A TBBPA and related compounds (bisphenol A, monobromobisphenol A, dibromobisphenol A, and tribromobisphenol A) were reported in sludge and sediment samples from Ebro river basin in Spain with values between 287 and 1,329 ng/g, which is higher than published data (Guerra et al. 2010). In Nakdong River basin, Korean, TBBPA content was found in sediment samples (Lee et al. 2015). In the industrialized region of East China, TBBPA can be detected from soil sample (Tang et al. 2014a). By forming ester- and ether-linked bound residues in an oxic sandy soil, TBBPA could have a linkage to soil and soil organic matters (Li et al. 2015). In the atmosphere, TBBPA was found from air conditioning filter dust collected from office building in Shenzhen in China (Ni and Zeng 2013). As an potential path for human exposure, TBBPA was observed 15 pg/m and 62ng/g from indoor air and dust from homes, respectively (Abdallah et al. 2008). The universal existence of the TBBPA indicated that the widespread utilization of TBBPA and it can be continuously released from commercial products and locations where BFRs are applied (Lee et al. 2015).

Moreover, the toxicity of TBBPA is a global concern for its acutely toxic at high concentration and can cause negative influence on ecosystem especially in aqueous environment (Hu et al. 2009). Toxicological effects of TBBPA on zebrafish (Danio rerio) were investigated under the analysis of a partial life cycle test (Kuiper et al. 2007). The result reported that shortly after beginning of exposure and were euthanized, adult fishes exposed to 3 and 6 μM showed severe disorientation and lethargy (Kuiper et al. 2007). The acute toxicity on mysid (Mysidopsis bahia) of three ages was also reported under a 96-h LC50 test (Goodman et al. 1988). Furthermore, the disruption of the hypothalamic-pituitary-thyroid axis in zebrafish embryo–larvae was reported under the

exposure of TBBPA in aqueous environment suggesting three genes of interest of thyroid receptor α, thyroid stimulating hormone, and transthyretin can be significantly induced by TBBPA (Chan and Chan 2012). Observations of hepatotoxicity of TBBPA in rats suggested that TBBPA metabolite involved the in vivo generation of radicals (Chignell et al. 2008). Similarly, in Carassius auratus, hydroxyl radical could be generated and caused oxidative damage to liver organs under the present of TBBPA (Shi et al. 2005). The generation of hydroxyl radical from TBBPA could also induce oxidative stress in the tissues of the earthworm (Eisenia fetida) (Xue et al. 2009). Scallop (Chlamys farreri) exhibited a bioaccumulation effect of TBBPA and chemical analysis showed that C. farreri rapidly absorbed TBBPA to achieve an approximate steady state within 6 days (Hu et al. 2015).

2.3 Immobilization of Environmental Pollutants on Adsorbents

During their fate and transport in environment, released pollutants from waste water, landfill site and industrial production could be immobilized on to certain adsorbents. A theoretical survey of molecular atmospheric pollutant adsorption on ice surface was carried out. Residence times of the pollutants between liquid and ice interfaces, with calculated transfer times from the interface to the bulk or to the gas phase and proposed scenarios at the molecular scale regarding the behavior of the pollutant species with respect to the substrate interface (Girardet and Toubin 2001). Polycation-exchanged clays were produced from polycation to be used as sorbents for organic pollutant removal including benzene and nitrophenol (Breen and Watson 1998). The results exhibited that polycation-treated clays could uptake maximum 28 and 46 mg $(g\ clay)^{-1}$ of nitrophenol compounds. With the increase loading of polycation on the clays, the

adsorption capacity of organic pollutant could be increased as well. In addition, the immobilization of inorganic pollutants was also investigated. As a water pollutant, the adsorption of arsenate was carried out on iron, manganese and iron–manganese-modified clinoptilolite-rich tuffs (Jiménez-Cedillo et al. 2009). Under a batch system of arsenate adsorption with a contact time from 5 min to 24 h, the kinetic experimentation was presented to investigate arsenate adsorption process on modified tuffs. The pseudo-second-order model was observed as the result and parameter k in the kinetic model was varied from 0.15 to 5.66 μg/g h, suggesting that the kinetic adsorption of arsenate on modified clinoptilolite-rich tuffs depend on the modified metallic specie on their surface including surface characteristics of the zeolitic material, the chemical nature of the metal as well as the association between different metallic chemical species in the zeolitic surface (Jiménez-Cedillo et al. 2009). In the field of application in wastewater treatment or soil remediation process, activated carbon membranes were used to efficiently immobilize pollutants (Baudu et al. 1991). A method based on the Polanyi−Dubinin−Manes (PDM) model of aqueous organic micropollutants on activated carbon was constructed to predicting parameters of adsorption isotherms (Li et al. 2005). Novel adsorbents, such as sulfonated graphene was used to manage persistent aromatic pollutant (Zhao et al. 2011). The results showed the adsorption capacity of sulfonated graphene nanomaterials could uptake 2.3–2.4 mmol/g for naphthalene and 1-naphthol, indicating a promising candidate of highly effective nano-adsorbent to remove aromatic compounds from aqueous solutions (Zhao et al. 2011). Mesosilica materials including MCM-41 and SBA-15 were also applied for removal organic pollutant of organic dyes, pharmaceuticals and chemical compounds in aqueous solution (Gibson 2014). Changed hydrophobicity was test by using different surface functionalization procedures on the mesoporous silica

materials in the adsorption process of organic pollutant (N,N-diethyl-m-toluamide, DEET) in aqueous solution, reporting DEET sorption capacity is 20 times higher for silylated than for parent materials (Trouvé et al. 2012). Based on the Grand Canonical Monte Carlo analysis, adsorption simulation of hydrogen sulphide removal from biogas on different zeolites was carried out to obtain structures and partial charges of some sorbates for the study of qualitative and quantitative insights into adsorption processes for removal environmental pollutant (Cosoli et al. 2008). Activated montmorillonite, an environment-friendly adsorbent was used for the removal of the persistent pollutant chlorobenzene (Sennour et al. 2009). In that study, the activated montmorillonite was produced and treated under chemical and thermal activation over 100-500 ℃, which can increase its adsorption capacity. Thermodynamic parameters in the adsorption, such as ΔH°, ΔS°, ΔG° and Ea were calculated, indicating the adsorption process was spontaneous and exothermic in nature (Sennour et al. 2009). A chitin/graphene oxide hybrid composite, a biologically friendly artificial material, was tested for removal of pollutant dyes, resulting in a solution pH and Chi:GO proportion dependent adsorption process with maximum adsorption capacity of 9.3×10^{-2} mmol/g and 57×10^{-2} mmol/g of Remazol Black and Neutral Red respectively (González et al. 2015). Biological materials, plants and microorganisms can help to immobilize pollutant from air, soil and water. Various plants exhibited purification capabilities to absorption and disintegration pollutants and waste gases in the air (Fujii et al. 2005). Heavy medal ions including copper (II), lead, cadmium and nicel can be adsorbed on sawdust from aqueous solution under different factors of solution pH, contact time and sorbate concentration, suggesting that sawdust could be a suitable adsorbent for removal metal ions in wastewater treatment (Bulut and Tez 2007, Yu et al. 2000). It was reported that dirhamnolipid biosurfactant could be adsorbed on four

microorganism of Gram-negative Pseudomonas aeruginosa, two Gram-positive Bacillus subtilis, and a yeast, Candida lipolytica and its effect on cell surface hydrophobicity (Zhong et al. 2007). Another report of immobilize thorium or uranium via cell-associated adsorption on various microorganisms highlighted that microorganism had the potential to adsorb large amount of certain pollutant from aqueous solution under different solution pH (Tsuruta 2004). Similarly, Sr can be adsorbed from wastewater on immobilized microorganisms (Watson et al. 1989). Moreover, microorganism in soil can help to enhance the adsorption capability on soil particles to adsorb virus from water content (Zhao et al. 2008).

2.4. Literature Review Summary

In the past decades, many research efforts have been made in the area of characterizing the transport of TBBPAs at solid-liquid interface, as well as exploring the remediation of organic contaminants through solvent extraction and composting. All the above noted efforts help to clarify the environmental fate of organic contaminants. However, improvements in the following areas are still required:

(1) The literature review indicated the relatively extensively manufactured and high adsorptive properties of TBBPA, result in the widely transportation and distribution in environment. Moreover, the major process of TBBPA immobilization is the adsorption of solid particles in soil from aqueous phase of leachate. Although many researches on the immobilization of TBBPA have been reported before, particularly on aspects relating to the effects of soil amendments and corresponding characteristics and analysis under the involvement of environmental factors. The investigations on

characteristics of complex composition in environment are relatively limited in scope. The behaviors and mechanisms of TBBPA influenced by environmental factors, especially inorganic fertilizer ions, remain poorly understood. Further study is necessary to better understand the immobility of TBBPA on biochar surface.

(2) Previous efforts using physical and chemical methods have been well documented for the removal of TBBPA. These methods include different types of approaches, such as degradation, oxidation and adsorption. Among these approaches, adsorption has been extensively used to increase as its cost-effective characteristic. As a more environmental-friendly and sustainable, pyrolyzed biomasses, such as pinecone-derived biochars, are starting to be widely used as a soil amendment. The application of biochar in the removal of organic pollutants from soil has been demonstrated in many previous studies. However, a good understanding of the various factors involved in biochar application is still a challenge in many respects. Further study is still necessary to enhance the efficiency of the application on BFRs.

(3) The adsorption of toxic metals, phosphate, fluoride, and boron, has been demonstrated in many previous studies. Adsorption of some organic compounds including dyes and phenolic compounds from aqueous solutions on inorganic fertilizer ions has also been reported. However, limited studies have focused on the interactions of TBBPA with inorganic fertilizer ions. In solid-liquid systems, the mechanism for the distribution and transportation of solute from bulk solution to solid surface is complicated. A number of issues about the immobilization of TBBPA with co-exist of inorganic fertilizer ions on biochar surface are poorly understood.

CHAPTER 3

ROLE OF INORGANIC FERTILIZER IONS IN THE IMMOBILIZATION OF TETRABROMOBISPHENOL A BY PINECONE-DERIVED BIOCHARS

3.1 Background

TBBPA, one of new brominated flame retardants, has been widely used in a variety of commercial and industrial sectors to improve fire resistance (Peng et al. 2017, Zhang et al. 2013). It accounts for around 60% of the total brominated flame retardant products in market (Han et al. 2013, Peng et al. 2013). TBBPA is of great concern as a relatively persistent organic pollutant, once released into the environment during manufacturing, recycling, and disposal of relevant fabrics and materials. It has been reported as a threat to environment and ecosystem across the world (Sellström and Jansson 1995, Zhang et al. 2014). TBBPA can induce a variety of adverse effects including cytotoxicity, immunotoxicity, hepato-toxicity, alteration of thyroid homeostasis, and disruption of estrogen signaling (Chen et al. 2012, Li et al. 2016). The International Agency for Research on Cancer has also recently upgraded this flame retardant to probable carcinogen (Group 2A) based on sufficient evidence in humans and in experimental animals (Abdallah 2016). Thus, there is an urgent need to explore the fate of TBBPA in the environment for minimizing human exposure and potential risk.

The environmental fate of pollutants is often governed by transport, retention and transformation processes (An et al. 2010, Wang et al. 2012, An et al.2016). Among these processes, sorption of pollutants on the soil complex may play an important role (An et al. 2012, Zhao et al. 2015a). When released into the environment, sorption of TBBPA on soil may retard its migration to surrounding soil, vegetation and stream (Li et al. 2011, Sun et al. 2008a). Soil is a complex porous media containing water mineral particles, water and organic matter (Western et al. 2002). TBBPA can be absorbed on minerals in the soil such as aluminum, magnesium and calcium (Han et al. 2013, Sun et al. 2008b). The binding between TBBPA and soil organic matter exists through a specific mechanism (Zou et al. 2007). Some inorganic fertilizer ions in the soil environment, especially ammonium and phosphorus in nature N and P cycle, can also affect the behavior of TBBPA through precipitation or co-precipitation (Potvin et al. 2012). Although these findings are encouraging, the knowledge about the transport and distribution of TBBPA coupled with complex land composition and contaminant interaction is still limited.

Biochars are carbon-rich materials which can be obtained by pyrolyzing biomass at a given temperature (Kołtowski et al. 2017, Li et al. 2017). Biochars derived from natural events such as grasslands and forest fires are present in soil around the world. A large amount of synthetic biochars are also used as soil amendments to improve soil fertility and sequester carbon in pedosphere (Novak et al. 2009). Recently, biochars are receiving increasing attention as a promising means of pollution control (An and Huang 2015, Wang et al. 2015). Compared with other carbon-related adsorbents (Jacquelin et al. 2016), biochars are considered as a cost-effective

alternative for immobilizing organic contaminants such as polycyclic aromatic hydrocarbons, polychlorinated biphenyls, pentachlorophenol, imidacloprid and atrazine (Cao et al. 2016). The surface of biochars contains various functional groups, among which oxygen containing functional groups are suitable for chemical reactions and surface adhesion (Vinh et al. 2014). Additionally, the hydrophobic surfaces of biochars may favor the adsorption of hydrophobic substances from water. It is expected that biochars have the potential for stabilizing TBBPA in the natural soil environment. To better understand the mobility of TBBPA, it is necessary to investigate the relevant behaviors of TBBPA in such process. However, the immobilization of TBBPA by biochars have not been studied. Little attention has been paid to the interaction of inorganic fertilizer ions in adsorption of TBBPA on biaochar.

In this study, therefore, the immobilization of TBBPA by pinecone-derived biochars at solid-liquid interface was studied. In detail, (1) pinecone biochars produced from different species and temperatures were characterized through synchrotron-assisted FTIR analysis; (2) the sorption of TBBPA on pinecone biochars were elucidated through isotherm models and the sorption mechanisms were explicated; (3) the effects of aqueous chemistry characteristics (pH, ionic strength, etc.) on TBBPA adsorption were explored; (4) particularly, the influences of inorganic fertilizer ions (NH_4^+, PO_4^{3-}, and NO_3^-) on the immobilization of TBBPA by pinecone biochars were revealed through fractional-factorial assisted analysis. The results have important implications for risk assessment of brominated flame retardants in the environment.

3.2 Materials and Methods

3.2.1 Chemicals

TBBPA (4,40-isopropylidenebis(2,6-dibromophenol)) was purchased from Sigma-Aldrich (MO, USA) with a purity greater than 97% and its chemical structure is shown in Figure 3.1. TBBPA stock solution was prepared by dissolving the TBBPA powder in methanol. High-performance liquid chromatography (HPLC) grade methanol was obtained from VWR (Ontario, Canada). High-purity water used in all experiments was prepared by processing deionized water through a Milli-Q system. All other chemicals were of analytical grade or higher.

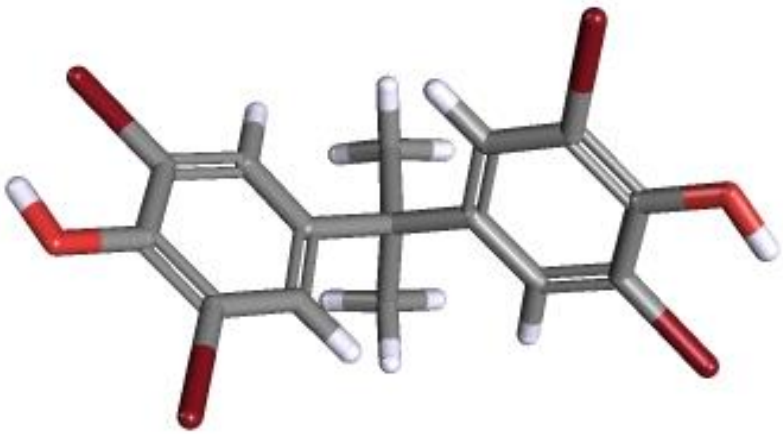

Figure 3.1 Chemical structure of Tetrabromobisphenol A

3.2.2 Biochar Preparation

Pinecones were collected from the western yellow pine (Pinus. ponderosa) and Scots pine (Pinus sylvestris L.) located in the campus of University of Regina, Canada. Biochars were prepared by charring two different pinecones under anaerobic conditions at certain temperatures. The procedure of preparing the biochars is in accordance with standard method. Briefly, the collected pinecones were separated and washed with deionized water to remove the impurities, and air-dried for 2 days before being oven-dried at 110 °C for 24 h. After drying, the biomass samples were grounded and passed through a 425 μm standard seive. The fine pinecone powder was tightly packed into a ceramic pot and covered with aluminum foil, followed by pyrolysis at different temperatures (300, 400, 500 and 600 °C) for 4 h in an oxygen-limited environment within muffle furnace. The heating rate was controlled at 5 °C /min for slow pyrolysis. The pinecone biochars were cooled at room temperature, washed with 1 M HCl for 6 h, centrifuged to remove the supernatant, and washed by distilled water to neutral pH. Then, the samples were oven-dried 24 h at 85 °C. Biochars produced at 300, 400, 500, and 600 °C from Western yellow pine were labeled as BCYP300, BCYP400, BCYP500 and BCYP600, respectively. Those produced from Scot pine at 300, 400, 500 and 600 °C were labeled respectively as BCBP300, BCBP400, BCBP500 and BCBP600.

3.2.3 Adsorption Studies

Batch adsorption experiments were carried out in 20-mL volumetric glass vial, capped with aluminum foil. Appropriate amount of biochars (10 mg) and TBBPA at certain concentration were added to each vial. To investigate the effects of different biochar sources and pyrolysis temperatures on TBBPA adsorption, 10 mg of BCYP and BCBP were added into each glass vial with a certain initial TBBPA concentration. To investigate the effects of pH, different amounts of 0.1 M NaOH and HCl were added into each glass vial with initial TBBPA concentration ranging from 0.5 to 2 mg/L. Sorption experiments for TBBPA conducted for all application rates of biochars. The TBBPA stock solution was prepared in methanol and then diluted by the background solution containing 0.01 mol/L $CaCl_2$ and 200 mg/L NaN_3 to simulate a constant ionic strength in environmental water and inhibit microbial activity, respectively. It should be noted that methanol concentrations (methanol/water, v/v) were controlled at less than 0.1% to avoid co-solvent effects. The initial concentrations (0.5–2.0 mg/L) were determined to cover the range between detection limit and aqueous solubility. Experiments were conducted in 20 mL glass vials at certain temperature. Blank controls (i.e., without sorbents) were run concurrently to investigate sorption to the walls of the glassware. The experiments were also conducted in the dark to prevent photolysis. To investigate the effects of ionic strength, different concentrations of NaCl were prepared by adding appropriate NaCl to TBBPA solution. The interactive effects of inorganic fertilizer ions and pH values on the adsorption of TBBPA by biochars were analyzed by a 25-1 fractional factorial design. The vials containing biochars and TBBPA solution were put into the temperature-controlled shaker at 200 rpm and 20 ± 1 °C for 24 hours to reach adsorption equilibrium. Preliminary experiments showed that 24 hours were enough for reaching equilibrium in adsorption process. Then the aqueous samples were taken

from vials and the concentration of TBBPA was measured after filtration.

3.2.4 Analytical Methods

Synchrotron based FTIR analysis (Figure 3.2) were carried out at the 01B1-01 (MidIR) beamline at the Canadian Light Source (Saskatoon, Canada). The Bruker Vertex 70v interferometer with a liquid nitrogen cooled mercury cadmium telluride (MCT) detector was used to analyze samples using synchrotron infrared light. The high-brilliant synchrotron radiation can achieve an adequate signal-to-noise ratio even using small apertures. Spectrum were measured with 512 co-added scans. Background spectra was taken for every sample to compensate for atmospheric and synchrotron ring current changes. Raw spectra were processed using 9-point smoothing with baseline correction (Shen et al. 2017, Wang et al. 2017b, Xin et al. 2017, Zhang et al. 2017). An Agilent Infinity 1260 high-performance liquid chromatography system (USA) equipped with a ZORBAX XDB-C18 column and a diode array detector (DAD) operated at a wavelength of 210 nm was used to measure the concentration of TBBPA. A mobile phase consisting of methonal/water (85:15, v/v) was used at a flow rate of 0.7 mL/min. SEM images were collected for the selected samples (BCYP300, BCYP 600, BCBP300 and BCBP 600) using a Zeiss Supra 55 VP SEM (Germany) with an accelerating voltage of 5.00 kV. The specific surface area of biochar was determined at 77 K with a TriStar II 3020 (Micromeritics, USA).

Figure 3.2 FTIR end station at Canadian Light Source

(http://midir.lightsource.ca/user-guide/infrared-microscopic-imaging/)

3.2.5 Data Analysis and Quality Assurance

The data from Synchrotron based FTIR were collected and analyzed using the OPUS 7.2 software (Bruker, USA). The data were analyzed through nonlinear regression using SigmaPlot software (Systat Software Inc., USA). Statistical analyses were undertaken through one-way ANOVA and least significant difference (LSD) analysis for comparisons of treatment means with $p < 0.05$. The fractional-factorial design was conducted using Design Expert 8.0.1 (Stat-Ease Inc., USA). All batch experiments were conducted in triplicate and average values were reported (relative standard deviation less than 5%). The quality assurance/quality control program was followed to ensure the accuracy and reliability of the collected data. The adsorption capacity of Q_t and the percentage removal were calculated using the following Equation (1) and equation (2) respectively.

$$Q_t = \frac{(C_i - C_e)V/1000}{W} \qquad (3\text{-}1)$$

$$\%\ \text{removal} = \frac{C_i - C_e}{C_i} \times 100 \qquad (3\text{-}2)$$

where Q_t is the adsorption capacity in mg g^{-1} at time t, C_i and C_e are the initial and equilibrium concentration in mg L^{-1}, V is the volume of solution mL and W is the total amount of adsorbent (g).

The quality assurance program was followed to ensure the accuracy and reliability of the collected data. All batch experiments were conducted in triplicate and average values were reported (relative standard deviation less than 5%). Blank tests were run

and corrections were applied if necessary. All containers used in this study has been previously cleaned with the particular washing liquid for laboratory purposes, triply rinsed with distilled water and oven dried. Experimental runs have been performed by using a TBBPA containing solution without addition of biochars. The corresponding results confirmed that the initial TBBPA concentration remained unchanged during the experiment. It indicated that the reduction of TBBPA concentration in experiments was only related to the adsorption on biochar samples.

3.3 Results and Discussion

3.3.1 Elemental Analysis and SEM Characterization of Pinecone-Derived Biochars

Due to the differences in lignin, cellulose and hemicelluloses content in pinecones, biochars produced from those biomasses had different chemical compositions and varied surface properties. The different formation of biochars pyrolyzed from the pinecone of yellow pine and scot pine could be preliminary analyzed according to their different physical and chemical properties. The elemental analysis results are shown in Table 3.1. The results showed that the oxygen contents of BCYP biochars decreased from 39.80% to 18.34% as pyrolysis temperature changed from 300 to 600 °C. On the surface of BCBP biochars, the relative high contents of oxygen were appeared on the surface of BCBP400 (42.08%) and BCBP600 (39.10%) and relative low oxygen contents were on BCBP300 (20.54%) and BCBP500 (20.25%). In addition, BCYP300 had a high H/C ratio (0.09) and the low O/C ratios appeared in biochars produced at high pyrolysis temperatures, such as BCYP500 (0.29),

BCYP600 (0.23) and BCBP500 (0.27). In general, the result of elemental analysis showed that the elemental characteristics of biochar varied with different pinecone sources and pyrolysis temperatures.

Adsorption of hydrophobic organic contaminants on biochars is mainly a surface phenomenon, which is related to surface characteristics (Peng et al. 2016). The SEM photomicrographs of biochar surfaces are shown in Figure 3.3. It showed the biochar surface was featured by porous structure. There are significant differences in the SEM images obtained from pinecone biochars produced at 300 and 600 °C. The surface of biochars produced at low temperatures had a relative smoother and less porous structure when compared with the biochar surface pyrolyzed at high temperatures. Moreover, the biochars produced at high pyrolysis temperatures had massive groove-like valleys across the compact mass and large visible pores with non-uniform distribution. Instead, the biochars produced at low pyrolysis temperatures exhibited layer-based smooth surface with random broken pores.

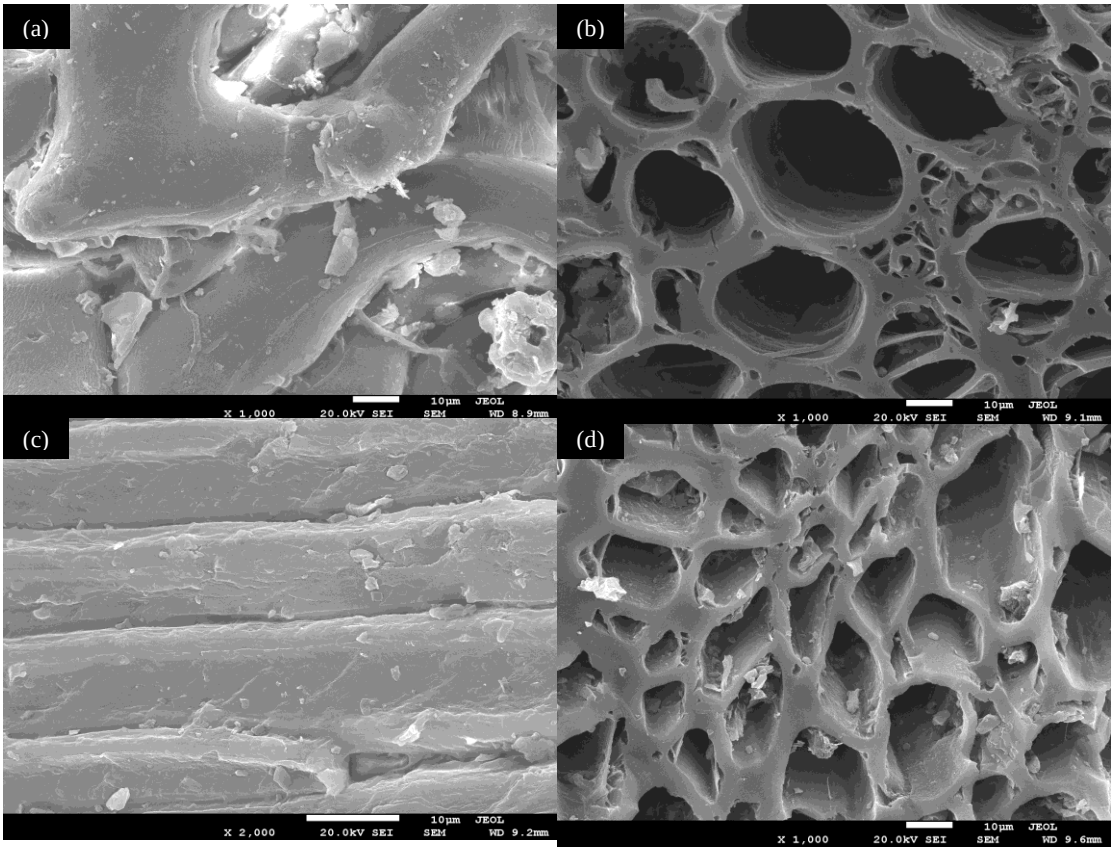

Figure 3.3 The SEM images of (a) BCYP300 (b) BCYP600 (c) BCBP300 and (d) BCBP600

Table 3.1 Characteristics of BCYP and BCBP biochars

Biomass	Pyrolysis Temperature (°C)	N_{ad} (%)	C_{ad} (%)	H (%)	$S_{t, ad}$ (%)	O (%)	H/C	O/C	Ash (%)
Scot pine cones	300	0.44	76.56	2.24	0.22	20.54	0.03	0.27	56.5
	400	0.49	54.64	2.59	0.20	42.08	0.05	0.77	61.3
	500	0.82	75.60	3.10	0.23	20.25	0.04	0.27	66.8
	600	0.43	58.34	1.94	0.19	39.10	0.03	0.67	71.2
Yellow pine cones	300	0.94	54.24	4.80	0.22	39.80	0.09	0.73	58.4
	400	1.00	69.46	3.16	0.20	26.18	0.05	0.38	61.2
	500	0.97	74.86	2.52	0.17	21.48	0.03	0.29	67.1
	600	0.92	78.44	2.12	0.18	18.34	0.03	0.23	68.5

3.3.2 Synchrotron-Based FTIR Analysis of Pinecone Biochars

With the IR light 100–1000 times brighter than a conventional thermal source, synchrotron light source has a great advantage of obtaining results with high resolution. Fine molecular features within the vibrational spectrum can be revealed through such synchrotron-assisted measurement. In complex biomass-derived samples, overlapping IR spectral bands of some functional groups are often observed. Therefore, second derivative analysis was used to better separate overlapping peaks and display remarkably sharp lines by yielding excellent signal-to-noise ratios. The synchrotron-based FTIR second-derivative spectra of BCYP and BCBP related to four pyrolysis temperatures are shown in Figure 3.4.

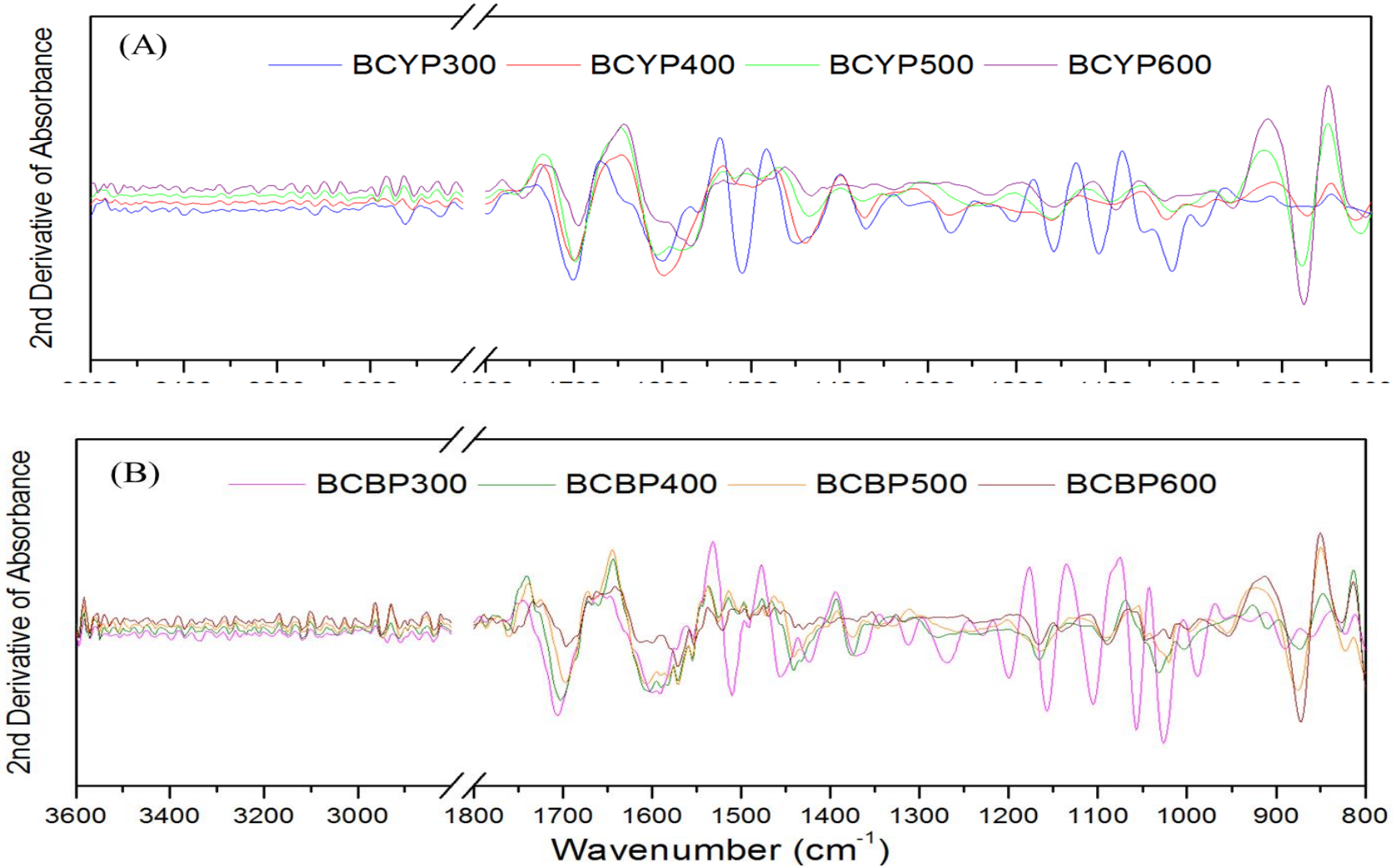

Figure 3.4: Second derivative FTIR spectra (3600–2600 cm^{-1}) and mid-infrared region (1800–800 cm^{-1}) of (A) BCYP and (B) BCBP biochars produced at various temperatures

Many peaks related to oxygen-contained functional groups and aromatic-related structure were found. Compared with biochars produced at low pyrolysis temperature, at high temperature, some peaks of saturated bond in hydroxy groups disappeared or shifted and new peaks of unsaturated bond in carbonyl groups were also detected. The transformation of pinecones to biochars at different pyrolysis temperatures can be regarded as an aromatization process. For both BCYP and BCBP, dissociable carboxyl and hydroxyl groups along with aromatic structure in uncarbonized biopolymer mainly exist at 300 and 400 °C. At 500 and 600 °C, more stabilized carboxyl and hydroxyl groups were observed.

Different patterns exist associated with different pinecone sources. For BCYP produced at 400, 500 and 600 °C, their main spectrum characteristics are similar. In the range of 1800–800 cm^{-1}, however, different band intensities at 880 cm^{-1} (C=C), 1275 cm^{-1} (carboxylic acid), 1425 cm^{-1} (C–O stretching), 1600 cm^{-1} (C=O stretching) and 1720 cm^{-1} (carbonyl) were observed. It suggests the carboxyl and aromatic contents in biochars changed from 400 to 600 °C. Compared with BCYP at 300 °C, stronger intensities for multiple bands in 1200–1000 cm^{-1} indicate the pyrolysis of polysaccharides structure above 400 °C (Shang et al. 2014). The band at 1520 cm^{-1} diminished above 300 °C might be attributed to the pyrolysis of non-conjugated nitro (Özhan et al. 2014). For BCYP changed from 300 to 600 °C, there are shifts in 1640 and 1425 cm^{-1}, suggesting the gradual pyrolysis of carboxylates and relevant change from carboxyl to alkenyl-ester structure. Furthermore, at 1600 cm^{-1}, the intensity increased from 300 to 400 °C, then decreased in 500 °C. The peaks shifted t from 1600 cm^{-1} at 300 °C to 1580 cm^{-1} at 600 °C. Similar shift from 1700 cm^{-1} to 1680 cm^{-1} also existed as temperature changed from 300 to 600 °C. The results show the

surface of BCYP are characterized by a large amount of acid functional groups at 300 °C, which can be transformed into ester and carbonized aromatic structures at higher temperature. Large amount of carboxyl and hydroxyl groups existed in BCYP produced at 300 °C. They were pyrolyzed into carboxyl and carbonyl groups at 400 °C, followed by the further transformation into alkenyl-ester content at 500 °C. When the temperature reached 600 °C, the aromatic carbonyl structure was formed.

Some different trends are observed in the spectrum results for BCBP. In the range of 1200–960 cm^{-1}, strong vibrations of C–O bending and stretching in ether and carbonate exist. Phenol O–H vibration at 3350 cm^{-1} indicates the presence of polysaccharides at 300 °C, which can be pyrolyzed into ether above 400 °C. The disappearance of peaks at 1320 cm^{-1} above 300 °C might suggest the pyrolysis of conjugated aromatic nitro group. The peak decrease at 1450 and 1425 cm^{-1} as well as the increase at 1435 cm^{-1} may be due to the transformation from carbonyl and aliphatics to carbonates from 300 to 500 °C and further formation of aromatic structure at 600 °C. Thus, BCBP is featured by various polysaccharides, graphene sheets and conjugated structures on its surface at low temperature, which can be transformed into unsaturated aliphatics and aromatic structures at higher temperature.

3.3.3 Adsorption of TBBPA at Biochar-Water Interface

Investigation into equilibrium adsorption curves can help understand the adsorption process (An et al. 2011, Wang et al. 2014, Zhao et al. 2015b). In this study, the adsorbed amount of TBBPA on biochars showed an increasing trend as the equilibrium TBBPA concentration in solution increased (Figure 3.5). The isotherm

results at different pyrolysis temperatures are significantly different ($P < 0.05$). Visual inspection results indicate pronounced nonlinearity in all isotherms. Langmuir and Freundlich adsorption isotherm models were therefore used to describe the data in this study (An et al. 2016b). Isotherm data were fitted to Langmuir model: $C_e / Q_e = C_e / Q_m + 1/(K_L Q_m)$, where Q_e is the amount of sorbate adsorbed per unit mass of adsorbent (mg/g), C_e is the concentration of sorbate in equilibrium solution (mg/L), Q_m is the adsorption capacity (mg/g), and K_L is the Langmuir adsorption constant (L/mg) and Freundlich model: $Q_e = K_f C_e^{1/n}$, where K_f is the Freundlich adsorption coefficient [(mg/kg)/(mg/L)^n] which provides an index of adsorption capacity, and n is the Freundlich exponent that describes isotherm nonlinearity.

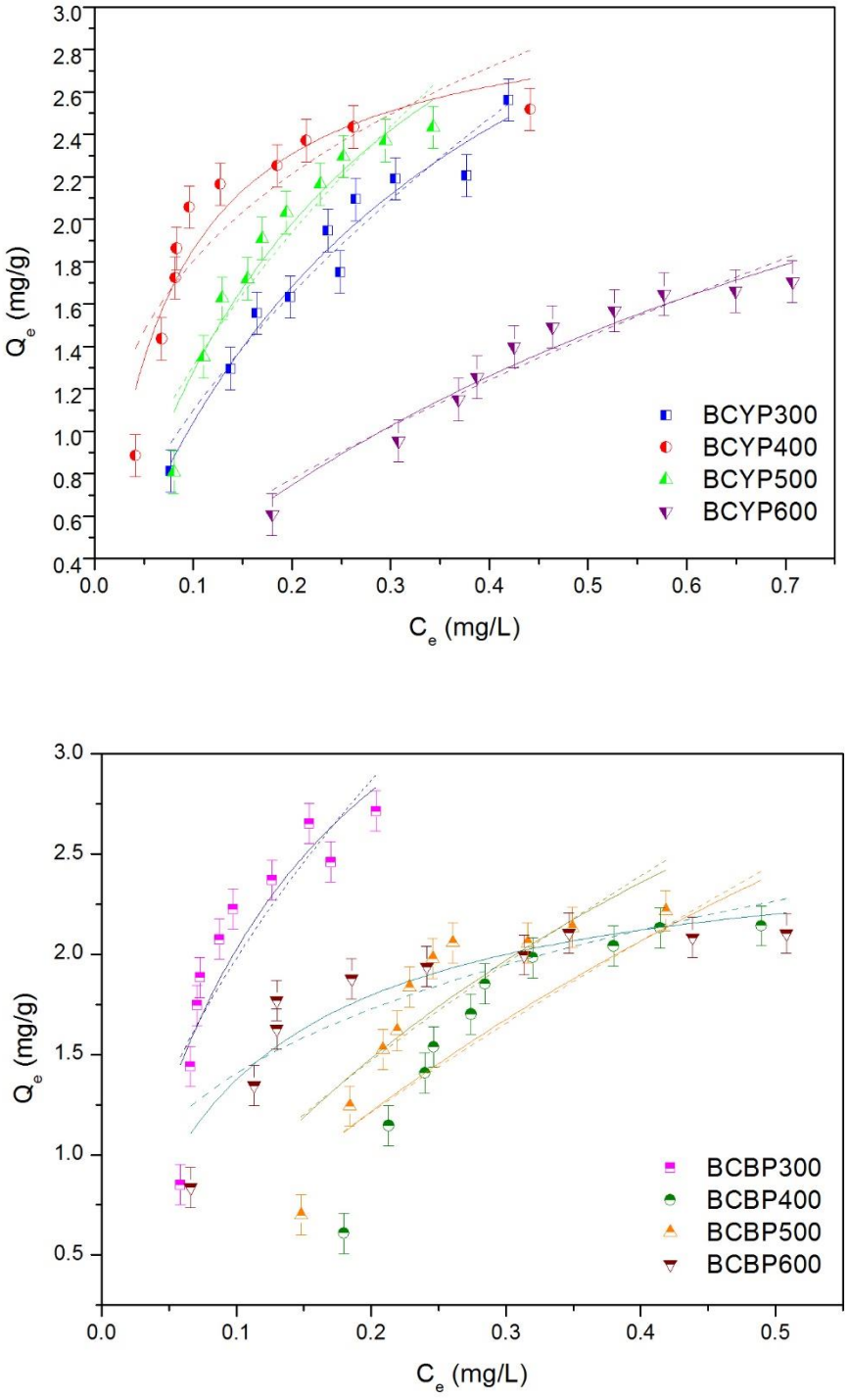

Figure 3.5 Sorption isotherms of TBBPA on (A) BCBP and (B) BCYP biochars (biochar = 10 mg, pH=7; the solid line represents non-linear curve fitting by Langmiur model the dotted lines represents non-linear curve fitting by Freundlich model.)

Table 3.2: Calculated Langmuir and Freundlich coefficient of TBBPA adsorption.

Biochar	Langmuir					Freundlich			
	q_m(mg/g)	K_L(mg/g)	R_L	r^2	RMSE	n	K_F(L/mg)	r^2	RMSE
BCYP300	4.32	3.18	0.14	0.96	0.10	1.72	4.20	0.94	0.11
BCYP400	3.03	15.80	0.03	0.90	0.15	3.45	3.55	0.75	0.23
BCYP500	4.31	4.23	0.11	0.93	0.11	1.79	4.78	0.88	0.15
BCYP600	3.91	1.92	0.21	0.95	0.07	1.08	2.30	0.93	0.09
BCBP300	4.56	8.00	0.06	0.78	0.24	1.92	6.70	0.74	0.27
BCBP400	6.78	1.09	0.31	0.77	0.21	1.32	4.16	0.74	0.23
BCBP500	5,68	1.76	0.22	0.73	0.22	1.45	4.51	0.71	0.23
BCBP600	2.57	11.70	0.04	0.86	0.13	3.54	2.77	0.74	0.19

The calculated parameters based on experimental data with the aid of regression analysis are given in Table 3.2. The results show that both of these two isotherm models could fit the data for TBBPA adsorption on pinecone-derived biochars. Compared with Freundlich adsorption model, Langmuir model can better represent the equilibrium data with higher correlation coefficients and lower root mean squared error (RMSE), indicating the involvement of homogeneous material adsorption in these processes. Similar results were also found in the adsorption of Arsenic(III), octadecane, octadecanoic acid and p-nitrophenol on biochars using the Langmuir isotherm model (Vinh et al. 2014, Wang et al. 2017a). BCYP and BCBP show satisfied adsorption capacity when compared with the some adsorbents such as multiwalled carbon nanotubes and MIEX resin (Fasfous et al. 2010).

There are higher values of Q_m for BCYP produced at 300 and 500 °C, while the higher values of Q_m for BCBP are related to 400 and 500 °C. The adsorption of TBBPA on biochars produced at different temperatures involved electrostatic attraction, hydrophobic interaction and microporous retention. Due to the presence of hydroxyl and amino groups as well as aromatic structures, TBBPA exhibits affinities to both polar and hydrophobic surface sites (Yu et al. 2015, Zhang et al. 2013). There are more polar dissociable acid groups and minerals in biochars produced at low pyrolysis temperature than those at high pyrolysis temperature. The relatively high carbon content would make biochar surface hydrophobic. It may affect the porosity development and chemical characteristics of the surface in small pores, which could be active for physical adsorption of TBBPA (Nielsen et al. 2015).

BCYP shows better fitting performance than BCBP, suggesting there are different

behaviors for adsorption of TBBPA on BCYP and BCBP biochars. There might be different mechanisms between adsorption of TBBPA on BCYP and BCBP, which could be attributed to their different surface properties. The surface of BCYP biochars had large amount of acid functional groups at 300 °C where the adsorption of TBBPA was relatively low. These functional groups can be transformed to carboxylic and carbonyl structure at 400 °C, followed by the transformation to oxide structure at 500 °C where the TBBPA adsorption was relatively higher. The low adsorption capacity was obtained for BCYP at 600 °C, with low aromatic structure and high nitro content. As for BCBP, the high polysaccharides and aliphatic content on the surface of biohcars at 300 °C resulted in relative high adsorption of TBBPA. When pyrolysis temperature increased from 400 to 600 °C, aromatic oxide graphene structure in BCBP was formed and the amount of adsorbed TBBPA exhibited increasing trend, indicating that unsaturated oxygen-containing structure of biochar could favor TBBPA adsorption.

3.3.4 pH-Dependent Adsorption of TBBPA on Biochars

pH often plays an important role in adsorption processes (An and Huang 2012, Li et al. 2012). This is especially true for the adsorption of TBBPA on biochars. As a hydrophobic and ionic organic compound, TBBPA can exist in solution as three forms including $TBBPA^0$, $TBBPA^-$ and $TBBPA^{2-}$ (Figure 3.6), with pKa values of 7.5 and 8.5 for the latter two forms, respectively (Fasfous et al. 2010). The species of TBBPA are influenced by pH and their initial concentrations. The net charge of surface functional group of biochars can also change at different pH levels.

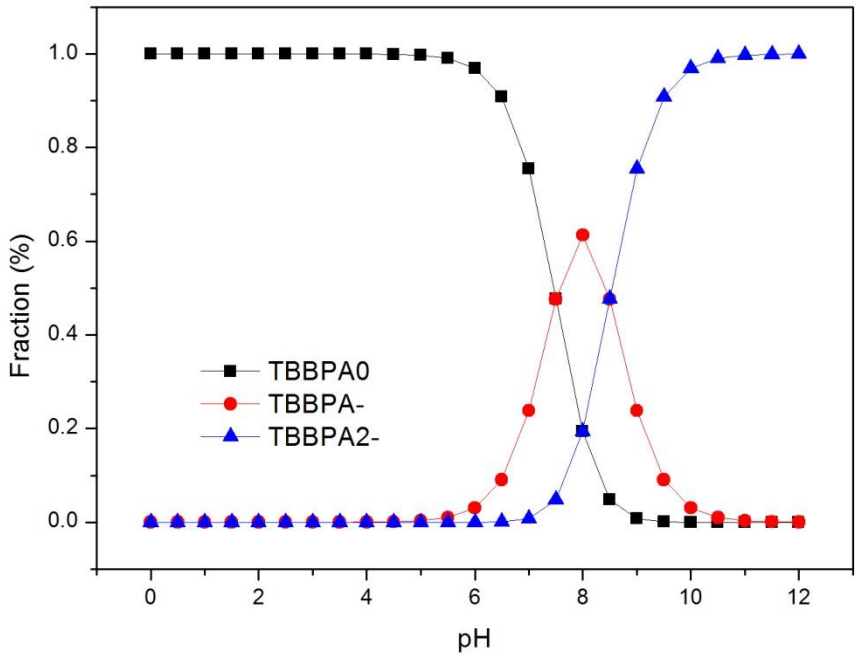

Figure 3.6 Species distribution of TBBPA as a function of pH

The adsorption of TBBPA on BCBP and BCYP is highly depended on solution pH and TBBPA concentration (Figure 3.7 and Figure 3.8). The maximum distribution coefficients (K_d) on biochars were observed in series with near neutral pH of 6–7. The enhanced TBBPA adsorption at high pH could be attributed to the decreasing presence of H^+ ions in solution. These ions could compete with TBBPA in adsorption (Ji et al. 2012). With decreased H^+ ions remained on surface, biochars had less competed ions and more available surface sites, which facilitated the adsorption of TBBPA.

With the decrease of pH, the surface acid functional groups resulted in enhanced surface acidity. It is favorable for the π^+-π electron donor-acceptor (EDA) interactions between the electrons of aromatic ring and surface, leading to an increase of adsorpqtion capacity (Teixidó et al. 2011). It was obvious that the adsorption on high-temperature biochars (BCYP600, BCBP600 and BCBP500) had relatively higher TBBPA removal in low concentration and decreased with increasing initial concentration at varied pH. The distribution coefficient (K_d) of high- temperature biochars at pH 4 was higher than low-temperature biochars. It suggested that hydrophobic effects and H^+ played an important role in such adsorption process. On the contrast, the decrease of adsorption on high-temperature biochars such as BCYP600 and BCBP600, might be due to the decrease of active functional groups and hydrophobic interaction between TBBPA molecular and aromatized biochar surface. It indicated that the effects of H^+ and hydrophobic interactions on the adsorption of molecular TBBPA are positive. The system "overcame" the competition between H^+ and TBBPA to high energy sites on biochars, and π^+-π EDA interactions was assumed to be involved in the adsorption (Teixidó et al. 2011). For

BCBP600 with high K_d in low concentration, it did not express higher adsorption in acid region as BCYP biochars. Hydrophobic interaction might be predominated with limited π^+-π EDA interaction involved. On the other hand, in the low pH range, plenty of stable molecular TBBPA existed and the water-solid phase energy increased , which could somehow weaken adsorption (Fasfous et al. 2010). It is also interesting to find there is a different trend for the adsorption of TBBPA on high-temperature biochars including BCYP600 and BCBP600 in the pH range 4–7. It could be explained by less active functional groups on such biochars.

For both low- and high-temperature biochars, the adsorption of TBBPA declined above pH 7. Due to the abundance of oxide functional groups, high pH could result in the repulsion between the negatively charged surfaces of biochars and TBBPA ions (Shao et al. 2010, Zhang et al. 2013). In such situation, the major interaction between biochars and TBBPA could be π–π bonding between TBBPA and the hexagonal skeleton structure, as well asand the H-bonding between hydroxyl and amino groups (Chin et al. 2007). Thus, high-temperature biochars favored π^+-π EDA and hydrophobic-hydrophobic interaction in acid region. Hydrophobic interaction dominated neutral and alkali conditions. However, given to the weaker adsoption of TBBPA on BCYP600 and BCBP600, π^+-π EDA interaction might not be the major factor to govern such process. Less adsorption of TBBPA on low-temperature biochars in acid region and alkali region revealed that the decrease of adsorption was due to the electrostatic repulsion. The adsorption on low-temperature biochars in neutral pH region was dominated by both electrostatic attraction and hydrophobic interactions.

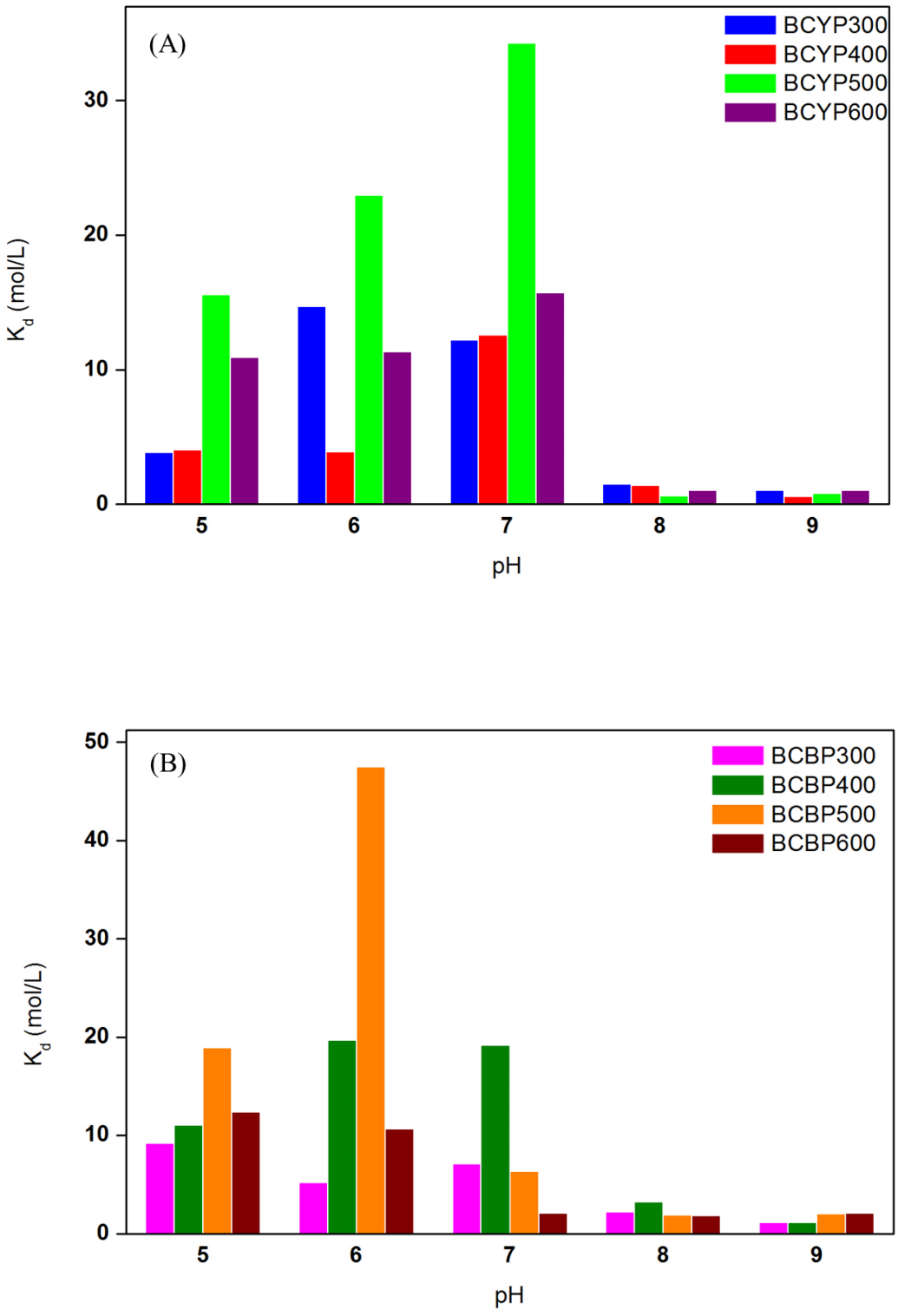

Figure 3.7 Effect of pH on distribution coefficient of TBBPA on (A) BCYP and (B) BCBP

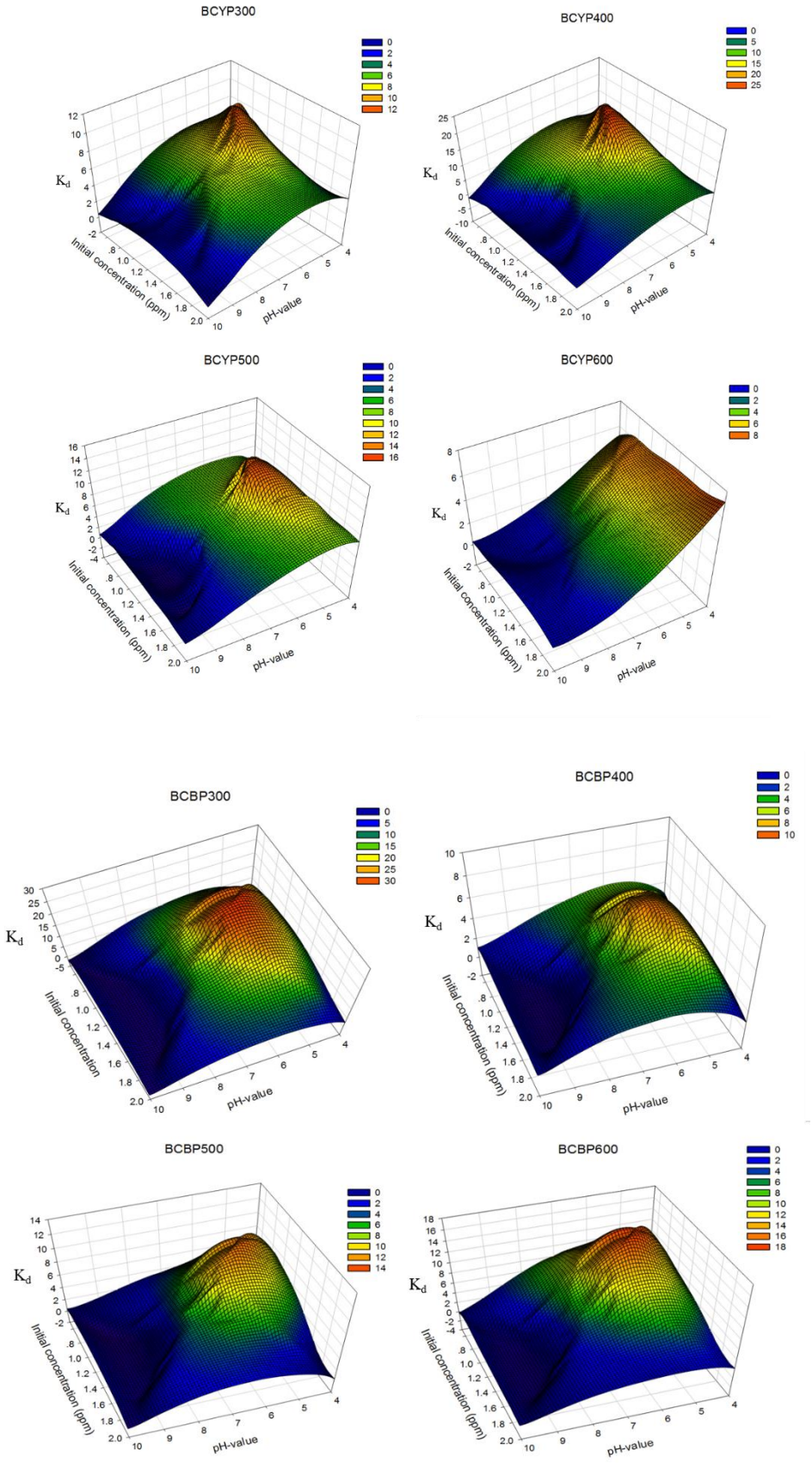

Figure 3.8 Influence of pH and concentration on distribution coefficient (K_d)

Figure 3.8 also showed the adsorption of TBBPA on biochars was influenced by initial TBBPA concentrations. With initial concentration of 1.0 to 1.4 mg/L, there was more adsorption of TBBPA than those with higher initial TBBPA concentrations in given pH range. With the initial TBBPA concentrations ranging from 0.5 to 1 mg/L, there was significant differences for the adsorption results relate to BCBP300, BCBP500 and BCBP600. As initial TBBPA concentration changed within that range, BCYP300, BCYP400, BCYP500, BCYP600 and BCBP400 showed less significant differences in adsorption. Such different performances influenced by initial TBBPA concentration might be attributed to the differences in adsorption mechanisms, biochars sources and production conditions. The adsorption of TBBPA on biochars is a concentration-pH driven process. Since pH could influence the fraction of TBBPA and the corresponding concentration, the concentration-pH adsorption might be further regarded as the TBBPA concentration-related process.

3.3.5 Factorial Analysis of Inorganic Fertilizer Ions Influencing the Adsorption Process

In the natural environment, inorganic fertilizer ions such as NH_4^+, NO_3^- and PO_4^{3-} play a major role in plant uptake, phosphorus cycle and nitrogen cycle. Such ions also widely exist in the leachate process in soils and fertilizers. When TBBPA enters the environment through a wide variety of sources the behavior of TBBPA can be influenced. Additionally, the presence of PO_4^{3-} and NH_4^+ may also result in the alteration of pH condition, which is relevant to the adsorption of TBBPA on biochars as discussed above. Therefore, it is necessary to understand the nature of TBBPA adsorption influenced by inorganic fertilizer ions. Environmental modeling has been

used extensively in data analysis (Ben-Awuah et al. 2015, Forsythe et al. 2015, Fu et al. 2015, Li et al. 2009, Qin et al. 2007, Xiao et al. 2015). In the present study, in the purpose of identifying behaviors of variable factors by applying effective analysis method, a 2^{5-1} fractional factorial-assisted analysis was used to determine the significant effects and interactions of pH, pyrolysis temperature, and concentrations of NH_4^+, PO_4^{3-} and NO_3^- (Table 3.3) where factors of pH (A), pyrolysis temperature (B), concentration of NH_4^+ (C), concentration of PO_4^{3-} (D) and concentration of NO_3^- (E) were considered independent variables. Figure 3.9 depicts the half-normal plot of standardized effects which can help determine the significant factors for the adsorption of TBBPA on biochars. It showed factors of A, B, C, D, E, AC, AD, AE, BD, BE, CD and DE in adsorption on BCYP as well as factors of A, C, AD and D on BCBP were considered significant. Figure 3.10 illustrates the interactions of main factors with low and high levels.

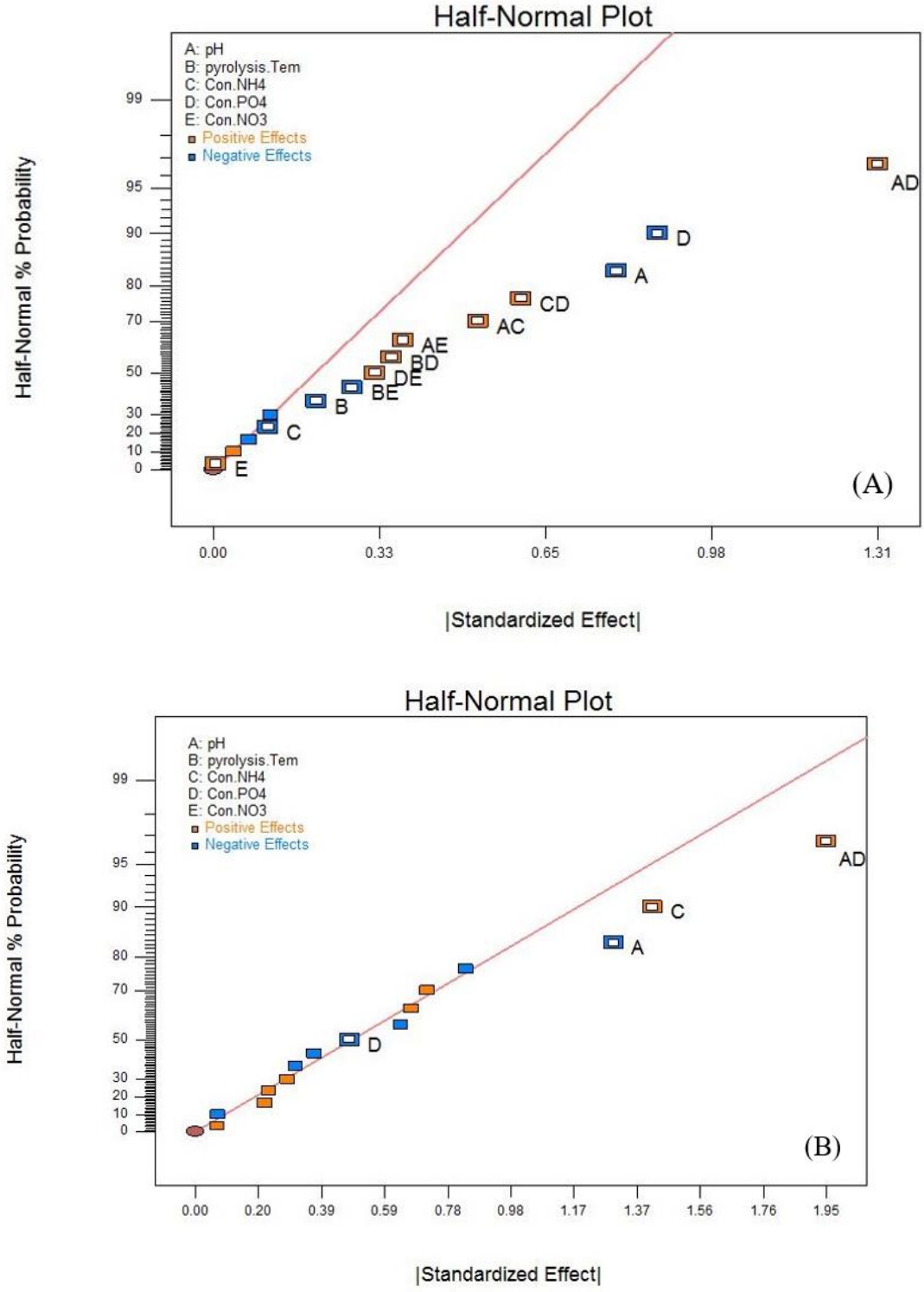

Figure 3.9 Half-Normal test for (a) BCYP and (b) BCBP

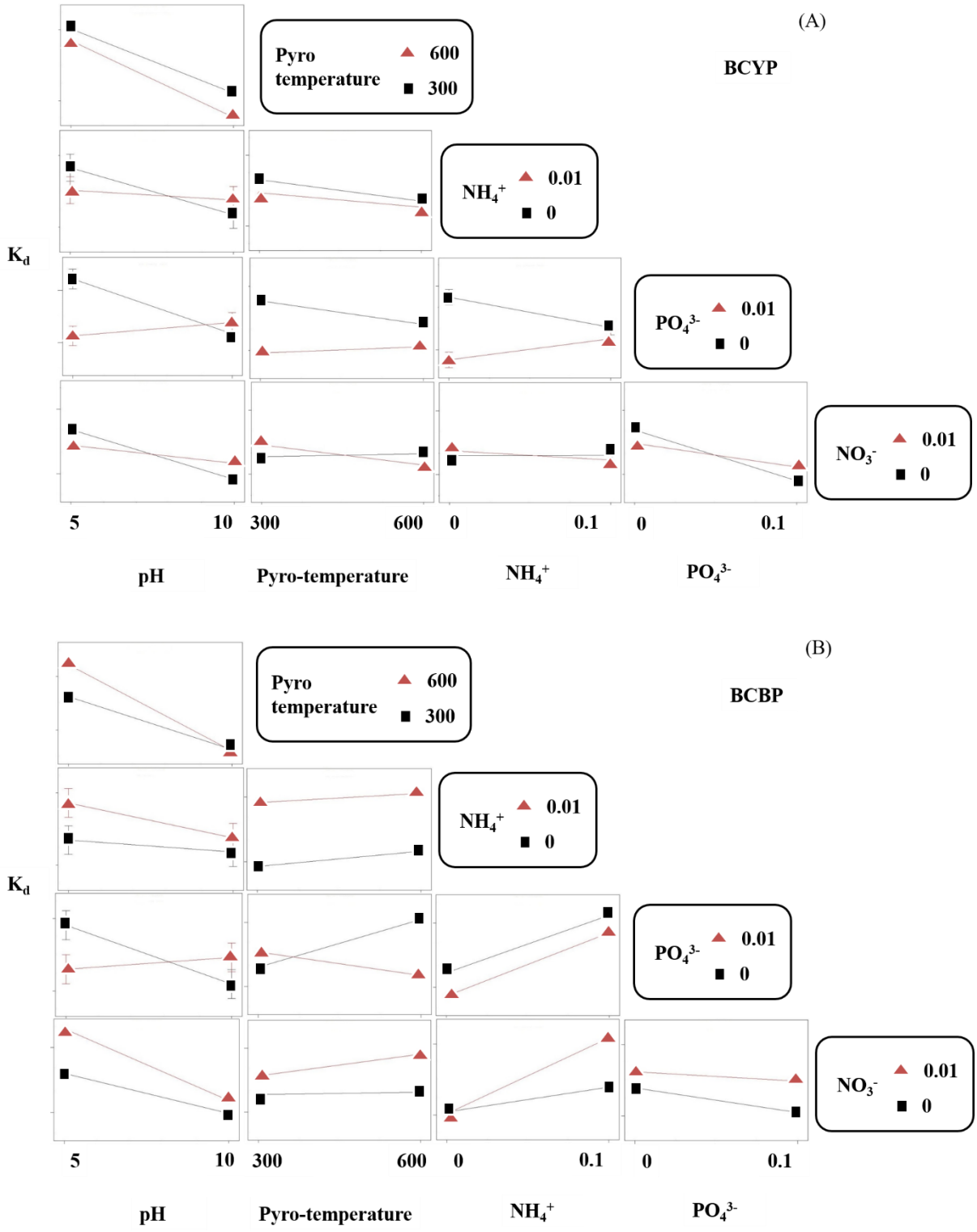

Figure 3.10 Interactive Effects of Inorganic Fertilizer Ions for adsorption of TBBPA on (A) BCYP and (B) BCBP biochars

Table 3.3 Independent factors and their levels in 2^{5-1} fractional factorial design.

Factors	Low level (-1)	High level (+1)
(A) pH of the solution	5	10
(B) Pyrolysis temperature (℃)	300	600
(C) Concentration of NH_4 (M)	0	0.01
(D) Concentration of PO_4 (M)	0	0.01
(E) Concentration of NO_3 (M)	0	0.01

Table 3.4 Results of fractional factorial analysis for BCBP

Source	Sum of Squares	df	Mean Square	F Value	p-value Prob > F	
Model	30.88	4.00	7.72	8.54	0.0022	significant
A-pH	6.71	1.00	6.71	7.42	0.0198	
C-Con.NH4	8.01	1.00	8.01	8.86	0.0126	
D-Con.PO4	0.91	1.00	0.91	1.01	0.3366	
AD	15.25	1.00	15.25	16.88	0.0017	
Residual	9.94	11.00	0.90			
Cor Total	40.82	15.00				
R-Squared	0.76		Adj R-Squared	0.67		
Pred R-Squared	0.48					

Table 3.5 Results of fractional factorial analysis for BCYP

Source	Sum of Squares	df	Mean Square	F Value	p-value Prob > F	
Model	16.87	12.00	1.41	55.04	0.0035	significant
A-pH	2.51	1.00	2.51	98.36	0.0022	
B-pyrolysis.Tem	0.16	1.00	0.16	6.42	0.0851	
C-Con.NH4	0.05	1.00	0.05	1.81	0.2712	
D-Con.PO4	3.05	1.00	3.05	119.22	0.0016	
E-Con.NO3	0.00	1.00	0.00	0.00	0.9540	
AC	1.08	1.00	1.08	42.35	0.0074	
AD	6.81	1.00	6.81	266.71	0.0005	
AE	0.555025	1	0.555025	21.73018	0.0186	
BD	0.49	1.00	0.49	19.18	0.0220	
BE	0.30	1.00	0.30	11.63	0.0421	
CD	1.46	1.00	1.46	57.32	0.0048	
DE	0.403225	1	0.403225	15.78695	0.0285	
Residual	0.076625	3	0.025541667			
Cor Total	16.9473	15				
R-Squared	0.99		Adj R-Squared	0.97		
Pred R-Squared	0.87					

As shown in Figure 3.10 and Figure 3.11, pH (A), pyrolysis temperature (B), concentration of NH_4^+ (C), concentration of PO_4^{3-} (D) and concentration of NO_3^- (E) were important factors in the adsorption of TBBPA on BCYP biochars and interactions of AC, AD, AE, BD, BE, CD, DE also showed important effects in adsorption (Table 3.6 and Table 3.7). In comparison, factors of pH (A), (C) concentration of NH_4^+, (D) concentration of PO_4^{3-} and AD interactions also played important roles in the adsorption of TBBPA on BCBP biochars. Their interactions and corresponding coefficients are shown in Table 3.6 and Table 3.7 The results indicated the adsorption behavior TBBPA could be significantly influenced by these factors and their interactions.

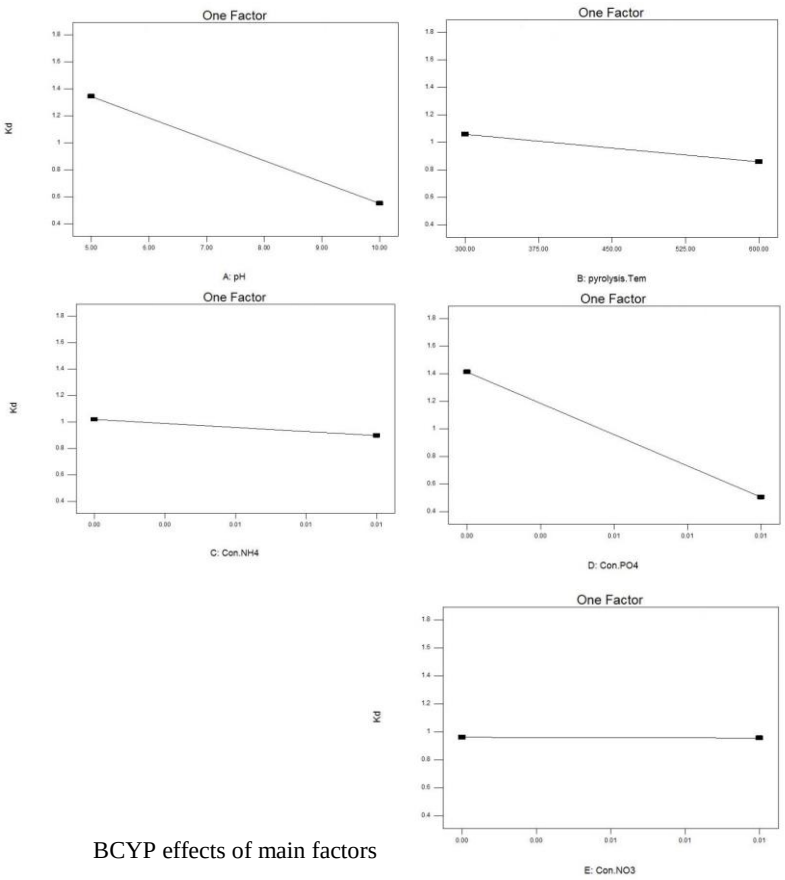

BCYP effects of main factors

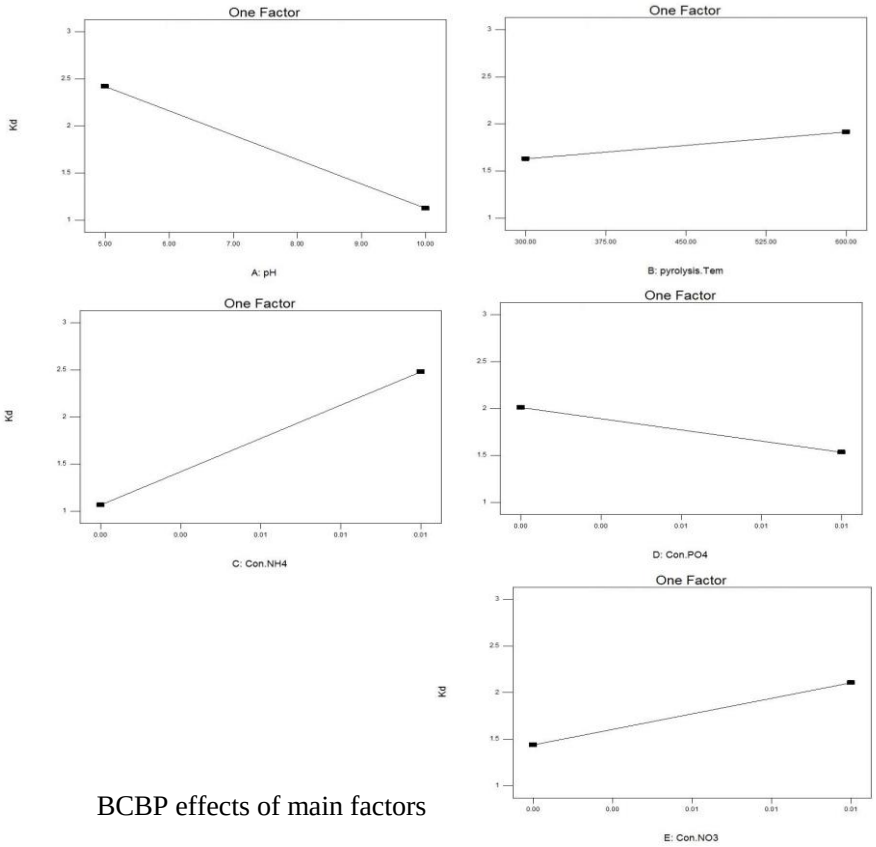

BCBP effects of main factors

Figure 3.11 Main factors for BCYP and BCBP

Table 3.6 Design matrix of 2^{5-1} fractional factorial design and corresponding responses for BCBP

Experiment	A	B	C	D	E	K_d
1	-1	1	1	-1	1	6.19
2	-1	1	1	1	-1	1.01
3	-1	-1	1	1	1	3.29
4	1	1	1	-1	-1	0.6
5	-1	1	-1	1	1	0.44
6	1	1	-1	1	-1	1.03
7	1	1	1	1	1	2.55
8	1	-1	-1	1	1	1.62
9	-1	-1	-1	1	-1	0.08
10	1	-1	1	1	-1	2.25
11	-1	-1	-1	-1	1	1.83
12	-1	-1	1	-1	-1	3.29
13	1	-1	1	-1	1	0.66
14	1	1	-1	-1	1	0.27
15	-1	1	-1	-1	-1	3.23
16	1	-1	-1	-1	-1	0.02

Table 3.7 Design matrix of 2^{5-1} fractional factorial design and corresponding responses for BCYP

Experiment	A	B	C	D	E	K_d
1	-1	1	1	-1	1	1.06
2	-1	1	1	1	-1	0.59
3	-1	-1	1	1	1	0.17
4	1	1	1	-1	-1	0.11
5	-1	1	-1	1	1	0.25
6	1	1	-1	1	-1	0.01
7	1	1	1	1	1	1.49
8	1	-1	-1	1	1	0.78
9	-1	-1	-1	1	-1	0.01
10	1	-1	1	1	-1	0.79
11	-1	-1	-1	-1	1	3.16
12	-1	-1	1	-1	-1	2.3
13	1	-1	1	-1	1	0.64
14	1	1	-1	-1	1	0.05
15	-1	1	-1	-1	-1	3.21
16	1	-1	-1	-1	-1	0.54

Effect of NH_4^+

It is known biochar may affect soil nitrogen transformations and is capable to taking up ammonia (Novak et al. 2009). NH_4^+ had significant positive effects (p = 0.013) for TBBPA adsorption on BCBP biochars and insignificant negative effects (p = 0.271) for that on BCYP biochars. The positive effects on TBBPA adsorption could be explained by the increase of electrostatic attraction as well as the increase of ionic strength. It was found the increase of NaCl concentration could result in increasing adsorption of TBBPA on low temperature BCYP and BCBP biochars as well as decreasing adsorption on high temperature BCYP and BCBP biochars (Figure 3.12). Along with the insignificant effects of NO_3^- factor (p =0.95) which ion strength took major part in adsorption, these results suggested that the role of ionic strength effects in NH_4^+ ions in the adsorption had limited positive effects. The significance of NH_4^+ might be due to the hydrophobic and electrostatic interaction between biochar surface and TBBPA. The acid functional groups existed on biochar surface as cation exchange sites. The negative effects on BCYP biochars could be related to the confliction between positive effects of ion strength interaction and negative effects of electrostatic repulsion. NH_4^+ ions favored TBBPA adsorption on aromatic-rich biochar surface.

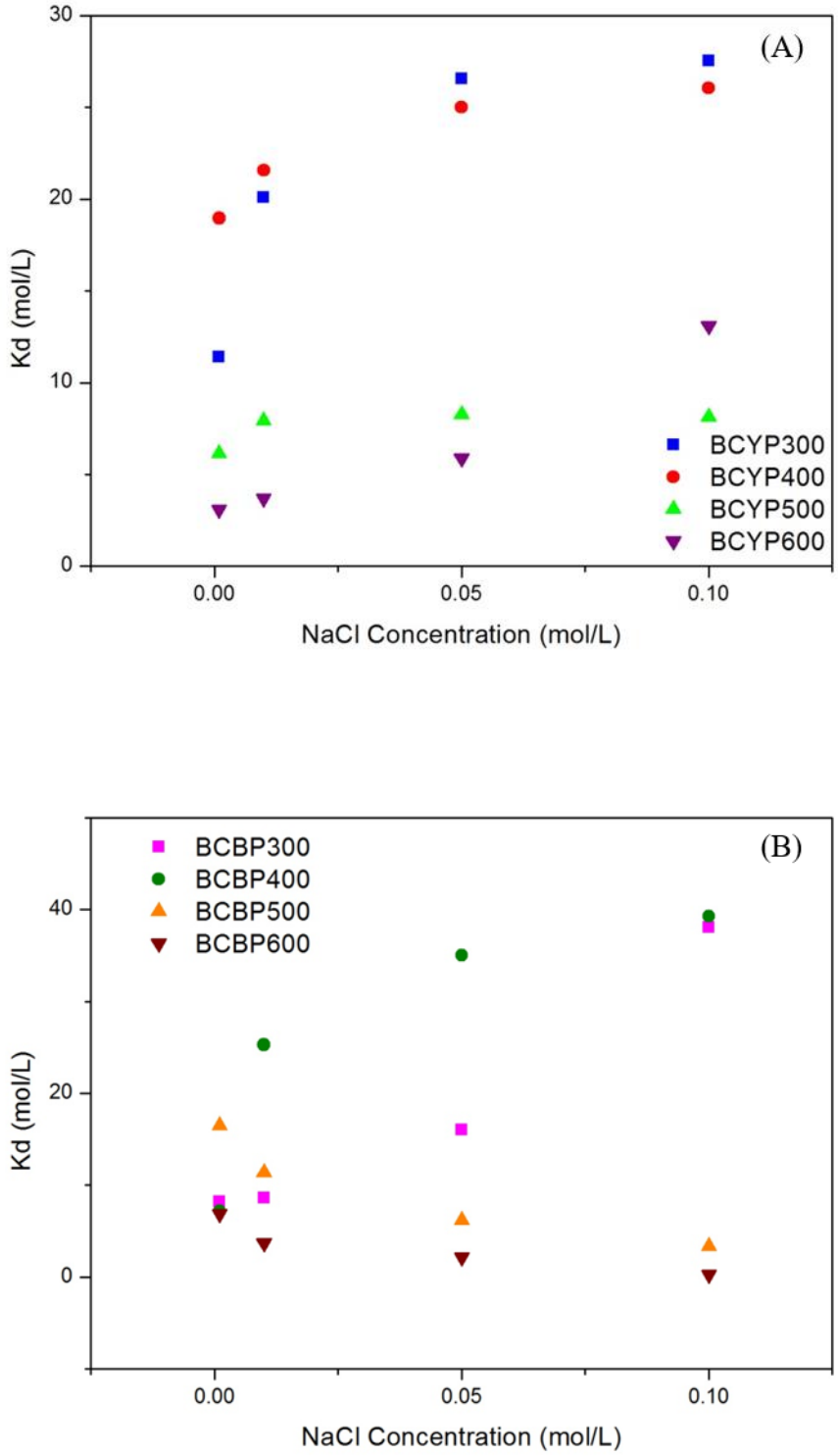

Figure 3.12 Effect of NaCl concentration for adsorption of TBBPA on (A) BCYP and (B) BCBP

Moreover, the two pinecone-derived biochars exhibited different adsorption characteristics of TBBPA in the presence of NH_4^+ ions. The adsorption on BCBP biochars decreased with the increase of pH (from K_d = 4.34 to K_d = 1.10), while the corresponding adsorption amounts were still higher than those without NH_4^+ ions (K_d = 2.92 in low pH to K_d = 0.02 in high pH). These results indicated that the electrostatic attraction on hydrophobic surface of BCBP biochars had positive effects on adsorption. In addition, NH_4^+ ions were able to bind with biochar surface via electrostatic exchange and hydrogen bond in alkali region where ionic TBBPA dominated in the solution (Wang et al. 2016). The adsorption on BCYP biochars exhibited the competition effect of cations, causing stronger negative effects on adsorption than positive effects of ion strength and hydrogen bond. Therefore, the effects of NH_4^+ ions, instead of improving electrostatic attraction on aromatic-rich surface, could cause electrostatic repulsion or competition on acid functional group-rich surface. It indicated NH_4^+ ions might have π–π bonding with aromatic structures on biochar surface, which would enhance electrostatic attraction on the surface. On the other hand, the competition of cationic and ionic strength effects varied for different pine cone-derived biochars as a result of different hydrophobicity and functional group characteristics on biochar surface. Such different effects on adsorption were related to the surface cation exchange capacity and hydrophobicity of biochars.

Effect of PO_4^{3-}

The effects of PO_4^{3-} on TBBPA adsorption were important, as PO_4^{3-} molecules can exchange compounds. PO_4^{3-} ions inhibited the adsorption of TBBPA. Such

inhibitive effect was significant for the adsorption on BCYP biochars ($p = 0.002$) and insignificant for that on BCBP biochars ($p = 0.337$). With the different forms of PO_4^{3-} and TBBPA at varied pH, the interactions of AD were significantly positive ($p < 0.001$). PO_4^{3-} showed inhibitive effects on TBBPA adsorption at low pH (K_d = 0.26 with PO_4^{3-} to K_d = 2.43 without PO_4^{3-}), which is similar with the pattern at low pH in the absence of PO_4^{3-}. When pH was higher than 8, the existence of PO_4^{3-} would facilitate adsorption (K_d = 1.16 with PO_4^{3-} to K_d = 0.02 without PO_4^{3-}). At low pH, $H_2PO_4^-$ and HPO_4^{2-} were the dominant forms in solution. The electrostatic interaction between biochars and TBBPA could be dramatically influenced by PO_4^{3-} ions. Since the surface hydrophobic and functional groups of two pine cone-derived biochars are different, the similarity of adsorption decrease for different biochar types may be attributed to the direct interactions between $H_2PO_4^-/HPO_4^{2-}$ ions and biochars surface. It could result in a competition between TBBPA and $H_2PO_4^-/HPO_4^{2-}$ ions (de Rozari et al. 2016, Gul and Whalen 2016).

On the other hand, when pH was higher than 8, PO_4^{3-} was the major species (Cui et al. 2016) and ionic TBBPA form dominated in solution. The interaction between PO_4^{3-} ions and biochar surface became less significant in alkali region. The presence of PO_4^{3-} ions could inhibit the acid functional groups on biochar surface and enhance ionic strength in solution, resulting in an increase of TBBPA adsorption on biochars. However, due to the higher amount of acid functional groups on BCYP biochars, the strong negative effect of PO_4^{3-} on functional groups lead to the decrease of hydrogen bond and the increase of electrostatic repulsion between TBBPA and BCYP biochars. PO_4^{3-} ions could bind with functional groups on biochar surface, which compete with TBBPA for adsorption sites on biochars. This

would compromise the adsorption of TBBPA in the presence of PO_4^{3-} when compared with that in the absence of PO_4^{3-}.

Effect of NO_3^-

As the insignificant main factor in the adsorption on both BCYP and BCBP, NO_3^- had little effect on biochar surface and TBBPA. The adsorption of TBBPA was slightly affected by NO_3^-. This might be related to the characteristics of NO_3^- which has limited ability to form chemical bonds with other substances under general conditions. In the presence of NO_3^-, the slightly positive effects on TBBPA adsorption might be the result of ionic strength change which could improve hydrophobic interaction.

Interactive effects of inorganic fertilizer ions

The interactions among inorganic fertilizer ions played an important role in the adsorption of TBBPA on biochars. As for the insignificance of BC interaction, the adsorption on biochars produced at different pyrolysis temperatures had insignificant changes with varied NH_4^+ concentrations. It suggested the biochar sources played more important role in determining surface properties such as the amount of cation exchange sites and hydrophobicity than pyrolysis temperature. The interactions of BD ($p = 0.022$) showed that the presence of PO_4^{3-} ions favored TBBPA adsorption by BCYP with pyrolysis temperature of 600 °C and BCBP with pyrolysis temperature of 300 °C. Compared with the positive effects of BC, where the adsorption of TBBPA increased with the increase of NH_4^+ concentration and pyrolysis temperature, the

effects of BD showed the adsorption was influenced via the interactions with PO_4^{3-} ions and pyrolysis temperatures. It indicated there were interactions with biochar surface properties which changed by biochar pyrolysis temperatures and PO_4^{3-} ions. The highly hydrophobic surface of BCBP produced at 300 °C transformed into oxygenated aromatic structures and ash contents at 600 °C. More cation exchange sites existed in BCYP produced in the range of 300 to 600 °C. The acid functional groups might decrease hydrophobic interactions between TBBPA and biochar surface. Therefore, hydrophobic interactions might play the major role in TBBPA adsorption.

The interaction of CD ($p = 0.005$) and DE ($p = 0.02$) showed the influence of NH_4^+ and NO_3^- ions. In the presence of PO_4^{3-} and NH_4^+ ions, the TBBPA adsorption on BCYP and BCBP was inhibited, while the co-existence of PO_4^{3-} and NO_3^- ions could improve adsorption. However, the effects on biochars derived from different pine cone sources were not exactly same. The interaction of PO_4^{3-} and NH_4^+ ions, as the significant factors for TBBPA adsorption on BCYP, exhibited an intersecting trend from low to high level of NH_4^+ ions, indicating interaction between ions among surface cation exchange sites of biochars. As for BCBP, the graph showed two approximately parallel lines, indicating there was no interaction between the effects of PO_4^{3-} and NH_4^+. The interaction of DE indicated NO_3^- ions could act as "stabilizer", which counteracted the negative effects of PO_4^{3-} ions in the adsorption of TBBPA on biochars. With the addition of PO_4^{3-} ions, K_d changed from 1.97 to 0.12. However, with the involvement of NO_3^- ions, K_d changed from 1.63 to 0.41. When compared the interactions of NO_3^- and PO_4^{3-} ions for BCYP and BCBP, NO_3^- ions caused more negative effects for BCYP. It suggested that the presence of

fertilizer anions had negative influences on cation exchange capacity of BCYP, resulting in the decreasing adsorption of TBBPA. The interactions of AE showed the different effects on BCYP and BCBP bicoahrs. The non-parallel lines of the NO_3^- ions for BCYP and BCBP biochars indicated the different situations occurred at low pH level, suggesting electrostatic interactions were involved. The interaction of BE showed varied adsorption on biochars produced at different pyrolysis temperatures. It might be due to the differences in hydrophobicity and functional groups on biochar surface.

More than two factors involved interactions could provide more information to TBBPA adsorption. The reverse trend for the interactions of BD with NO_3^- ions was found. When PO_4^{3-} was involved, K_d changed from 0.02 to 0.32 without NO_3^- and shifted from 0.47 to 0.35 with NO_3^- as pyrolysis temperature increased. It indicated the change of TBBPA adsorption could be related to the change of acid group content on biochar surface. In addition to the effects of ionic strength, NO_3^- ions could improve the adsorption of TBBPA on the biochar surface enriched by acid groups. DE interaction exhibited a "stabilizer" effects which offset both negative and positive influences of PO_4^{3-} ions and these effects could be improved via the involvement of NH_4^+ ions. With the presence of NH_4^+ and NO_3^- ions, K_d changed from 0.89 to 0.88 after PO_4^{3-} being added. It indicated the decrease of adsorption via PO_4^{3-} ions could be due to the decrease of hydrophobic interaction and competition with TBBPA on biochars. NO_3^- and NH_4^+ ions increased ionic strength and interfered with the interactions between TBBPA and surface functional groups of biochars.

3.4 Conclusions

The study related to trace organic contaminant in the complex land system is an emerging area in environmental research. This is the first study to reveal the behaviors of TBBPA at the biochar-water interface as influence by environmental factors. The results indicated the TBBPA adsorption on pine cone-derived biochars were related to biochar characteristics. Hydrophobic interaction played a major role in the adsorption of TBBPA on biochars and electrostatic attraction could also improve the adsorption. The adsorption behaviors of TBBPA on biochars were significantly affected by pH and inorganic fertilizer ions. NH_4^+ ions had significant positive effects for the adsorption of TBBPA on biochars with aromatic-rich surface. Strong negative effects of PO_4^{3-} existed for TBBPA adsorption. The insignificant effects of NO_3^- was observed and NO_3^- could act as a "stabilizer" to offset the influences of other fertilizer ions. The overall influence of various factors on the adsorption of TBBPA could be an integration of multiple processes with interactions. The results of this study can help understand migration patterns of TBBPA and analyze the immobilization on biochars in the presence of inorganic fertilizer ions. It will have important implications for risk assessment and site remediation regarding overall environmental performance. Further studies are desired to define the fate and transport of TBBPA on biochars in combination with the other components and obtain more theoretical foundation for analyzing TBBPA mobility in the land system.

CHAPTER 4

KINETICS AND SURFACE FUNCTIONALITY IN THE REMOVAL OF TETRABROMOBISPHENOL A BY PINECONE-DERIVED BIOCHARS

4.1. Background

Attention has been recently drawn to the environmental behaviors of TBBPA, a widely used brominated flame retardant which accounts for 60% of total commercial market (Covaci et al. 2011, Widmer et al. 2005, Zhang et al. 2015). TBBPA is a relatively persistent organic pollutant which can be released into the environment through manufacturing, recycling, and disposal of various fabrics and materials. It posts potential threat to soil, water, atmosphere and living organisms (Geens et al. 2009, Labadie et al. 2010, Ni and Zeng 2013, Sellström and Jansson 1995). The exposure to TBBPA can induce a variety of adverse health effects including cytotoxicity, immunotoxicity and hepato-toxicity. TBBPA also has the potential to disrupt thyroid homeostasis and estrogen signaling (Hendriks and Westerink 2015, Nakajima et al. 2009). Moreover, the International Agency for Research on Cancer listed this flame retardant into group 2A (probably carcinogenic to humans). Human exposure to TBBPA on the environmental occurrence has become an important public issue (Abdallah 2016). Therefore, the efficient and environmental friendly technologies are desired for the removal of TBBPA from water.

Some treatment approaches such as chemical oxidation, photocatalytic degradation

and membrane filtration have been studied for the removal of TBBPA in the past decade(Potvin et al. 2012, Sun et al. 2008b, Tang et al. 2014b). Adsorption is an effective method, and has been used in the removal of a wide variety of pollutants (Wu et al. 2017). It is often featured with high efficiency and simple operation. Moreover, adsorption is a key process to influence transport, bioavailability and degradation of organic contaminants in the natural environment (Han et al. 2013). Some adsorbents such as carbon nanotubes and graphene oxide have been used for the removal of TBBPA (Tang et al. 2014b, Yang et al. 2013, Yu et al. 2015). There is also an increasing interest in biochar which is a cost-effective adsorbent. Charcoals can be produced through the pyrolysis of natural biomass. Charcoal surface has a large number of exchangeable cations and surface adsorption sites. It contains various function groups, especially oxygen containing function groups. Its adsorption performance can be improved by suitable chemical activation. In previous studies, Wu et al. (Wu et al. 2017) used the modified bamboo charcoal in the removal of hexavalent chromium. Karaer and Kaya (2016) reported the adsorption of methylene blue on biochar. Pingree et al. (2016) observed the high adsorption affinity to phenol using wildfire-produced charcoal from woody material. Pinecone biomass is widely available as a low-cost biomass from pine plantations, public park and residential backyard. Pinecone charcoals have a well-developed carbon structure with porous structure, which is favorable for the adsorption of contaminants (Benyoucef and Amrani 2011, Das et al. 2015). Hydrophobic sites can form on the surface of activated pinecone charcoals, which may also favor the adsorption of hydrophobic compounds (Keiluweit et al. 2010, Li et al. 2014, Teixidó et al. 2011). Therefore, there is a potential for using pinecone-derived biochar as an effective adsorbent for the removal of TBBPA from aqueous solution.

In general, some efforts have been made to investigate the adsorption of TBBPA on soil particles and modified adsorbents such as graphene nanotubes. However, there are few reports on the adsorption of TBBPA by biochars. No comprehensive observation has been undertaken to understand the effects of surface area and surface-element composition, as well as the roles of surface functional groups in TBBPA adsorption.

Based on the above reasoning, this study seeks to explore the interactions between TBBPA and activated-charcoal surface, as well as the corresponding effects of functionality and adsorption capacities. In detail, (i) the change of surface functional groups on biochars derived from different temperatures will be analyzed via synchrotron FTIR analysis; (ii) batch experiments will be conducted to investigate the distribution and kinetics for the adsorption of TBBPA on the surface of biochars; (iii) surface behaviors and their interactions with TBBPA concentrations will be revealed by correlating adsorption behaviors of TBBPA with compositions of surface on different biochars. This study can provide a feasible adsorbent for the removal of TBBPA from aqueous solution. Kinetics and surface functionality features will be discovered to better understand the process of TBBPA adsorption. Moreover, it is expected that the results can help to develop a sound treatment strategy for TBBPA and evaluate the mobility of TBBPA in the environment with charcoals produced from wildfire or other natural processes.

4.2. Materials and Methods

4.2.1 Chemicals

TBBPA (4,40-isopropylidenebis(2,6-dibromophenol)) was purchased from Aldrich Chemical Co. (WI, USA) with a purity greater than 97%. Methanol (HPLC grade) was obtained from VWR Scientific (AB, Canada). The standard solution was prepared by dissolving TBBPA into methanol for a concentration of 200 mg/L. All other chemicals used were of reagent grade quality or higher. High-purity water used in all experiments was prepared by processing deionized water through a Milli-Q system.

4.2.2 Preparation of Acid Biochars

Pinecones biomass were collected from the Scots pine (Pinus sylvestris L.) and Yellow pine (Pinus. ponderosa) in the south of Saskatchewan, Canada. The procedure of preparing the acid biochars was in accordance with standard method (Peng et al. 2016). Briefly, the collected pinecones were separated and washed with deionized water to remove impurities, and air-dried for 2 days before being oven-dried at 110 °C for 24 h. After drying, the biomass samples were grounded and passed through a 0.425 mm standard sieve. Fine pinecone powder was tightly packed into a ceramic pot and covered with aluminum foil. The powder was pyrolyzed for 4 h at different temperatures (400, 500, 600 °C) in muffle furnace under an oxygen-limited atmosphere. The heating rate was controlled at 5 °C /min. The obtained pinecone charcoals were cooled at room temperature and were washed with 1M HCl for 6 h for activation, centrifuged to remove the supernatant, and washed by pure water to

neutral pH. The samples were further oven-dried 24 h at 85 °C. The biochars produced at 400, 500 and 600 °C were labeled respectively as BCSP400, BCSP500 and BCSP600 from Scots pine, and BCYP400, BCYP500 and BCYP600 from Yellow pine. In addition, the biochars produced from Yellow pine were labeled as BCYPs as well as produced from Scot pine were labeled as BCSPs.

4.2.3 Characterization of Charcoal Adsorbents

Surface functional group on charcoal surface was analyzed by synchrotron FTIR analysis method. The high-brilliant synchrotron radiation can help obtain results with adequate signal-to-noise ratio even using small apertures (Xin et al. 2017). Synchrotron FTIR analysis were carried out at the 01B1-01 (MidIR) beamline of the Canadian Light Source (Saskatoon, Canada). The Bruker Vertex 70v interferometer with a liquid nitrogen cooled mercury cadmium telluride (MCT) detector was applied to analyze samples using synchrotron infrared light. To compensate for atmospheric and synchrotron ring current changes, background spectra was taken for each sample. Spectrum were measured with 512 co-added scans and the data were collected and analyzed using the OPUS 7.2 software (Bruker, USA). Raw spectra were processed using 12-point smoothing and baseline correction. The elemental composition (C, H and N) of different biochar sample was determined using an elemental analyzer (Elementar Analysensysteme GmbH, vario EL, Germany). The specific surface area and porosity were measured at 77 K with a TriStar II 3020 (Micromeritics, USA) using BET nitrogen gas sorption method. Images of the surface morphology of the selected samples were obtained by using a Zeiss Supra 55 VP SEM (Zeiss, Oberkochen, Germany) with an accelerating voltage of 5.00 kV. The surface

elemental compositions of biochars were determined on dry ash-free basis using a vario MACRO cube elemental analyzer (Elementar, Germany)

4.2.4 Adsorption Experiments

Batch adsorption experiments were conducted in 20-mL glass vials. Appropriate amounts of biochars, TBBPA stock solutions and pure water were added. Methanol concentrations (methanol/water, v/v) were controlled at less than 0.1% to avoid co-solvent effects. Blank controls without sorbents were performed with no addition of biochars. Vials were placed in a reciprocal shaker at 20 °C and 200 rpm for 24 hours to reach adsorption equilibrium. Preliminary experiments showed that 24 hours were enough for the adsorption process to reach equilibrium. In kinetics experiments, TBBPA concentrations were monitored at different time points. After adsorption, supernatant was taken out and analyzed by high-performance liquid chromatography (HPLC, Agilent 1260 Infinity, USA) equipped with ZORBAX Eclipse XDB-C18 column (5 μm particle size, 4.6 × 150 mm), thermostated column compartment (set to 30 °C), and diode array detector operated at wavelength of 210 nm. A mobile phase consisting of methanol/water (85:15, v/v) was used at a flow rate of 0.7 mL/min. The adsorption amounts and removal efficiency were calculated:

$$Q_t = \frac{(C_0 - C_i)V/1000}{W} \quad (4\text{-}1)$$

$$\%\ \text{removal} = \frac{C_0 - C_i}{C_0} \times 100 \quad (4\text{-}2)$$

where Q_t is the adsorption amount in mg/g at time t; C_0 and C_i in mg/L are the

initial concentration and concentration at time t; V is the volume of solution in mL and W is the total amount of adsorbent in g.

4.2.5 Quality Assurance and Quality Control

The quality assurance program was followed to ensure the accuracy and reliability of the collected data. All batch experiments were conducted in triplicate and average values were reported (relative standard deviation less than 5%). Blank tests were run and corrections were applied if necessary. All containers used in this study has been previously cleaned with the particular washing liquid for laboratory purposes, triply rinsed with distilled water and oven dried. Experimental runs have been performed by using a TBBPA containing solution without addition of biochars. The corresponding results confirmed that the initial TBBPA concentration remained unchanged during the experiment. It indicated that the reduction of TBBPA concentration in experiments was only related to the adsorption on biochars samples.

4.3. Results and Discussion

4.3.1 Surface Characterization of Pinecone-Derived Biochars

In order to explore the nature of adsorption process, the produced pinecone-derived biochars were characterized through some different approaches. Surface interaction and pore filling played a role in the adsorption of hydrophobic organic contaminants on carbon (Peng et al. 2016). SEM analysis of biochars were carried out to determine surface structure and porosity of biochars. Figure 4.1 shows the SEM images of pinecone-derived charcoals produced at different temperatures. Different features of surface morphology were observed for the charcoals derived from different sources and production temperatures. BCSP600 showed a compact structure with groove-like valleys on its top and large pores on its side. BCYP400 and BCSP400 had layered structure with indistinct pores distributed on the surface. BCYP600 had the structure where numerous visible pores distributed on the charcoal surface. As shown in Table 4.1, the surface area ranged from 0.9 to 10 m^2/g for the charcoals derived from two pinecone sources, while such difference was not significant for the charcoals from same pinecone source.

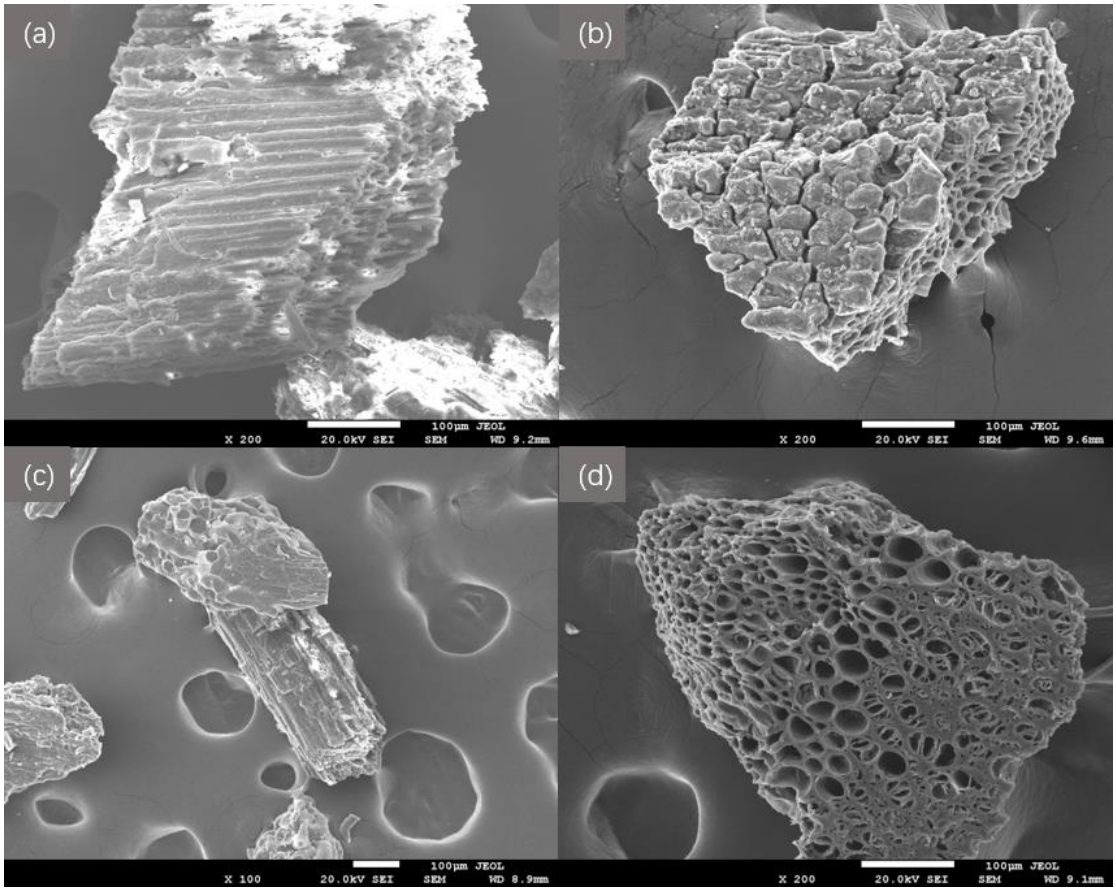

Figure 4.1 SEM images of (a) BCSP400 (b) BCSP600 (c) BCYP400 (d) BCYP600

Table 4.1 Elemental composition of biochars

	N_{ad} (%)	C_{ad} (%)	H (%)	O (%)	H/C	O/C	BET (m^2/g)
BCSP 400	0.49	54.64	2.59	42.08	0.05	0.77	2.40
BCSP 500	0.82	75.60	3.10	20.25	0.04	0.27	6.30
BCSP 600	0.43	58.34	1.94	39.10	0.03	0.67	10.21
BCYP 400	1.00	69.46	3.16	26.18	0.05	0.38	1.50
BCYP 500	0.97	74.86	2.52	21.48	0.03	0.29	7.40
BCYP 600	0.92	78.44	2.12	18.34	0.03	0.23	10.44

The results of elemental analysis showed that biochars were featured by high carbon content from 54.64% to 78.44% (Table 4.1). BCYP600 had the highest total carbon content of 78.44%, while BCYP500 and BCSP500 also had relatively high carbon contents of 74.86% and 75.60%, respectively. BCSP400 had the highest oxygen content (42.08%) and the least total carbon content (54.64%)., Hydrogen contents among these produced charcoals decreased in the order of: BCYP400 (3.16%) > BCSP500 (3.10%) > BCSP400 (2.59%) > BCYP500 (2.52%) > BCYP600 (2.12%) > BCSP600 (1.94%). A highest oxygen content was observed in BCSP400, indicating the existence of large quantity of oxygen or oxygen-content function groups. BCSP600 had both high content of oxygen (39.10%) and low content of hydrogen (1.94%). It could be due to the formation of combined oxygen-involved aromatic structure on charcoal surface at high pyrolysis temperature. Relative low content of total carbon and high content of oxygen in carbon adsorbents produced from agricultural wastes could also be related to the negative surface charge (Sewu et al.).

The aromaticity and polarity of charcoal surface were further evaluated via hydro-carbon ratio (H/C) and oxygen-carbon ratio (O/C), respectively. In general, H/C decreased with the increase of pyrolysis temperature. The lowest H/C of these biochars was 0.03 in BCYP600 and BCSP600, indicating their high aromaticity. The highest H/C of 0.05 was obtained in BCYP400 and BCSP400, suggesting their low aromaticity. At the same production temperature, BCYP400 and BCSP400 had the same H/C but different O/C The same aromaticity and different polarity suggested their different surface function groups and carbon structure. Similar characteristics were also observed in BCSP600 and BCYP600. However, due to their high

aromaticity, BCYP600 and BCSP600 might have less functional groups on surface and more aromatic structures.

BCYP600 had graphene-like aromatic sheet on the surface and BCSP600 had graphene-oxide-like aromatic surface containing more oxygen and negative charges. Such differences in surface polarity could contribute to their adsorption affinity and selectivity for apolar or polar molecules. In the natural aqueous environment, pH is usually less than pKa_1 = 7.5 of TBBPA, where most TBBPA compounds are in their molecular forms. BBPA is a polar compound. The increase in surface polarity and aromatic structure of biochar might favor the adsorption of TBBPA. Due to the interactions of functional groups and chemical properties of TBBPA, such influence of polarity and aromaticity to TBBPA adsorption could be complicated.

4.3.2 Insight from Synchrotron FTIR Analysis

To better understand the difference among biochars derived from different pyrolysis temperatures and sources, synchrotron FTIR analysis was performed and the corresponding spectra are shown in Figure 4.2. The high-intensity peaks at 1700 and 1600 cm^{-1}were associated with C=O stretching vibration. The vibration of C=C at 885 cm^{-1} were observed in most produced charcoals except BCSP400 and BCYP400. It suggested the carbon structure with oxygen-containing aromatic compounds on BCSP500, BCSP600, BCYP500 and BCYP600 (Shin et al. 1997, Siengchum et al. 2013). The band at 3390 cm^{-1} is corresponding to O—H vibration and the peaks at 1310~1250 cm^{-1} is indicative of acid —C—OH vibration (Cuba-Chiem et al. 2008). The results indicated acid functional groups were formed on the surface of BCYP400

and BCYP500. In addition, the strong band at 1440 and 1380 cm^{-1} can be attributed to bending vibration of O—H.C=O stretching vibration occurred at 1600 cm^{-1}, indicating the existence of carboxylate groups (—COOH). The wide absorption band arising at 1200 ~ 1000 cm^{-1} on BCSP500 and BCSP600 represented C—O and O—H vibration (Shin et al. 1997), which could be related to acid phenol groups rather than acid carboxylate groups. On BCYP600, BCSP400 and BCSP500, the peaks at 1200~1100 cm^{-1} could be related to C—O—C, indicating the presence of ether groups and ester groups including anhydride groups, aliphatic ethers and relatively low content of carboxylate groups (Sclavons et al. 2000, Sclavons et al. 2005, Yang et al. 2003).

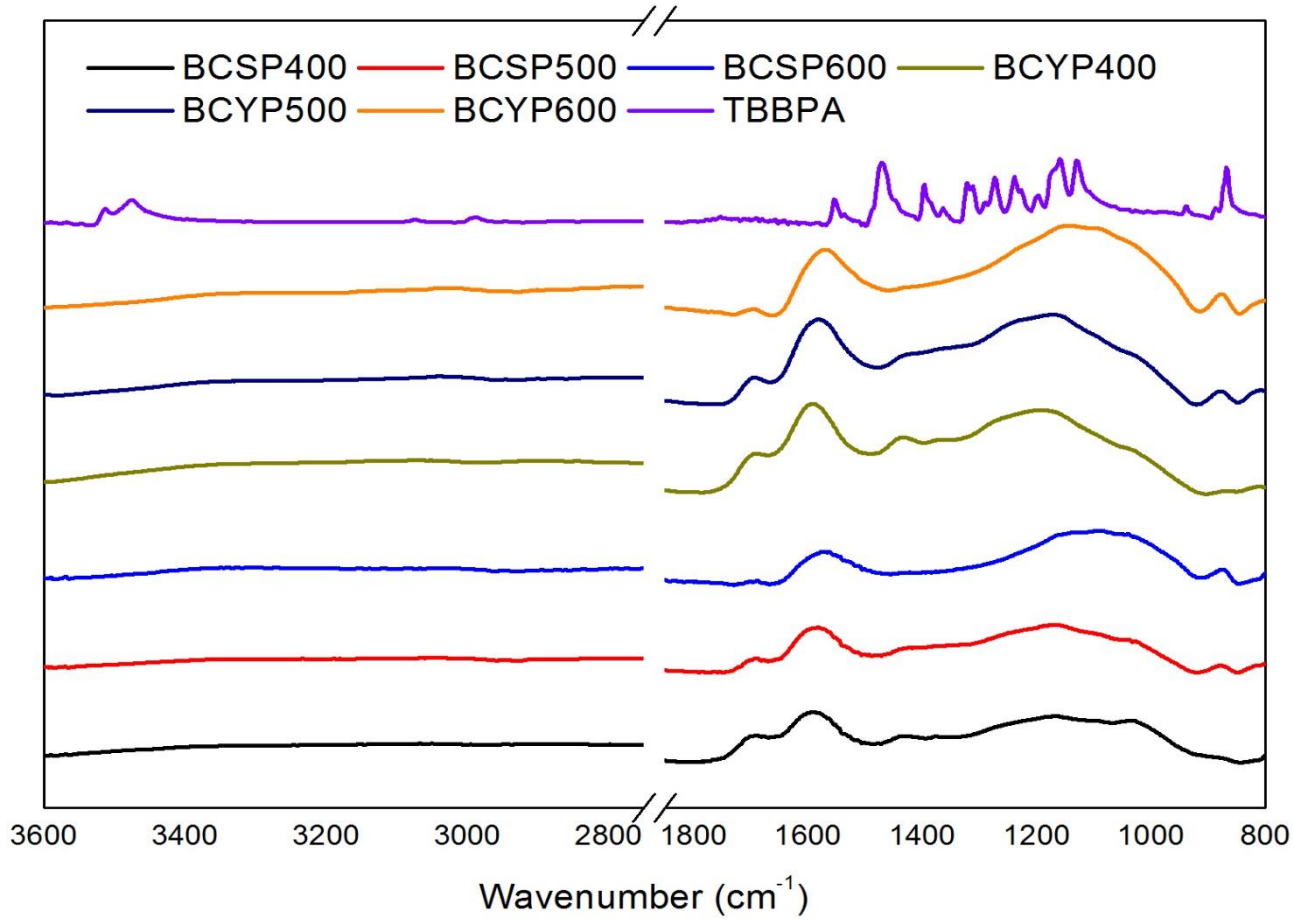

Figure 4.2 Synchrotron FTIR spectra of biochars BCSPs, BCYPs and TBBPA

The different function groups and structures on the charcoal surface contributed to the different adsorption mechanisms. As shown in Figure 4.3, high intensity peak in 1550 cm^{-1} and a series of serrated peaks from 1800 to 1300 cm^{-1} were observed in BCYP and BCBP after TBBPA adsorption. These bands are corresponding to those main functional groups in the chemical structure of pure TBBPA. This result indicated that TBBPA was successfully adsorbed on the surface of biochars. Different FTIR results were observed in TBBPA-BCYP and TBBPA-BCSP from different pyrolysis temperatures. It suggested different functional groups on charcoal surface were involved during the adsorption of TBBPA. The major spectrum change of strong doublet peaks of C—O vibration appeared at 1060 and 1040 cm^{-1} (Bhutto et al. 2003), which could be ascribed to hydrogen bonding between O—H groups (Zhang et al. 2013). Moreover, the decreasing peak intensity in 3000 ~ 2900 cm^{-1} of C—H stretching vibration (Figure 4.4) could be related to less ethyl and methyl groups on TBBPA-BCYP surface. In addition, TBBPA-BCSP400 showed similar changes with TBBPA-BCYPs, indicating a similar mechanism of TBBPA adsorption on the surface of BCSP400 and BCYP. However, TBBPA-BCSP500 and TBBPA-BCSP600 presented different spectrum changes compared with TBBPA-BCYP and TBBPA-BCSP400. Three sharp peaks of C—O stretching vibration appeared at 1060, 1040 and 1020 cm^{-1}, which could be due to hydrogen bonding and hydroxyl contents (Pandey 1999). Moreover, strong peaks in 2950~2850 cm^{-1} exhibited as a result from aliphatic CH_3 asymmetric and symmetric stretching vibration (Hossain et al. 2011). It could be attributed to the interaction between TBBPA and alkene chains on the surface of biochars.

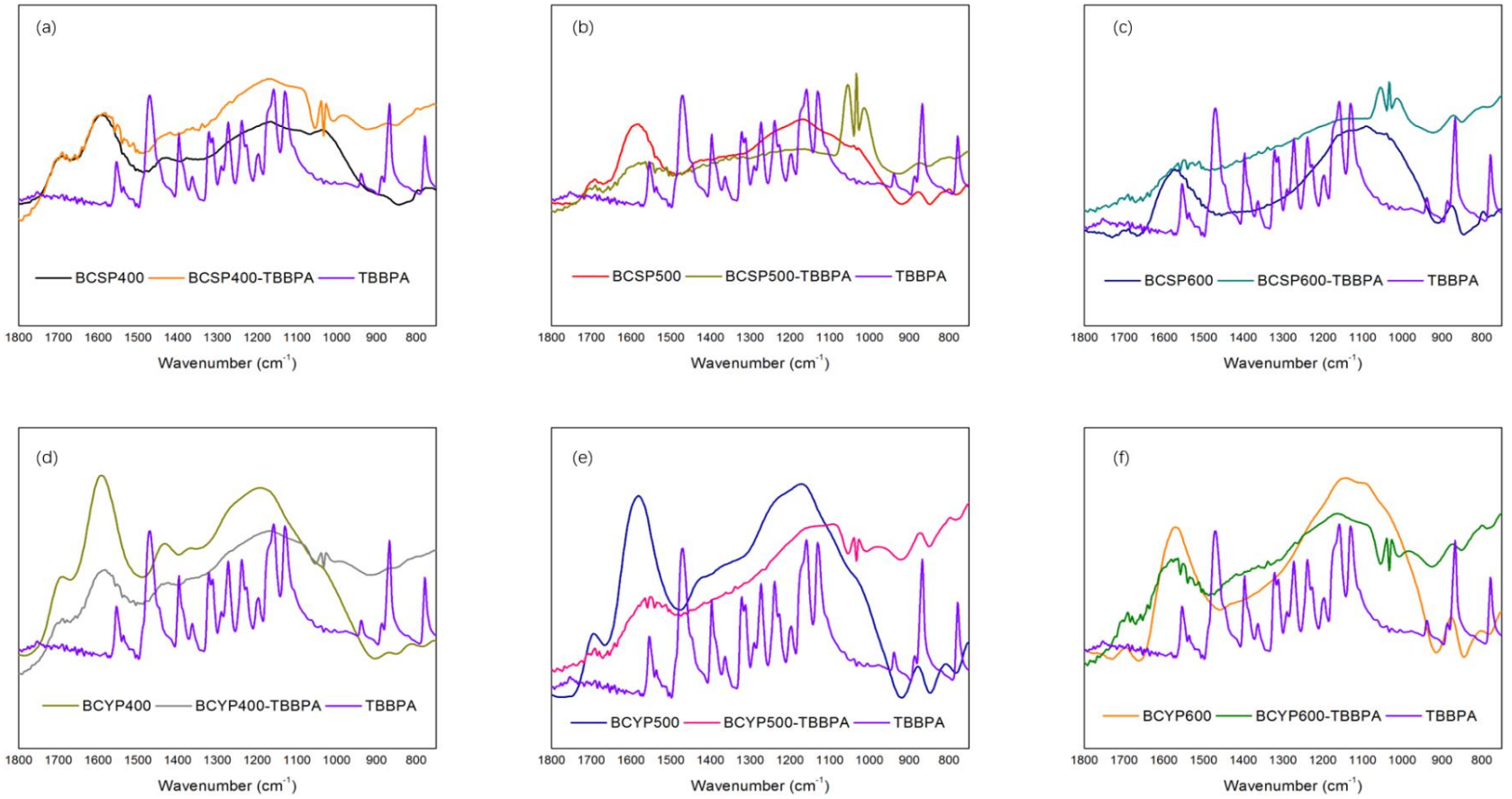

Figure 4.3 Synchrotron FTIR spectra of (a) BCSP400 and adsorbed TBBPA, (b) BCSP500 and adsorbed TBBPA, (c) BCSP600 and adsorbed TBBPA, (d) BCYP400 and adsorbed TBBPA, (e) BCYP500 and adsorbed TBBPA, (f) BCYP600 and adsorbed TBBPA

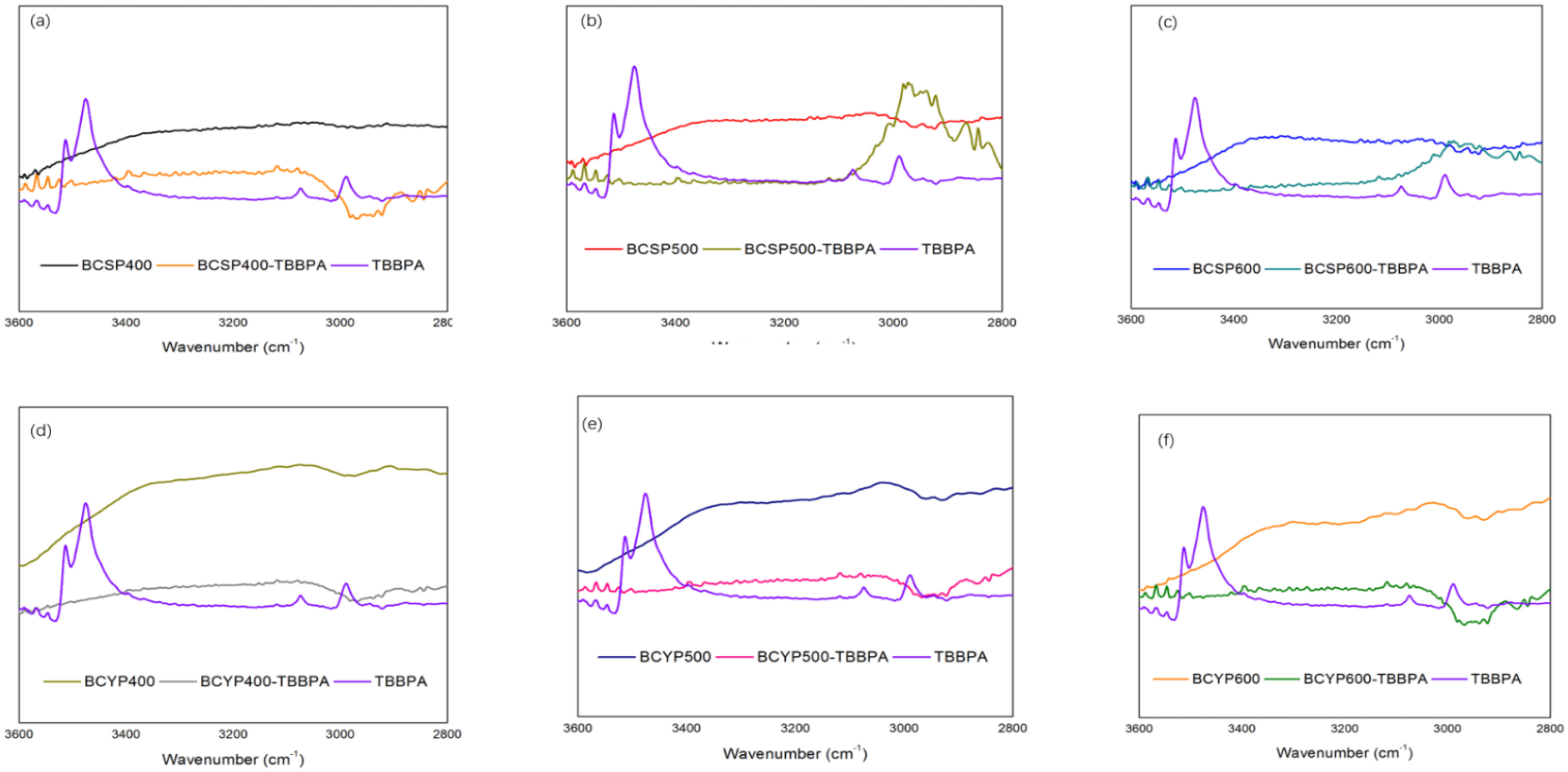

Figure 4.4 FT-IR spectrum of adsorbed TBBPA on BCYPs, BCBPs and TBBPA molecular in wavenumber 3600 to 2800 cm^{-1}

The function groups on the surface of biochars can contribute to the adsorption of TBBPA (Figure 4.5). Hydroxyl interaction existed between TBBPA and acid functional groups on biochars such as carboxyl groups on BCYPs and BCSP400, and phenol groups on BCSP500 and BCSP600. π-π interaction between carbon aromatic structures was also reported (Kim et al. 2011).

Therefore, it can be concluded that hydrogen bonding and π-π interactions on the charcoal surface played an important role in the adsorption of TBBPA. Meanwhile, interactions between hydroxyl groups on both biochars and TBBPA can be influenced by conjugated π-π interaction in aromatic structures. In addition, anhydride, aliphatic ester and ether groups on the biochars might also be involved in hydrogen bonding for the adsorption of TBBPA. These FTIR spectroscopy results can help better understand the interactions between TBBPA and biochars.

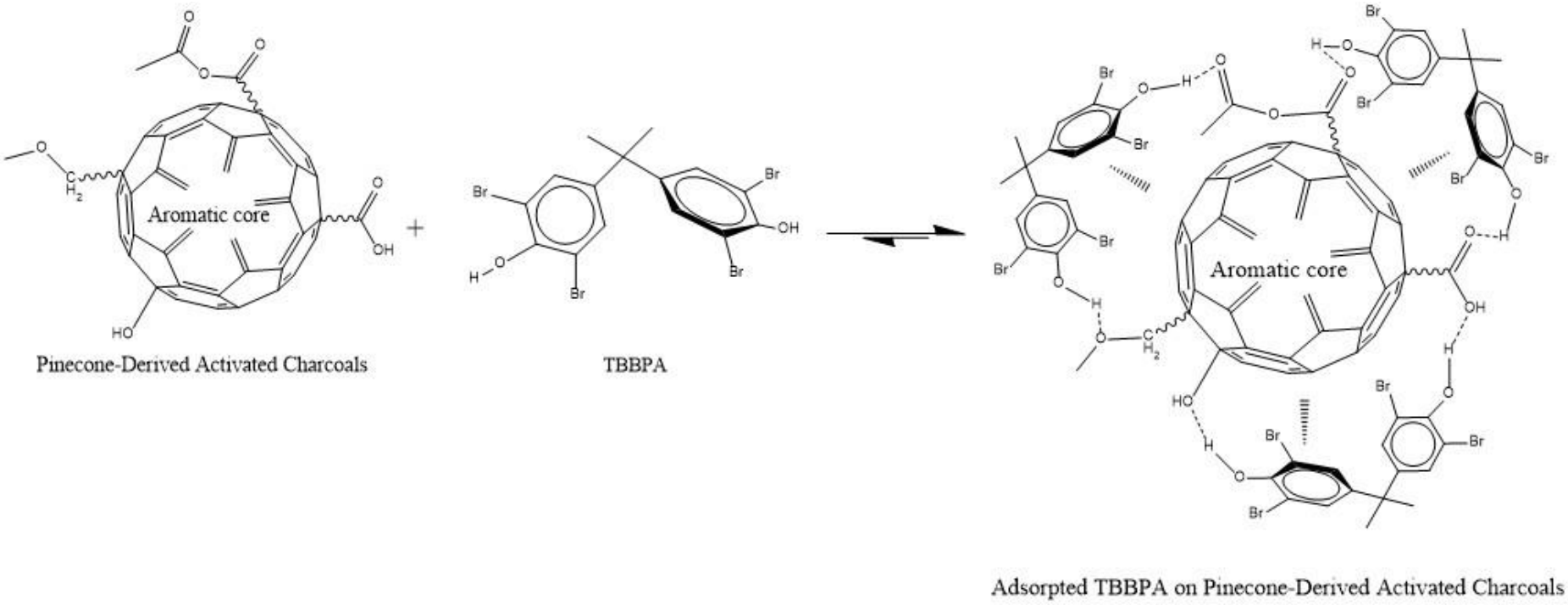

Figure 4.5 Possible mechanism in adsorption of TBBPA on biochar

4.3.3. Effect of Contact Time on the Adsorption of TBBPA by Biochars

The contact time in adsorption is an important factor for practical application (An et al. 2016b, Zhang et al. 2017). It can help determine the optimum time for maximum adsorption. The effect of contact time on the extraction and removal of TBBPA from aqueous solutions by biochars is shown in Figure 4.6. In general, the quantity of adsorbed TBBPA increased as contact time went on. During the first 30-50 min, there was a rapidly increase in the quantity of adsorbed TBBPA. 61.40% ~ 90.50% of TBBPA was removed by adsorption on biochars. The rapid adsorption could be due to the large number of activated sites for adsorption and specific properties of charcoal surface. When compared with the ionic form of TBBPA, TBBPA in molecular form could show a faster adsorption on biochar surface due to its hydrophobic characteristic. This rapid adsorption was followed by a gradual increase in adsorption quantity and removal efficiencies. When approaching the saturation of the biochars adsorbents, the adsorption of TBBPA tended to reach an equilibrium. The apparent equilibrium for the adsorption of TBBPA on BCYP 400, BCYP600, BCSP500 and BCSP400 was reached in less in 100 min, while it took BCSP600 and BCYP500 around 240 min to obtain such equilibrium. Although the adsorption of TBBPA on BCSP500 and BCYP400 occurred faster than that on other biochars, the adsorbed amount of TBBPA in equilibrium was similar with those on BCSP400, BCSP600 and BCYP500. It indicated these biochars had similar adsorption capacity and different affinity to TBBPA. The different affinity could be explained by the heterogeneous surface and structure characteristics of these biochars.

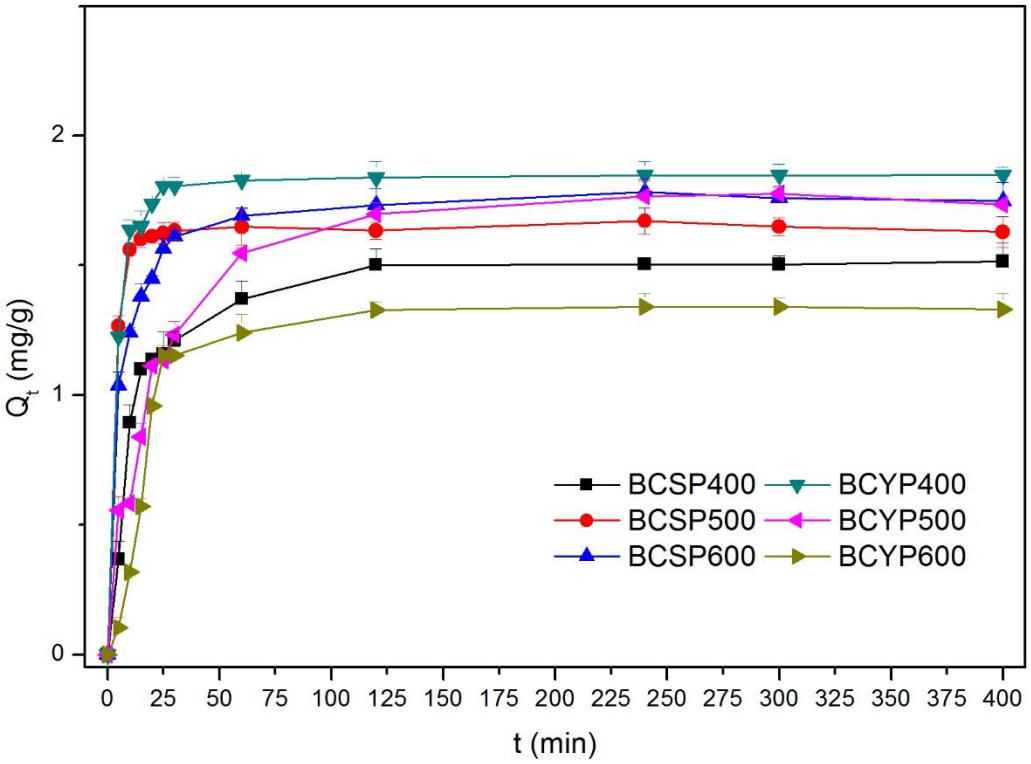

Figure 4.6 Effect of contact time on the adsorption of TBBPA by BCYPs and BCSPs.

4.3.4. Adsorption Kinetics

Analysis of adsorption kinetics can help further provide information of the adsorption mechanism. The adsorption kinetics was analyzed using pseudo-first-order, pseudo-second-order and intraparticle diffusion models. The pseudo-first order kinetics model is expressed as:

$$Q_t = Q_e(1 - e^{-k_1 t}) \qquad (4\text{-}3)$$

where Q_t (mg/g) represents amount of adsorbate adsorbed at time t, t (min) and Q_e (mg/g) is the amount of adsorbate adsorbed at equilibrium and k_1 (1/min) is the rate constant.

The pseudo-second order kinetics model is defined as:

$$Q_t = \frac{Q_e^2 k_2 t}{1 + Q_e k_2 t} \quad \text{and} \quad h = k_2 Q_e^2 \qquad (4\text{-}4)$$

where k_2 (g/mg min) is the pseudo-second order rate constant and h (mg/g min) is the initial adsorption rate.

Intra-particle diffusion model can help determine the rate-controlling step of pore diffusion in adsorption and it is described as:

$$Q_t = k_p t^{0.5} + C \qquad (4\text{-}5)$$

where k_p (mg/g $min^{0.5}$) is the intra-particle diffusion rate constant and C (mg/g) is a constant that describes the boundary layer effect. Higher C values are indicative of higher boundary layer effect and thus are descriptive of the inapplicability of pore diffusion as the sole rate-determining step in describing the dynamics of the adsorption process (Sewu et al. 2017). If $C = 0$, the adsorption kinetics are controlled only by intraparticle diffusion. If $C \neq 0$, the adsorption process is quite complex (Wang et al. 2014). Furthermore, the increase of parameter C is often corresponding to the increase of k_1, k_2 and h. The enhanced adsorption rate may be attributed to the increase in boundary layer thickness.

The calculated kinetic parameters for the adsorption of TBBPA on produced charcoals are shown in Table 4.2. For both BCYPs and BCSPs, the fitting to pseudo-first-order and pseudo-second-order kinetic models possessed relative higher correlation coefficients (0.8923-0.9989) and lower root-mean-square (0.0002-0.0284). It indicated that these two models could well describe the corresponding kinetic adsorption process (Figure 4.7). The low correlation coefficients of intra-particle model and positive C values suggested intra-particle diffusion was not a major process in the adsorption of TBBPA on biochars. The kinetic process about TBBPA adsorption on BCSP500, BCYP400 and BCYP600 could be better described by the pseudo-first-order kinetic model. In comparison, the kinetic process about TBBPA adsorption on BCSP400, BCSP600 and BCYP500 could be better descried with pseudo-second-order kinetic model. The different adsorption capacities of pinecone-derived biochars were also reflected in the analysis of adsorption kinetics. The order of Q_e for pseudo-first-order kinetic model decreased as BCYP400 > BCYP500 > BCSP600 > BCSP500 > BCYP600 > BCSP400 and the order of Q_e for

pseudo-second-order kinetic model decreased as BCYP400 > BCYP500 > BCSP600 > BCSP500 > BCSP400 > BCYP600. The initial adsorption rate h exhibited a decreasing order as BCSP500 > BCYP400 > BCSP600 > BCSP400 > BCYP600 > BCYP 500.

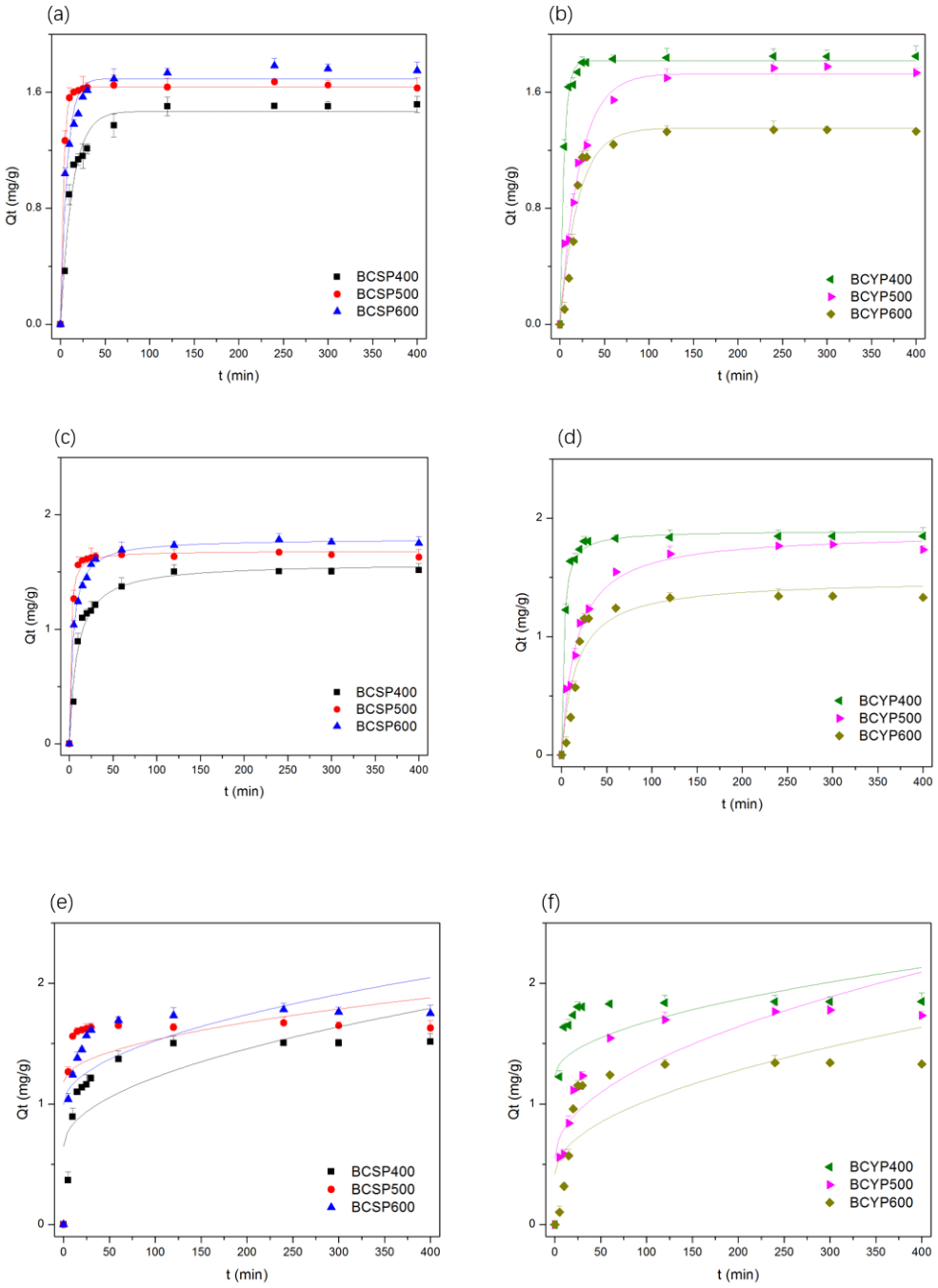

Figure 4.7 Kinetic analysis of pseudo-first model of (a) BCSP and (b) BCYP; pseudo-second model of (c) BCSP and (d) BCYP; intra-particle model of (e) BCSP and (f) BCYP

The pseudo-second order model is used to explain the external liquid film diffusion, surface adsorption and intra-particle diffusion processes (Park et al.). This model could provide a more comprehensive reflection of the adsorption mechanism of TBBPA onto the biochar when compared with the pseudo-first order model. The well-fit pseudo second-order model implies that the rate limiting step is chemical adsorption involving electronic forces through the sharing or exchange of electrons between the adsorbent and ionized adsorbate (Jung et al. 2013). π- π bonding and hydro-bonding could be considered as two possible interactions between biochar surface and TBBPA. Similar π- π bonding and hydro-bonding interactions on pyrolyzed carbon surface were also reported in the adsorptions of carbamazepine, sulfamethoxazole and reactive red 195 A dye (Chen et al. 2017, Jung et al. 2013, Mahmoud et al. 2016).

Table 4.2 Kinetic models and parameters of TBBPA adsorption on biochars

Adsorbent	Pseudo-first-order				Pseudo-second-order					Intra-particle model			
	$Q_{e\ cal}$ (mg/g)	k_1	R^2	RMSE	$Q_{e\ cal}$ (mg/g)	k_2	h	R^2	RMSE	k_p	C	R^2	RMSE
BCSP400	1.469	0.075	0.972	0.0064	1.578	0.071	0.243	0.9737	0.0060	0.057	0.649	0.5515	0.0838
BCSP500	1.637	0.297	0.9989	0.0002	1.682	0.474	1.497	0.9918	0.0018	0.035	1.182	0.1522	0.1891
BCSP600	1.693	0.137	0.9633	0.0093	1.789	0.140	0.252	0.9965	0.0009	0.052	0.997	0.4047	0.1505
BCYP400	1.818	0.217	0.9939	0.0017	1.894	0.243	0.782	0.9909	0.0026	0.045	1.231	0.2310	0.2166
BCYP500	1.728	0.046	0.9806	0.0065	1.877	0.033	0.097	0.9844	0.0052	0.077	0.549	0.7236	0.0927
BCYP600	1.353	0.049	0.9377	0.0164	1.482	0.042	0.130	0.8923	0.0284	0.061	0.417	0.5510	0.1182

4.3.5. Effect of Biochar Dosage

The impact of adsorbent dosage on the adsorption of TBBPA by biochars was investigated with the initial TBBPA concentration of 1 mg/L. As shown in Figure 4.8, the removal efficiency increased as the dosage of biochars increased. The adsorption efficiency increased from 39.82% to 87.42% and 24.11% to 65.29% as BCYP500 and BCYP600 dosage changed from 5 to 25mg, respectively. The enhanced adsorption can be attributed to the results of enlarged surface area and increasing adsorption sites (Garg et al. 2003). As the charcoal dosage further increased, the relative stable removal efficiency would be achieved. That could be due to the overlapping of available adsorption sites and competition with other adsorbents when there is limited adsorbate concentration or large amount of adsorbents (Namasivayam et al. 1998).

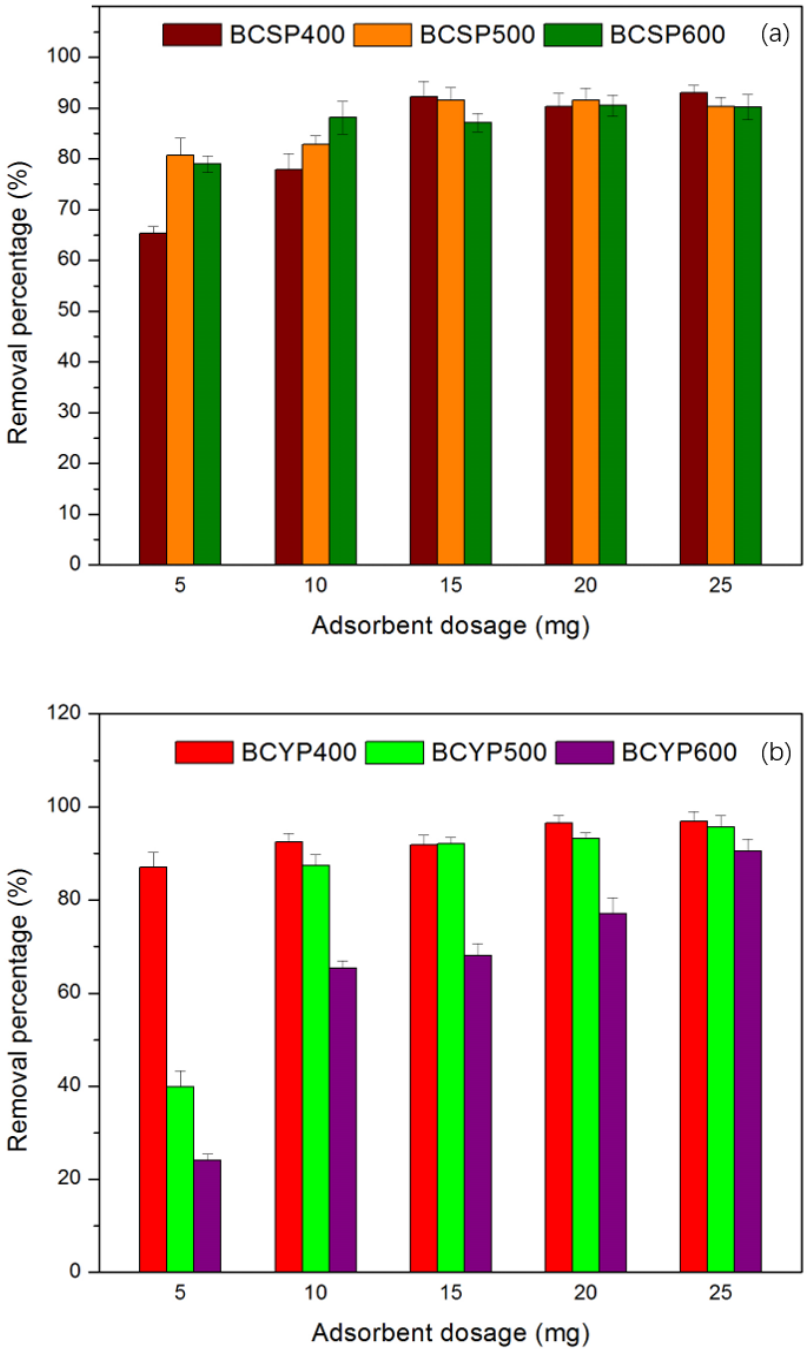

Figure 4.8 Effect of activated carbon dosage on the removal of TBBPA by BCSPs and (b) BCYPs.

The removal of TBBPA by pinecone-derived biochars as influenced by initial TBBPA concentration is illustrated in Figure 4.9. As the initial TBBPA concentration increased, a general increase was followed by a gradual decrease of removal efficiency. For most initial TBBPA concentrations, the removal efficiencies were enhanced when using BCSP with increasing pyrolysis temperature. At the initial TBBPA concentration of 1 mg/L, the removal efficiencies for BCSP400, BCSP500 and BCSP600 were 75.17%, 80.74% and 86.65%, respectively. The adsorption of TBBPA on BCYP exhibited a different trend. The high TBBPA removal was observed in the tests with BCYP400, while low TBBPA removal was associated with the tests using BCYP600. It is interesting to note that BCYP produced at low temperature with a relatively low surface area can uptake more TBBPA than those highly aromatized carbon particle produced at high temperature with relatively high surface area. The chemical structure of TBBPA exhibited affinities to both polar and hydrophobic surface sites (Han et al. 2013, ten Dam et al. 2012). The adsorption of TBBPA could include the external liquid film diffusion, surface adsorption and intra-particle diffusion processes. For BCYP produced at low pyrolysis temperature, the polar content of dissociable acid groups and mineral is higher than other BCYP produced at high pyrolysis temperature. The relatively high content of carbon phase would enhance surface hydrophobicity, which could also affect the structure porosity and the surface chemistry of small pores. These pores could be very active for the physical adsorption of TBBPA. A similar result regarding the role of porosity was also reported in the adsorption of carbamazepine on sludge/fish waste-derived charcoal adsorbents (Nielsen et al. 2015).

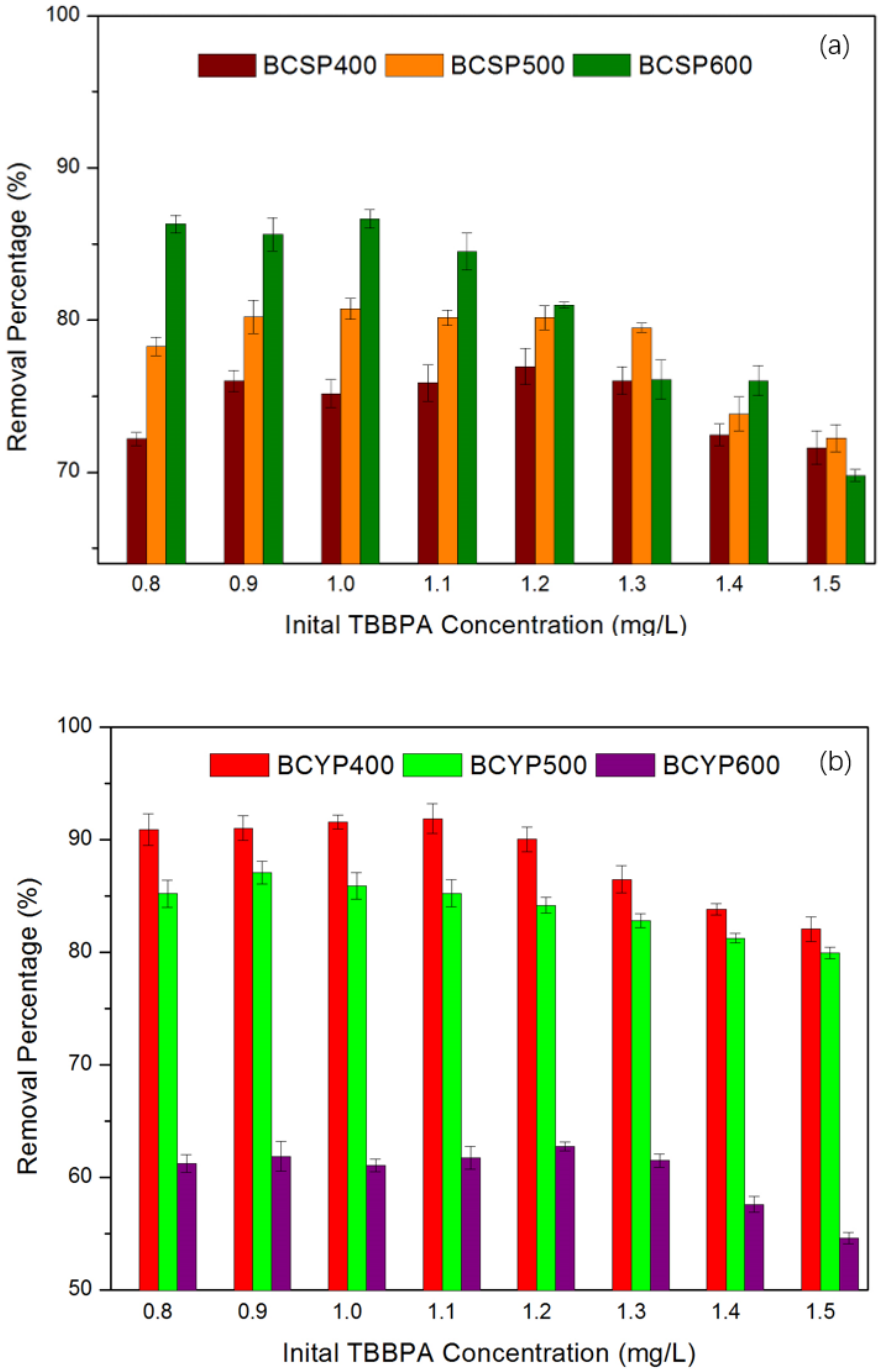

Figure 4.9 Effect of initial TBBPA concentrations on the removal performance with (a) BCSPs and (b) BCYPs.

4.3.6. Role of Charcoal Surface Functionality in the Adsorption of TBBPA

The distribution coefficient (K_d) is closely related to the characteristics of carbon-based adsorbents (Zielińska and Oleszczuk 2015). The role of charcoal surface functionality in TBBPA adsorption was evaluated through correlating K_d and physical-chemical properties of pinecone-derived biochars such as specific surface area (S_{BET}), total carbon content (C%), total oxygen content (O%), hydrogen-carbon ratio (H/C) and oxygen-carbon ratio (O/C). As shown in Figure 4.10, the correlation parameters varied with the charcoal sources and pyrolysis temperatures. The high correlations were present between K_d obtained in the initial TBBPA concentrations of 0.5, 1.0 and 1.5 mg/L and BCYP properties of S_{BET} (r = -0.999), C% (r = -0.993), O% (r = 0.992), H/C (r = 0.999) and O/C (r = 0.998). As for BCSP, the relative low correlations obtained at low initial TBBPA concentrations of 0.5 and 1.0 mg/L were observed. The above correlations suggested that the adsorption of TBBPA on BCYPs primarily occurred on the charcoal surface, as the result of interaction between TBBPA and surface contents. However, less significant correlations about S_{BET} and H/C were found for the adsorption of TBBPA on BCSP. It indicated the aromaticity and porosity played the less important role in the adsorption of TBBPA on BCSPs. There was negative correlation between K_d and S_{BET} (-0.999) for BCYPs, indicating the adsorption of TBBPA on BCYP did not only occur on charcoal outer surface. The surface adsorption might not be the dominated mechanism. In addition, the positive correlations between (K_d and S_{BET} showed the adsorption of BCSPs primarily occurred on the outer surface of BCSP. The lack of correlation between K_d and specific surface area was confirmed the difficult access of TBBPA molecular to surface of micropores and groove-like gullies on BCSP surfaces.

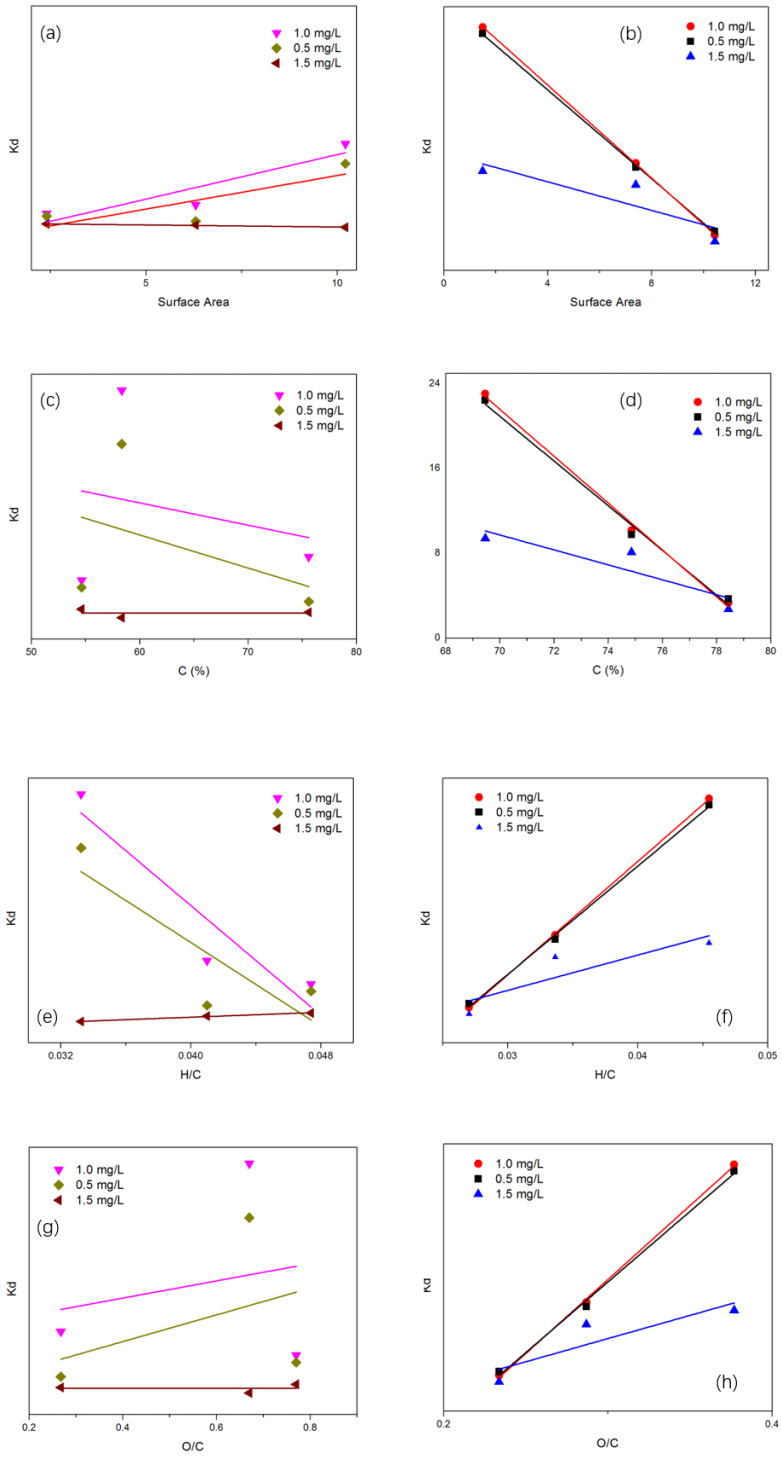

Figure 4.10 Interactions between TBBPA adsorption and (a) surface area of BCSPs; (b) surface area of BCYPs; (c) carbon content of BCSPs; (d) carbon content of BCYPs; (e) hydrogen-oxygen ratio of BCSPs; (f) hydrogen-oxygen ratio of BCYPs; (g) oxygen-carbon ratio of BCSPs, and (h) oxygen-carbon ratio of BCYPs.

The adsorption of TBBPA on BCYP and BCSP was additionally determined by the charcoal elemental composition and surface properties. H/C and O/C are indicative of substance aromaticity and polarity, respectively (Al-Wabel et al. 2013). Negative correlations were found between K_d and C% on the surface of sorbents as well as the significant positive correlations were found between K_d and (H%, O%, H/C) and O/C. The increase of C% would result in the decrease of TBBPA adsorption. The results suggested the decrease of aromaticity and increase of polarity could facilitate TBBPA adsorption. The surface acid groups showed electrical attraction with TBBPA molecules. Therefore, a relatively abundant acid groups on the surface of BCYP could create favorable conditions for TBBPA adsorption. As for BCSP, the negative correlations between K_d and H/C were obtained. It indicated the existence of aromatic structures, which could improve the adsorption of TBBPA. Different forms of acid groups have positive or negative influence on adsorption (Qiu et al. 2009). On the one hand, some acid functional groups such as carboxyls and lactones could diminish π-π interactions due to their electron-withdrawing ability which would reduce the density of π electron on charcoal surface. On the other hand, the electron-donating ability of phenolic hydroxyls could strengthen π-π interactions. The dramatic change of K_d with the increasing of O/C and C% could be due to such different forms of acid groups on the BCSP surface, which caused different effects on TBBPA adsorption. The interactions between TBBPA molecular and charcoal surface properties can be influenced by the initial TBBPA concentration. For BCSPs, the interactions between S_{BET} and K_d significantly changed at different initial TBBPA concentrations. K_d increased with the increase of S_{BET} with the TBBPA concentrations of 0.5 and 1.0 mg/L, while K_d gradually decreased with the increase of S_{BET} with the concentration of TBBPA of 1.5 mg/L. Similarly, the changing interactions between K_d and C%, H/C

and O/C were also observed when the initial TBBPA concentration was 1.5 mg/L. The variations were also observed for the results about BCYPs. However, such variation exhibited an opposite trend. and lower adsorption capacity was accompanied with the TBBPA initial concentration of 1.5 mg/L rather than 0.5 and 1.0 mg/L.

In addition, the correlations of charcoal surface parameters and TBBPA adsorption were also affected by the initial TBBPA concentration. For the adsorption of TBBPA on BCSPs, lower correlations ($r^2 < 0.7$) between S_{BET} and K_d with initial TBBPA concentration of 0.5 and 1.0 mg/L were observed than correlation ($r^2 = 0.944$) with initial TBBPA concentration of 1.5 mg/L. The higher correlation indicated that the effect of surface porosity could play an important role when the initial TBBPA concentration was 1.5 mg/L. For the adsorption of TBBPA on BCYPs, however, higher correlations ($r^2=0.999$) of S_{BET} and K_d with initial TBBPA concentration of 0.5 and 1.0 mg/L were obtained than correlation ($r^2=0.508$) with the initial TBBPA concentration of 1.5 mg/L. Low correlations suggested the involvement of other interactions and the influence of other characteristics. When the initial TBBPA concentration was 1.5 mg/L, the adsorption of TBBPA could not easily access the interior area of BCYPs surface. and some effects other than surface porosity would favor the adsorption process. In addition, significant changes of correlations of K_d and parameters such as C%, H/C and O/C were also observed with TBBPA concentration of 1.5 mg/L. That indicated more factors and interactions for the adsorption on biochar would be involved at higher TBBPA concentration than those at lower TBBPA concentration.

At relatively low concentration of TBBPA, high-energy sites with specific acid functional groups or pores on the surface of BCYP and BCSP would be occupied at first in the adsorption process. At low TBBPA concentration, the adsorption of TBBPA on BCYP would be favored by higher polarity, low aromaticity and acid functional groups on charcoal surface. π-π interactions and electrostatic attraction could show positive effect. Nevertheless, according to the different correlations obtained, some specific functional groups and structures of activated carbon could also contribute to the adsorption process. Both electrostatic and hydrophobic interactions facilitated the adsorption of TBBPA. At high TBBPA concentrations, those high-energy sites tended to be fully occupied and the TBBPA continued to fill other unoccupied sites. For the adsorption on BCYP, the decreasing correlations with the initial TBBPA concentration of 1.5 mg/L might due to the less interaction between TBBPA and hydrophobicity, specific functional groups and specific structures when compared with the results for BCSP. Similarly, as the TBBPA concentrations increased, the increase of adsorption on BCSP surface happened as the results of porosity and hydrophilic interactions.

Moreover, given to the results of SR-FTIR analysis and contact times of TBBPA adsorption on biochars, the surface function groups of biochars can affect the adsorption capacity and efficiency. The high removal efficiency and relative fast adsorption of BCYP400 (91%), BCYP500 (85%) and BCSP600 (86%) at TBBPA concentration of 1.0 mg/L showed a similar structure of —C—OH and oxygen-contenting groups such as anhydrides and esters on the surface. The results of sorped TBBPA on BCYP400, BCYP500 and BCSP600 were observed the decrease of acid —C—OH structures. It indicated that the structures of the acid functional groups

played an important role both in the adsorption capacity and efficiency. Moreover, groups of anhydride and esters might have less positive effects on TBBPA adsorption than acid —C—OH structures, which suggested that the π-π interaction on C = O structures and the hydroxyl interactions on anhydride groups might cause less impacts on TBBPA adsorption than hydroxyl interaction with acid functional groups. Furthermore, though BCSP400 (75%) and BCYP600 (60%) might showed a similar adsorption mechanism with BCYP400 and BCYP500, the relative low removal efficiency and slow adsorption might be ascribed to the low contents of acid function groups. In addition, the weak response of —C—OH structures showed that BCSP400 might have much lower content of acid functional groups, which might lead to a lower adsorption performance than BCYP400 and BCYP500. Identically, as the spectrum showed, the relatively low removal efficiency of TBBPA on BCYP600 also exhibited that, on the surface of BCYP600, it might content rich aromatic structures, unsaturated ether and ester groups but little acid functional groups. Furthermore, on the present of aromatic structures on the surface of BCYP600 and BCSP600, the different adsorption performances were due to the acid functional groups, which suggesting that π-π interaction was less impacts on TBBPA adsorption than hydroxyl interaction with acid functional groups as well as groups of anhydride and esters might have less positive effects on TBBPA adsorption than acid —C—OH structures.

4.4. Conclusions

In this study, it was demonstrated that the pinecone-derived biochars are effective in adsorbing TBBPA. The contact time, adsorbent dosage and initial concentration on TBBPA removal efficiency were investigated. The surface properties, kinetic models

and surface functionalities of different biochars were studied. The roles of elemental composition, porosity and surface functional group in TBBPA adsorption were analyzed.

Based on synchrotron FTIR analysis, kinetic model evaluation and elemental composition study, we discovered that (a) adsorption of TBBPA on biochar occurred mainly due to the existence of multiple hydroxyls and their interactive effects. (b) Acid functional groups (including carboxyl and phenol groups) had an important role in the adsorption of TBBPA. In addition, (c) other oxygen-containing groups could help to stabilize the adsorption performance under high initial concentrations. (d) π-π interactions could have insignificant impacts on TBBPA adsorption. In association with adsorption performance, through examining the properties and sorption behavior of biochar surface, we revealed that the adsorption performance could be influenced by porosity, initial concentration, adsorbent dosage and elemental composition. In detail, the adsorption of TBBPA on BCYP might be favored by the conditions of high polarity, low aromaticity, and low surface area; in comparison, the adsorption of TBBPA on BCSP would be favored by the conditions of high aromaticity and high surface area. During the adsorption on BCSP, the effect of polarity can be interfered with other factors. Moreover, the adsorption capacity and removal efficiency of TBBPA was significantly dependent upon the contents of acid functional groups on surface.

Based on this conclusion, the study for investigating the adsorption of TBBPA by pinecone-derived biochars shows that a developed black carbon material can be used as a potential remediation agent to purify effluent, river and lakes contaminated with

TBBPA. The new presented proofs of interactions between functional groups and TBBPA can provide potential methods and materials to be applied for the immobilization of halogenated biphenyls. In addition, the revealed interactions between TBBPA and pinecone-derived charcoals are helpful for exploring the fate and transport of such a contaminant in forest, wetland, grassland, and various cultivated agricultural systems. Such study of biogeochemical cycle of TBBPA can also suggest the role of charcoals and their behaviors with pollutant in environment. Base on the research of their aspects in environment, the results will have extensive implications for the environmental simulation, ecological system modeling and pollutant migration estimations.

CHAPTER 5

CONCLUSIONS

5.1 Summary

This study is an emerging area in environmental research in associate with trace organic contaminant in the complex land system. Pinecone produced biochars under multiple pyrolysis temperatures were prepared and investigated for their surface properties and TBBPA adsorption behaviors. Due to the complex interactions and environmental aspects, immobilization capability of TBBPA on biochar is investigated with the involvement of environmental relevant factors. Effects of inorganic fertilizer ions, including ammonia, nitrate and phosphate which present in natural nitro-cycle and phosphor-cycle are studied under different solution pH levels and initial sorbate concentrations on biochar from different pinecones and pyrolysis temperatures. Thus, a 2^{5-1} factorial design was contracted to reveal their interactions. Surface functionality and adsorption efficiency of TBBPA immobilization on biochar were also investigated through SR-FTIR analysis, SEM method and BET surface study. Equilibrium isotherms and kinetic study under different contact time and initial concentrations were carried out to explore TBBPA adsorption mechanism on biochar surface.

5.2 Research Achievements

This is the first study to reveal the behaviors of TBBPA at the biochar-water interface under the effects of environmental factors. The results indicated biochar characteristics

can affect the performance of TBBPA adsorption. The TBBPA immobilization on biochar surface can be influenced by hydrophobic interaction as a major effect and such adsorption can be improved under electrostatic interaction. In addition, pH and inorganic fertilizer ions were also the significant factors which can impact interactions between biochar surface and TBBPA. NH_4^+ ions had significant positive effects for the adsorption of TBBPA on biochars with aromatic-rich surface. Strong negative effects of PO_4^{3-} existed for TBBPA adsorption. The insignificant effects of NO_3^- was observed and NO_3^- could act as a "stabilizer" to offset the influences of other fertilizer ions. The overall influence of various factors on the adsorption of TBBPA could be an integration of multiple processes with interactions. The results of this study can help understand migration patterns of TBBPA and analyze the immobilization on biochars in the presence of inorganic fertilizer ions. Moreover, based on SR-FTIR analysis, kinetic model evaluation and elemental composition study, we discovered that, the adsorption of TBBPA on biochar occurred mainly due to the existence of multiple hydroxyls and their interactive effects. Acid functional groups including carboxyl and phenol groups can impact the adsorption of TBBPA as an important role. Furthermore, other oxygen-containing groups could help to stabilize the adsorption performance under high initial concentrations. The results also revealed that π-π interactions between TBBPA and biochar surface could have insignificant impacts on the adsorption. Through examining the properties and sorption behavior of biochar surface, the adsorption performance could be influences by porosity, initial concentration, adsorbent dosage and elemental composition. In detail, the adsorption of TBBPA on BCYP might favor conditions of high polarity, low aromaticity, and low surface area; in comparison, the adsorption of TBBPA on BCSP would favor conditions of high aromaticity and high surface area. During the adsorption on BCSP, the effect of polarity

can be interfered with other factors. Additionally, the adsorption capacity and removal efficiency of TBBPA was significantly dependent upon the contents of acid functional groups on surface. Based on this conclusion, the study for the investigating adsorption of TBBPA by pinecone derived biochar show that a developed black carbon material can be used as a potential remediation agent to purify field, river and lakes contaminated with TBBPA. The revealed interactions between TBBPA and wood-derived charcoals are helpful for exploring fate and transport of such a contaminant in forest, wetland, grassland, and various cultivated agricultural systems. Such study of biogeochemical cycle of TBBPA can also suggest the role of charcoals and their behaviors with pollutant in environment.

5.3 Recommendations for the Future Study

It will have important implications for risk assessment and site remediation regarding overall environmental performance. Further studies are desired to define the fate and transport of TBBPA on biochars in combination with the other components and obtain more theoretical foundation for analyzing TBBPA mobility in the land system. Base on the research of their aspects in environment, the biochars will have extensive applications and understanding on the environmental simulation, ecological system modeling and pollutant migration estimations. Moreover, the new presented proofs of interactions between functional groups and TBBPA can provide potential methods and materials to be applied for the immobilization of halogenated biphenyls.

REFERENCES

Abdallah, M.A.E. (2016) Environmental occurrence, analysis and human exposure to the flame retardant tetrabromobisphenol-A (TBBP-A)-A review. Environment International 94, 235-250.

Abdallah, M.A.E., Harrad, S. and Covaci, A. (2008) Hexabromocyclododecanes and Tetrabromobisphenol-A in Indoor Air and Dust in Birmingham, UK: Implications for Human Exposure. Environmental Science & Technology 42(18), 6855-6861.

Ahmad, M., Ok, Y.S., Rajapaksha, A.U., Lim, J.E., Kim, B.-Y., Ahn, J.-H., Lee, Y.H., Al-Wabel, M.I., Lee, S.-E. and Lee, S.S. (2016) Lead and copper immobilization in a shooting range soil using soybean stover- and pine needle-derived biochars: Chemical, microbial and spectroscopic assessments. Journal of Hazardous Materials 301, 179-186.

Ahmad, M., Rajapaksha, A.U., Lim, J.E., Zhang, M., Bolan, N., Mohan, D., Vithanage, M., Lee, S.S. and Ok, Y.S. (2014) Biochar as a sorbent for contaminant management in soil and water: A review. Chemosphere 99, 19-33.

Al-Wabel, M.I., Al-Omran, A., El-Naggar, A.H., Nadeem, M. and Usman, A.R.A. (2013) Pyrolysis temperature induced changes in characteristics and chemical composition of biochar produced from conocarpus wastes. Bioresource Technology 131, 374-379.

Alaee, M., Arias, P., Sjödin, A. and Bergman, Å. (2003) An overview of commercially used brominated flame retardants, their applications, their use patterns in different countries/regions and possible modes of release. Environment International 29(6), 683-689.

An, C., Huang, G, Wei, J. and Yu, H. (2011) Effect of short-chain organic acids on the enhanced desorption of phenanthrene by rhamnolipid biosurfactant in soil–water environment. Water Research 45(17), 5501-5510.

An, C.., Huang, G., Yu, H. and Wei, J. (2012) Influence of short-chain aliphatic acids on the phenanthrene desorption and mobilization from contaminated soil. Soil and Sediment Contamination: An International Journal 21(2), 192-206.

An, C. and Huang, G. (2012) Stepwise adsorption of phenanthrene at the fly ash–water interface as affected by solution chemistry: experimental and modeling studies. Environmental Science & Technology 46(22), 12742-12750.

An, C. and Huang, G. (2015) Environmental concern on biochar: capture, then what? Environmental Earth Sciences 74(12), 7861-7863.

An, C., Huang, G., Yu, H., Wei, J., Chen, W. and Li, G. (2010) Effect of short-chain organic acids and pH on the behaviors of pyrene in soil–water system. Chemosphere 81(11), 1423-1429.

An, C., McBean, E., Huang, G., Yao, Y., Zhang, P., Chen, X. and Li, Y. (2016a) Multi-Soil-Layering Systems for Wastewater Treatment in Small and Remote Communities. Journal of Environmental Informatics 27(2), 131-144.

An, C., Yang, S., Huang, G., Zhao, S., Zhang, P. and Yao, Y. (2016b) Removal of sulfonated humic acid from aqueous phase by modified coal fly ash waste: Equilibrium and kinetic adsorption studies. Fuel 165, 264-271.

Baudu, M., Le Cloirec, P. and Martin, G. (1991) Pollutant Adsorption onto Activated Carbon Membranes. Water Science and Technology 23(7-9), 1659.

Ben-Awuah, E., Elkington, T., Askari-Nasab, H. and Blanchfield, F. (2015) Simultaneous Production Scheduling and Waste Management Optimization for an Oil Sands Application. Journal of Environmental Informatics 26(2), 80-90.

Benyoucef, S. and Amrani, M. (2011) Adsorption of phosphate ions onto low cost Aleppo pine adsorbent. Desalination 275(1–3), 231-236.

Bhutto, A.A., Vesely, D. and Gabrys, B.J. (2003) Miscibility and interactions in polystyrene and sodium sulfonated polystyrene with poly(vinyl methyl ether) PVME blends. Part II. FTIR. Polymer 44(21), 6627-6631.

Birnbaum, L.S. and Staskal, D.F. (2004) Brominated flame retardants: cause for concern? Environmental Health Perspectives 112(1), 9-17.

Breen, C. and Watson, R. (1998) Polycation-Exchanged Clays as Sorbents for Organic Pollutants: Influence of Layer Charge on Pollutant Sorption Capacity. Journal of Colloid and Interface Science 208(2), 422-429.

Bruun, E.W., Ambus, P., Egsgaard, H. and Hauggaard-Nielsen, H. (2012) Effects of slow and fast pyrolysis biochar on soil C and N turnover dynamics. Soil Biology and Biochemistry 46, 73-79.

Bulut, Y. and Tez, Z. (2007) Removal of heavy metals from aqueous solution by sawdust adsorption. Journal of Environmental Sciences 19(2), 160-166.

Buss, W., Graham, M.C., Shepherd, J.G. and Mašek, O. (2016) Suitability of marginal biomass-derived biochars for soil amendment. Science of the Total Environment 547, 314-322.

Cao, X. and Harris, W. (2010) Properties of dairy-manure-derived biochar pertinent to its potential use in remediation. Bioresource Technology 101(14), 5222-5228.

Cao, X., Ma, L., Gao, B. and Harris, W. (2009) Dairy-Manure Derived Biochar Effectively Sorbs Lead and Atrazine. Environmental Science & Technology 43(9), 3285-3291.

Cao, Y., Yang, B., Song, Z., Wang, H., He, F. and Han, X. (2016) Wheat straw biochar amendments on the removal of polycyclic aromatic hydrocarbons (PAHs) in

contaminated soil. Ecotoxicology and Environmental Safety 130, 248-255.

Chan, W.K. and Chan, K.M. (2012) Disruption of the hypothalamic-pituitary-thyroid axis in zebrafish embryo–larvae following waterborne exposure to BDE-47, TBBPA and BPA. Aquatic Toxicology 108, 106-111.

Chen, B., Zhou, D. and Zhu, L. (2008) Transitional Adsorption and Partition of Nonpolar and Polar Aromatic Contaminants by Biochars of Pine Needles with Different Pyrolytic Temperatures. Environmental Science & Technology 42(14), 5137-5143.

Chen, J., Zhang, D., Zhang, H., Ghosh, S. and Pan, B. (2017) Fast and slow adsorption of carbamazepine on biochar as affected by carbon structure and mineral composition. Science of the Total Environment 579, 598-605.

Chen, Y.P., Wang, D.-N., Yin, Y.-M., Wang, L.-Y., Wang, X.-F. and Xie, M.-X. (2012) Quantum Dots Capped with Dummy Molecularly Imprinted Film as Luminescent Sensor for the Determination of Tetrabromobisphenol A in Water and Soils. Journal of Agricultural and Food Chemistry 60(42), 10472-10479.

Cheng, Y., Cai, Z., Chang, S.X., Wang, J. and Zhang, J. (2012) Wheat straw and its biochar have contrasting effects on inorganic N retention and N2O production in a cultivated Black Chernozem. Biology and Fertility of Soils 48(8), 941-946.

Chignell, C.F., Han, S.K., Mouithys-Mickalad, A., Sik, R.H., Stadler, K. and Kadiiska, M.B. (2008) EPR studies of in vivo radical production by 3,3′,5,5′-tetrabromobisphenol A (TBBPA) in the Sprague–Dawley rat. Toxicology and Applied Pharmacology 230(1), 17-22.

Chin, C.J.M., Shih, L.C., Tsai, H.J. and Liu, T.K. (2007) Adsorption of o-xylene and p-xylene from water by SWCNTs. Carbon 45(6), 1254-1260.

Choi, K.I., Lee, S.H. and Osako, M. (2009) Leaching of brominated flame retardants

from TV housing plastics in the presence of dissolved humic matter. Chemosphere 74(3), 460-466.

Cosoli, P., Ferrone, M., Pricl, S. and Fermeglia, M. (2008) Hydrogen sulphide removal from biogas by zeolite adsorption: Part I. GCMC molecular simulations. Chemical Engineering Journal 145(1), 86-92.

Covaci, A., Harrad, S., Abdallah, M.A.E., Ali, N., Law, R.J., Herzke, D. and de Wit, C.A. (2011) Novel brominated flame retardants: A review of their analysis, environmental fate and behaviour. Environment International 37(2), 532-556.

Cuba-Chiem, L.T., Huynh, L., Ralston, J. and Beattie, D.A. (2008) In Situ Particle Film ATR FTIR Spectroscopy of Carboxymethyl Cellulose Adsorption on Talc: Binding Mechanism, pH Effects, and Adsorption Kinetics. Langmuir 24(15), 8036-8044.

Cui, X., Dai, X., Khan, K.Y., Li, T., Yang, X. and He, Z. (2016) Removal of phosphate from aqueous solution using magnesium-alginate/chitosan modified biochar microspheres derived from Thalia dealbata. Bioresource Technology 218, 1123-1132.

Das, O., Sarmah, A.K. and Bhattacharyya, D. (2015) A sustainable and resilient approach through biochar addition in wood polymer composites. Science of the Total Environment 512–513, 326-336.

Das, O., Sarmah, A.K., Zujovic, Z. and Bhattacharyya, D. (2016) Characterisation of waste derived biochar added biocomposites: chemical and thermal modifications. Science of the Total Environment 550, 133-142.

de Rozari, P., Greenway, M. and El Hanandeh, A. (2016) Phosphorus removal from secondary sewage and septage using sand media amended with biochar in constructed wetland mesocosms. Science of the Total Environment 569–570,

123-133.

Di Carlo, F.J., Seifter, J. and DeCarlo, V.J. (1978) Assessment of the hazards of polybrominated biphenyls. Environmental Health Perspectives 23, 351-365.

Fan, S., Tang, J., Wang, Y., Li, H., Zhang, H., Tang, J., Wang, Z. and Li, X. (2016) Biochar prepared from co-pyrolysis of municipal sewage sludge and tea waste for the adsorption of methylene blue from aqueous solutions: Kinetics, isotherm, thermodynamic and mechanism. Journal of Molecular Liquids 220, 432-441.

Fasfous, I.I., Radwan, E.S. and Dawoud, J.N. (2010) Kinetics, equilibrium and thermodynamics of the sorption of tetrabromobisphenol A on multiwalled carbon nanotubes. Applied Surface Science 256(23), 7246-7252.

Feng, A.H., Chen, S.-J., Chen, M.Y., He, M.J., Luo, X.J. and Mai, B.X. (2012) Hexabromocyclododecane (HBCD) and tetrabromobisphenol A (TBBPA) in riverine and estuarine sediments of the Pearl River Delta in southern China, with emphasis on spatial variability in diastereoisomer- and enantiomer-specific distribution of HBCD. Marine Pollution Bulletin 64(5), 919-925.

Forsythe, K., Irvine, K.N., Atkinson, D., Perrelli, M., Aversa, J., Swales, S., Gawedzki, A. and Jakubek, D. (2015) Assessing lead contamination in Buffalo River sediments. Journal of Environmental Informatics 26(2), 106-111.

Fu, H., Huang, G., Zhang, M., Gao, P. and Chai, T. (2015) Interactions of Factors for Effluent Quality in Membrane Bioreactor. Journal of Environmental Informatics 25(1), 14-22.

Fujii, S., Cha, H., Kagi, N., Miyamura, H. and Kim, Y.-S. (2005) Effects on air pollutant removal by plant absorption and adsorption. Building and Environment 40(1), 105-112.

Garg, V.K., Gupta, R., Bala Yadav, A. and Kumar, R. (2003) Dye removal from aqueous

solution by adsorption on treated sawdust. Bioresource Technology 89(2), 121-124.

Geens, T., Roosens, L., Neels, H. and Covaci, A. (2009) Assessment of human exposure to Bisphenol-A, Triclosan and Tetrabromobisphenol-A through indoor dust intake in Belgium. Chemosphere 76(6), 755-760.

Gibson, L.T. (2014) Mesosilica materials and organic pollutant adsorption: part B removal from aqueous solution. Chemical Society Reviews 43(15), 5173-5182.

Girardet, C. and Toubin, C. (2001) Molecular atmospheric pollutant adsorption on ice: a theoretical survey. Surface Science Reports 44(7–8), 159-238.

González, J.A., Villanueva, M.E., Piehl, L.L. and Copello, G.J. (2015) Development of a chitin/graphene oxide hybrid composite for the removal of pollutant dyes: Adsorption and desorption study. Chemical Engineering Journal 280, 41-48.

Goodman, L.R., Cripe, G.M., Moody, P.H. and Halsell, D.G. (1988) Acute toxicity of malathion, tetrabromobisphenol-A, and tributyltin chloride to mysids (Mysidopsis bahia) of three ages. Bulletin of Environmental Contamination and Toxicology 41(4), 746-753.

Guerra, P., Eljarrat, E. and Barceló, D. (2010) Simultaneous determination of hexabromocyclododecane, tetrabromobisphenol A, and related compounds in sewage sludge and sediment samples from Ebro River basin (Spain). Analytical and Bioanalytical Chemistry 397(7), 2817-2824.

Gul, S. and Whalen, J.K. (2016) Biochemical cycling of nitrogen and phosphorus in biochar-amended soils. Soil Biology and Biochemistry 103, 1-15.

Han, W., Luo, L. and Zhang, S. (2013) Adsorption of tetrabromobisphenol A on soils: Contribution of soil components and influence of soil properties. Colloids and Surfaces A: Physicochemical and Engineering Aspects 428, 60-64.

Hendriks, H.S. and Westerink, R.H.S. (2015) Neurotoxicity and risk assessment of brominated and alternative flame retardants. Neurotoxicology and Teratology 52, Part B, 248-269.

Hossain, M.K., Strezov, V., Chan, K.Y., Ziolkowski, A. and Nelson, P.F. (2011) Influence of pyrolysis temperature on production and nutrient properties of wastewater sludge biochar. Journal of Environmental Management 92(1), 223-228.

Hossain, M.K., Strezov, V., Yin Chan, K. and Nelson, P.F. (2010) Agronomic properties of wastewater sludge biochar and bioavailability of metals in production of cherry tomato (Lycopersicon esculentum). Chemosphere 78(9), 1167-1171.

Hu, F., Pan, L., Xiu, M., Jin, Q., Wang, G. and Wang, C. (2015) Bioaccumulation and detoxification responses in the scallop Chlamys farreri exposed to tetrabromobisphenol A (TBBPA). Environmental Toxicology and Pharmacology 39(3), 997-1007.

Hu, J., Liang, Y., Chen, M. and Wang, X. (2009) Assessing the toxicity of TBBPA and HBCD by zebrafish embryo toxicity assay and biomarker analysis. Environmental Toxicology 24(4), 334-342.

Jacquelin, D.K., Perez, M.A., Euti, E.M., Arisnabarreta, N., Cometto, F.P., Paredes-Olivera, P. and Patrito, E.M. (2016) A pH-Sensitive Supramolecular Switch Based on Mixed Carboxylic Acid Terminated Self-Assembled Monolayers on Au(111). Langmuir 32(4), 947-953.

Ji, L., Zhou, L., Bai, X., Shao, Y., Zhao, G., Qu, Y., Wang, C. and Li, Y. (2012) Facile synthesis of multiwall carbon nanotubes/iron oxides for removal of tetrabromobisphenol A and Pb(ii). Journal of Materials Chemistry 22(31), 15853-15862.

Jiménez-Cedillo, M.J., Olguín, M.T. and Fall, C. (2009) Adsorption kinetic of arsenates as water pollutant on iron, manganese and iron–manganese-modified clinoptilolite-rich tuffs. Journal of Hazardous Materials 163(2–3), 939-945.

Jin, H., Hanif, M.U., Capareda, S., Chang, Z., Huang, H. and Ai, Y. (2016) Copper(II) removal potential from aqueous solution by pyrolysis biochar derived from anaerobically digested algae-dairy-manure and effect of KOH activation. Journal of Environmental Chemical Engineering 4(1), 365-372.

Joseph, S., Anawar, H.M., Storer, P., Blackwell, P., Chia, C., Lin, Y., Munroe, P., Donne, S., Horvat, J., Wang, J. and Solaiman, Z.M. (2015) Effects of Enriched Biochars Containing Magnetic Iron Nanoparticles on Mycorrhizal Colonisation, Plant Growth, Nutrient Uptake and Soil Quality Improvement. Pedosphere 25(5), 749-760.

Jung, C., Park, J., Lim, K.H., Park, S., Heo, J., Her, N., Oh, J., Yun, S. and Yoon, Y. (2013) Adsorption of selected endocrine disrupting compounds and pharmaceuticals on activated biochars. Journal of Hazardous Materials 263, Part 2, 702-710.

Karaer, H. and Kaya, İ. (2016) Synthesis, characterization of magnetic chitosan/active charcoal composite and using at the adsorption of methylene blue and reactive blue4. Microporous and Mesoporous Materials 232, 26-38.

Karhu, K., Mattila, T., Bergström, I. and Regina, K. (2011) Biochar addition to agricultural soil increased CH4 uptake and water holding capacity – Results from a short-term pilot field study. Agriculture, Ecosystems & Environment 140(1–2), 309-313.

Keiluweit, M., Nico, P.S., Johnson, M.G. and Kleber, M. (2010) Dynamic Molecular Structure of Plant Biomass-Derived Black Carbon (Biochar). Environmental

Science & Technology 44(4), 1247-1253.

Kim, Y.H., Lee, B., Choo, K.H. and Choi, S.J. (2011) Selective adsorption of bisphenol A by organic–inorganic hybrid mesoporous silicas. Microporous and Mesoporous Materials 138(1–3), 184-190.

Kołtowski, M., Hilber, I., Bucheli, T.D., Charmas, B., Skubiszewska-Zięba, J. and Oleszczuk, P. (2017) Activated biochars reduce the exposure of polycyclic aromatic hydrocarbons in industrially contaminated soils. Chemical Engineering Journal 310, Part 1, 33-40.

Kuiper, R.V., van den Brandhof, E.J., Leonards, P.E.G., van der Ven, L.T.M., Wester, P.W. and Vos, J.G. (2007) Toxicity of tetrabromobisphenol A (TBBPA) in zebrafish (Danio rerio) in a partial life-cycle test. Archives of Toxicology 81(1), 1-9.

Labadie, P., Tlili, K., Alliot, F., Bourges, C., Desportes, A. and Chevreuil, M. (2010) Development of analytical procedures for trace-level determination of polybrominated diphenyl ethers and tetrabromobisphenol A in river water and sediment. Analytical and Bioanalytical Chemistry 396(2), 865-875.

Law, R.J., Allchin, C.R., de Boer, J., Covaci, A., Herzke, D., Lepom, P., Morris, S., Tronczynski, J. and de Wit, C.A. (2006) Levels and trends of brominated flame retardants in the European environment. Chemosphere 64(2), 187-208.

Lee, I.S., Kang, H.H., Kim, U.J. and Oh, J.E. (2015) Brominated flame retardants in Korean river sediments, including changes in polybrominated diphenyl ether concentrations between 2006 and 2009. Chemosphere 126, 18-24.

Li, F., Wang, J., Jiang, B., Yang, X., Nastold, P., Kolvenbach, B., Wang, L., Ma, Y., Corvini, P.F.-X. and Ji, R. (2015) Fate of Tetrabromobisphenol A (TBBPA) and Formation of Ester- and Ether-Linked Bound Residues in an Oxic Sandy Soil.

Environmental Science & Technology 49(21), 12758-12765.

Li, G., Wang, S., Wu, Q., Wang, F., Ding, D. and Shen, B. (2017) Mechanism identification of temperature influence on mercury adsorption capacity of different halides modified bio-chars. Chemical Engineering Journal 315, 251-261.

Li, H., Huang, G., An, C. and Zhang, W.-x. (2012) Kinetic and equilibrium studies on the adsorption of calcium lignosulfonate from aqueous solution by coal fly ash. Chemical Engineering Journal 200, 275-282.

Li, J., Li, Y., Wu, Y. and Zheng, M. (2014) A comparison of biochars from lignin, cellulose and wood as the sorbent to an aromatic pollutant. Journal of Hazardous Materials 280, 450-457.

Li, L., Quinlivan, P.A. and Knappe, D.R.U. (2005) Predicting Adsorption Isotherms for Aqueous Organic Micropollutants from Activated Carbon and Pollutant Properties. Environmental Science & Technology 39(9), 3393-3400.

Li, X., Zhang, Y., Jing, L. and He, X. (2016) Novel N-doped CNTs stabilized Cu2O nanoparticles as adsorbent for enhancing removal of Malachite Green and tetrabromobisphenol A. Chemical Engineering Journal 292, 326-339.

Li, Y., Zhou, Q., Wang, Y. and Xie, X. (2011) Fate of tetrabromobisphenol A and hexabromocyclododecane brominated flame retardants in soil and uptake by plants. Chemosphere 82(2), 204-209.

Li, Y.P., Huang, G., Huang, Y.F. and Zhou, H.D. (2009) A multistage fuzzy-stochastic programming model for supporting sustainable water-resources allocation and management. Environmental Modelling & Software 24(7), 786-797.

Liu, K., Li, J., Yan, S., Zhang, W., Li, Y. and Han, D. (2016) A review of status of tetrabromobisphenol A (TBBPA) in China. Chemosphere 148, 8-20.

Mahmoud, M.E., Nabil, G.M., El-Mallah, N.M., Bassiouny, H.I., Kumar, S. and Abdel-Fattah, T.M. (2016) Kinetics, isotherm, and thermodynamic studies of the adsorption of reactive red 195 A dye from water by modified Switchgrass Biochar adsorbent. Journal of Industrial and Engineering Chemistry 37, 156-167.

Meerts, I.A., Letcher, R.J., Hoving, S., Marsh, G., Bergman, A., Lemmen, J.G., van der Burg, B. and Brouwer, A. (2001) In vitro estrogenicity of polybrominated diphenyl ethers, hydroxylated PDBEs, and polybrominated bisphenol A compounds. Environmental Health Perspectives 109(4), 399-407.

Morose, G. (2006) An overview of alternatives to tetrabromobisphenol A (TBBPA) and hexabromocyclododecane (HBCD). Lowell Center for Sustainable Production, University of Massachusetts, Lowell http://sustainableproduction. org/downloads/AternativestoTBBPAandHBCD. pdf.

Morris, S., Allchin, C.R., Zegers, B.N., Haftka, J.J.H., Boon, J.P., Belpaire, C., Leonards, P.E.G., van Leeuwen, S.P.J. and de Boer, J. (2004) Distribution and Fate of HBCD and TBBPA Brominated Flame Retardants in North Sea Estuaries and Aquatic Food Webs. Environmental Science & Technology 38(21), 5497-5504.

Nakajima, A., Saigusa, D., Tetsu, N., Yamakuni, T., Tomioka, Y. and Hishinuma, T. (2009) Neurobehavioral effects of tetrabromobisphenol A, a brominated flame retardant, in mice. Toxicology Letters 189(1), 78-83.

Namasivayam, C., Prabha, D. and Kumutha, M. (1998) Removal of direct red and acid brilliant blue by adsorption on to banana pith. Bioresource Technology 64(1), 77-79.

Ni, H.-G. and Zeng, H. (2013) HBCD and TBBPA in particulate phase of indoor air in

Shenzhen, China. Science of the Total Environment 458–460, 15-19.

Nielsen, L., Zhang, P. and Bandosz, T.J. (2015) Adsorption of carbamazepine on sludge/fish waste derived adsorbents: Effect of surface chemistry and texture. Chemical Engineering Journal 267, 170-181.

Novak, J.M., Busscher, W.J., Laird, D.L., Ahmedna, M., Watts, D.W. and Niandou, M.A.S. (2009) Impact of Biochar Amendment on Fertility of a Southeastern Coastal Plain Soil. Soil Science 174(2), 105-112.

Osako, M., Kim, Y.J. and Sakai, S.-i. (2004) Leaching of brominated flame retardants in leachate from landfills in Japan. Chemosphere 57(10), 1571-1579.

Özhan, A., Şahin, Ö., Küçük, M.M. and Saka, C. (2014) Preparation and characterization of activated carbon from pine cone by microwave-induced ZnCl2 activation and its effects on the adsorption of methylene blue. Cellulose 21(4), 2457-2467.

Pandey, K. (1999) A study of chemical structure of soft and hardwood and wood polymers by FTIR spectroscopy. Journal of Applied Polymer Science 71(12), 1969-1975.

Park, C.M., Han, J., Chu, K.H., Al-Hamadani, Y.A.J., Her, N., Heo, J. and Yoon, Y. Influence of solution pH, ionic strength, and humic acid on cadmium adsorption onto activated biochar: Experiment and modeling. Journal of Industrial and Engineering Chemistry.

Peng, P., Lang, Y.H. and Wang, X.M. (2016) Adsorption behavior and mechanism of pentachlorophenol on reed biochars: pH effect, pyrolysis temperature, hydrochloric acid treatment and isotherms. Ecological Engineering 90, 225-233.

Peng, X., Tian, Y., Liu, S. and Jia, X. (2017) Degradation of TBBPA and BPA from aqueous solution using organo-montmorillonite supported nanoscale zero-

valent iron. Chemical Engineering Journal 309, 717-724.

Peng, X., Zhang, Z., Luo, W. and Jia, X. (2013) Biodegradation of tetrabromobisphenol A by a novel Comamonas sp. strain, JXS-2-02, isolated from anaerobic sludge. Bioresource Technology 128, 173-179.

Pingree, M.R.A., DeLuca, E.E., Schwartz, D.T. and DeLuca, T.H. (2016) Adsorption capacity of wildfire-produced charcoal from Pacific Northwest forests. Geoderma 283, 68-77.

Potvin, C.M., Long, Z. and Zhou, H. (2012) Removal of tetrabromobisphenol A by conventional activated sludge, submerged membrane and membrane aerated biofilm reactors. Chemosphere 89(10), 1183-1188.

Qin, X.S., Huang, G., Zeng, G.M., Chakma, A. and Huang, Y.F. (2007) An interval-parameter fuzzy nonlinear optimization model for stream water quality management under uncertainty. European Journal of Operational Research 180(3), 1331-1357.

Qiu, Y., Zheng, Z., Zhou, Z. and Sheng, G.D. (2009) Effectiveness and mechanisms of dye adsorption on a straw-based biochar. Bioresource Technology 100(21), 5348-5351.

Roberts, K.G., Gloy, B.A., Joseph, S., Scott, N.R. and Lehmann, J. (2010) Life Cycle Assessment of Biochar Systems: Estimating the Energetic, Economic, and Climate Change Potential. Environmental Science & Technology 44(2), 827-833.

Sclavons, M., Franquinet, P., Carlier, V., Verfaillie, G., Fallais, I., Legras, R., Laurent, M. and Thyrion, F.C. (2000) Quantification of the maleic anhydride grafted onto polypropylene by chemical and viscosimetric titrations, and FTIR spectroscopy. Polymer 41(6), 1989-1999.

Sclavons, M., Laurent, M., Devaux, J. and Carlier, V. (2005) Maleic anhydride-grafted polypropylene: FTIR study of a model polymer grafted by ene-reaction. Polymer 46(19), 8062-8067.

Sellström, U. and Jansson, B. (1995) Analysis of tetrabromobisphenol A in a product and environmental samples. Chemosphere 31(4), 3085-3092.

Sennour, R., Mimane, G., Benghalem, A. and Taleb, S. (2009) Removal of the persistent pollutant chlorobenzene by adsorption onto activated montmorillonite. Applied Clay Science 43(3–4), 503-506.

Sewu, D.D., Boakye, P. and Woo, S.H. (2017) Highly efficient adsorption of cationic dye by biochar produced with Korean cabbage waste. Bioresource Technology 224, 206-213.

Shang, J., He, W. and Fan, C. (2014) Adsorption of dimethyl trisulfide from aqueous solution on a low-cost adsorbent: thermally activated pinecone. Chinese Journal of Oceanology and Limnology 33(1), 169-175.

Shao, D., Hu, J., Chen, C., Sheng, G., Ren, X. and Wang, X. (2010) Polyaniline Multiwalled Carbon Nanotube Magnetic Composite Prepared by Plasma-Induced Graft Technique and Its Application for Removal of Aniline and Phenol. The Journal of Physical Chemistry C 114(49), 21524-21530.

Shen, J., Huang, G., An, C., Zhao, S. and Rosendahl, S. (2017) Immobilization of tetrabromobisphenol A by pinecone-derived biochars at solid-liquid interface: Synchrotron-assisted analysis and role of inorganic fertilizer ions. Chemical Engineering Journal 321, 346-357.

Shi, H., Wang, X., Luo, Y. and Su, Y. (2005) Electron paramagnetic resonance evidence of hydroxyl radical generation and oxidative damage induced by tetrabromobisphenol A in Carassius auratus. Aquatic Toxicology 74(4), 365-

371.

Shimabuku, K.K., Kearns, J.P., Martinez, J.E., Mahoney, R.B., Moreno-Vasquez, L. and Summers, R.S. (2016) Biochar sorbents for sulfamethoxazole removal from surface water, stormwater, and wastewater effluent. Water Research 96, 236-245.

Shin, S., Jang, J., Yoon, S.H. and Mochida, I. (1997) A study on the effect of heat treatment on functional groups of pitch based activated carbon fiber using FTIR. Carbon 35(12), 1739-1743.

Siengchum, T., Isenberg, M. and Chuang, S.S.C. (2013) Fast pyrolysis of coconut biomass – An FTIR study. Fuel 105, 559-565.

Sun, Z., Mao, L., Xian, Q., Yu, Y., Li, H. and Yu, H. (2008a) Effects of dissolved organic matter from sewage sludge on sorption of tetrabromobisphenol A by soils. Journal of Environmental Sciences 20(9), 1075-1081.

Sun, Z., Yu, Y., Mao, L., Feng, Z. and Yu, H. (2008b) Sorption behavior of tetrabromobisphenol A in two soils with different characteristics. Journal of Hazardous Materials 160(2–3), 456-461.

Taghizadeh-Toosi, A., Clough, T.J., Sherlock, R.R. and Condron, L.M. (2012) Biochar adsorbed ammonia is bioavailable. Plant and Soil 350(1), 57-69.

Tang, J., Feng, J., Li, X. and Li, G. (2014a) Levels of flame retardants HBCD, TBBPA and TBC in surface soils from an industrialized region of East China. Environmental Science: Processes & Impacts 16(5), 1015-1021.

Tang, Y., Li, S., Zhang, Y., Yu, S. and Martikka, M. (2014b) Sorption of tetrabromobisphenol A from solution onto MIEX resin: Batch and column test. Journal of the Taiwan Institute of Chemical Engineers 45(5), 2411-2417.

Teixidó, M., Pignatello, J.J., Beltrán, J.L., Granados, M. and Peccia, J. (2011)

Speciation of the Ionizable Antibiotic Sulfamethazine on Black Carbon (Biochar). Environmental Science & Technology 45(23), 10020-10027.

ten Dam, G., Pardo, O., Traag, W., van der Lee, M. and Peters, R. (2012) Simultaneous extraction and determination of HBCD isomers and TBBPA by ASE and LC–MSMS in fish. Journal of Chromatography B 898, 101-110.

Trouvé, A., Batonneau-Gener, I., Valange, S., Bonne, M. and Mignard, S. (2012) Tuning the hydrophobicity of mesoporous silica materials for the adsorption of organic pollutant in aqueous solution. Journal of Hazardous Materials 201–202, 107-114.

Tsuruta, T. (2004) Cell-Associated Adsorption of Thorium or Uranium from Aqueous System Using Various Microorganisms. Water, Air, and Soil Pollution 159(1), 35-47.

Van Zwieten, L., Kimber, S., Morris, S., Chan, K.Y., Downie, A., Rust, J., Joseph, S. and Cowie, A. (2010) Effects of biochar from slow pyrolysis of papermill waste on agronomic performance and soil fertility. Plant and Soil 327(1), 235-246.

Vinh, N., Zafar, M., Behera, S.K. and Park, H.-S. (2014) Arsenic(III) removal from aqueous solution by raw and zinc-loaded pine cone biochar: equilibrium, kinetics, and thermodynamics studies. International Journal of Environmental Science and Technology 12(4), 1283-1294.

Wang, F., Ren, X., Sun, H., Ma, L., Zhu, H. and Xu, J. (2016) Sorption of polychlorinated biphenyls onto biochars derived from corn straw and the effect of propranolol. Bioresour Technol 219, 458-465.

Wang, J., Tsuzuki, T., Tang, B., Hou, X., Sun, L. and Wang, X. (2012) Reduced Graphene Oxide/ZnO Composite: Reusable Adsorbent for Pollutant Management. ACS Applied Materials & Interfaces 4(6), 3084-3090.

Wang, P., Cao, M., Wang, C., Ao, Y., Hou, J. and Qian, J. (2014) Kinetics and thermodynamics of adsorption of methylene blue by a magnetic graphene-carbon nanotube composite. Applied Surface Science 290, 116-124.

Wang, P., Tang, L., Wei, X., Zeng, G., Zhou, Y., Deng, Y., Wang, J., Xie, Z. and Fang, W. (2017a) Synthesis and application of iron and zinc doped biochar for removal of p-nitrophenol in wastewater and assessment of the influence of co-existed Pb(II). Applied Surface Science 392, 391-401.

Wang, P., Yin, Y., Guo, Y. and Wang, C. (2015) Removal of chlorpyrifos from waste water by wheat straw-derived biochar synthesized through oxygen-limited method. RSC Advances 5(89), 72572-72578.

Wang, W., Huang, G., An, C., Xin, X., Zhang, Y. and Liu, X. (2017b) Transport behaviors of anionic azo dyes at interface between surfactant-modified flax shives and aqueous solution: Synchrotron infrared and adsorption studies. Applied Surface Science 405, 119-128.

Watanabe, I., Kashimoto, T. and Tatsukawa, R. (1983) Identification of the flame retardant tetrabromobisphenol-a in the river sediment and the mussel collected in Osaka. Bulletin of Environmental Contamination and Toxicology 31(1), 48-52.

Watson, J.S., Scott, C.D. and Faison, B.D. (1989) Adsorption of Sr by immobilized microorganisms. Applied Biochemistry and Biotechnology 20(1), 699-709.

Western, A.W., Grayson, R.B. and Blöschl, G. (2002) Scaling of Soil Moisture: A Hydrologic Perspective. Annual Review of Earth and Planetary Sciences 30(1), 149-180.

Widmer, R., Oswald-Krapf, H., Sinha-Khetriwal, D., Schnellmann, M. and Böni, H. (2005) Global perspectives on e-waste. Environmental Impact Assessment

Review 25(5), 436-458.

Wu, F., Jia, Z., Wang, S., Chang, S.X. and Startsev, A. (2013) Contrasting effects of wheat straw and its biochar on greenhouse gas emissions and enzyme activities in a Chernozemic soil. Biology and Fertility of Soils 49(5), 555-565.

Wu, Y., Ming, Z., Yang, S., Fan, Y., Fang, P., Sha, H. and Cha, L. (2017) Adsorption of hexavalent chromium onto Bamboo Charcoal grafted by Cu2+-N-aminopropylsilane complexes: Optimization, kinetic, and isotherm studies. Journal of Industrial and Engineering Chemistry 46, 222-233.

Xiao, W., Wang, J., Huang, Y., Sun, S. and Zhou, Y. (2015) An Approach for Estimating the Nitrobenzene (NB) Emission Effect in Frozen Rivers: A Case Study of Nitrobenzene Pollution in the Songhua River, China. Journal of Environmental Informatics 26(2), 140-147.

Xin, X., Huang, G., Liu, X., An, C., Yao, Y., Weger, H., Zhang, P. and Chen, X. (2017) Molecular toxicity of triclosan and carbamazepine to green algae Chlorococcum sp.: A single cell view using synchrotron-based Fourier transform infrared spectromicroscopy. Environmental Pollution 226, 12-20.

Xue, Y., Gu, X., Wang, X., Sun, C., Xu, X., Sun, J. and Zhang, B. (2009) The hydroxyl radical generation and oxidative stress for the earthworm Eisenia fetida exposed to tetrabromobisphenol A. Ecotoxicology 18(6), 693-699.

Yang, L., Zhang, F., Endo, T. and Hirotsu, T. (2003) Microstructure of Maleic Anhydride Grafted Polyethylene by High-Resolution Solution-State NMR and FTIR Spectroscopy. Macromolecules 36(13), 4709-4718.

Yang, X., Sun, L., Xiang, J., Hu, S. and Su, S. (2013) Pyrolysis and dehalogenation of plastics from waste electrical and electronic equipment (WEEE): A review. Waste Management 33(2), 462-473.

Yu, B., Zhang, Y., Shukla, A., Shukla, S.S. and Dorris, K.L. (2000) The removal of heavy metal from aqueous solutions by sawdust adsorption — removal of copper. Journal of Hazardous Materials 80(1–3), 33-42.

Yu, J.G., Yu, L.Y., Yang, H., Liu, Q., Chen, X.H., Jiang, X.Y., Chen, X.Q. and Jiao, F.-P. (2015) Graphene nanosheets as novel adsorbents in adsorption, preconcentration and removal of gases, organic compounds and metal ions. Science of the Total Environment 502, 70-79.

Zhang, Y., Huang, G., An, C., Xin, X., Liu, X., Raman, M., Yao, Y., Wang, W. and Doble, M. (2017) Transport of anionic azo dyes from aqueous solution to gemini surfactant-modified wheat bran: Synchrotron infrared, molecular interaction and adsorption studies. Science of the Total Environment 595, 723-732.

Zhang, Y., Liu, G., Yu, S., Zhang, J., Tang, Y., Li, P. and Ren, Y. (2014) Kinetics and Interfacial Thermodynamics of the pH-Related Sorption of Tetrabromobisphenol A onto Multiwalled Carbon Nanotubes. ACS Applied Materials & Interfaces 6(23), 20968-20977.

Zhang, Y., Tang, Y., Li, S. and Yu, S. (2013) Sorption and removal of tetrabromobisphenol A from solution by graphene oxide. Chemical Engineering Journal 222, 94-100.

Zhang, Z., Cai, R., Long, F. and Wang, J. (2015) Development and application of tetrabromobisphenol A imprinted electrochemical sensor based on graphene/carbon nanotubes three-dimensional nanocomposites modified carbon electrode. Talanta 134, 435-442.

Zhao, B., Zhang, H., Zhang, J. and Jin, Y. (2008) Virus adsorption and inactivation in soil as influenced by autochthonous microorganisms and water content. Soil

Biology and Biochemistry 40(3), 649-659.

Zhao, G., Jiang, L., He, Y., Li, J., Dong, H., Wang, X. and Hu, W. (2011) Sulfonated Graphene for Persistent Aromatic Pollutant Management. Advanced Materials 23(34), 3959-3963.

Zhao, S., Huang, G., An, C., Wei, J. and Yao, Y. (2015a) Enhancement of soil retention for phenanthrene in binary cationic gemini and nonionic surfactant mixtures: Characterizing two-step adsorption and partition processes through experimental and modeling approaches. Journal of Hazardous Materials 286, 144-151.

Zhao, S., Huang, G., Wei, J., An, C. and Zhang, P. (2015b) Phenanthrene Sorption on Palygorskite Modified with Gemini Surfactants: Insights from Modeling Studies and Effects of Aqueous Solution Chemistry. Water, Air, & Soil Pollution 227(1), 17.

Zhong, H., Zeng, G.m., Yuan, X.Z., Fu, H.y., Huang, G.H. and Ren, F.Y. (2007) Adsorption of dirhamnolipid on four microorganisms and the effect on cell surface hydrophobicity. Applied Microbiology and Biotechnology 77(2), 447-455.

Zhou, X., Guo, J., Lin, K., Huang, K. and Deng, J. (2013) Leaching characteristics of heavy metals and brominated flame retardants from waste printed circuit boards. Journal of Hazardous Materials 246–247, 96-102.

Zielińska, A. and Oleszczuk, P. (2015) Evaluation of sewage sludge and slow pyrolyzed sewage sludge-derived biochar for adsorption of phenanthrene and pyrene. Bioresource Technology 192, 618-626.

Zou, M.Y., Ran, Y., Gong, J., Mai, B.X. and Zeng, E.y. (2007) Polybrominated diphenyl ethers in watershed soils of the Pearl River Delta, China: occurrence,

inventory, and fate. Environmental Science & Technology 41(24), 8262-8267.